UNIVERSITÉ DE SHERBROOKE

Faculté de Génie

Département de génie chimique et biotechnologique

SYNTHÈSES D'UN CATALYSEUR COMPOSÉ D'UNE SAPO-34 AVEC UNE HAUTE SÉLECTIVITÉ VERS LES OLÉFINES LÉGÈRES ET RÉSISTANCE À LA FORMATION DE COKE

SYNTHESIS OF A SAPO-34-BASED CATALYST WITH HIGH SELECTIVITY TO LIGHT OLEFINS AND RESISTANCE TO COKE FORMATION

Thèse de doctorat

Spécialité: Génie chimique

Ignacio J. CASTELLANOS-BELTRAN

Jury: Prof. Jean-Michel LAVOIE (Directeur)

Dr. Stéphane MARIE-ROSE (Enerkem)

Prof. Marco J. CASTALDI (External evaluator)

Prof. Nicolas ABATZOGLOU (Rapporteur)

Sherbrooke (Québec) Canada 2 May 2018

SUMMARY:

Ethylene and propylene are commodities extensively used in the petrochemical industry for the fabrication of added-value products such as polymers. However, their current production rely on inefficient, energy-intensive technologies that use fossil fuels as raw material. As alternative, the conversion of methanol to olefins (MTO) using microporous solid acids as catalyst represented a major landmark for the reduction of energy expenditure and carbon dioxide generation. Furthermore, methanol can be produced through the gasification of sustainable sources, thus opening the opportunity for the development of "*green*" alternatives. In industry, SAPO-34 is employed for the production of polymer-grade olefins due to its exceptional selectivity. However, the catalyst undergoes deactivation due to coke deposition at a relatively fast pace. This study focused on the fabrication and testing in the MTO reaction of a hierarchical-type SAPO-34, composed of a micro- and mesoporous structure. In literature, this novel configuration is reported to enhance the selectivity towards light olefins, since it reduces products residence time and their corresponding secondary reactions.

First, an alkaline treatment using NaOH was explored for the formation of a secondary structure in a microporous SAPO-34 (purchased), which presented a conventional microporous structure. The effect of the treatment on the physico-chemical properties was investigated and samples were tested for the accumulation of coke using DME as carbon source. Afterwards, the effect of temperature (300 and 500°C) was investigated on the MTO reaction using an extruded SAPO-34 as catalyst. An extrusion process was customized to allow testing different catalysts in a bench-scale, fixed-bed reactor. Reactions were done at similar conditions: water content (80 wt%), weight hour space velocity (WHSV, 1.21 – 1.40 h^{-1}) and extruded catalyst mass (30 g per experiment). Then, a SAPO-34 was synthesized using an organosilane-directed method and tested in the MTO reaction. The latter method led to positive results for the fabrication of a hierarchical SAPO-34, unlike the alkaline treatment method, and its testing at the optimal temperature (450°C) led to a remarkable selectivity to light olefins of 79.1% and 90.9% methanol conversion hydrocarbons in the gas phase (carbon basis), while minimizing the formation of coke (7.7%) and propane (1.6%). The higher selectivity was attributed to the suppression of secondary reactions, in particular, those involving propylene, since this species was the only one changing in selectivity in parallel with those of coke and propane. Finally, other parameters, such as metal incorporation and diluting gas, are suggested for boosting further the selectivity to light olefins.

Keywords: MTO, SAPO-34, hierarchization, temperature effect, coke deposition, catalyst extrusion, organosilane method.

RÉSUMÉ:

L'éthylène et le propylène sont des produits largement utilisés dans l'industrie pétrochimique pour la fabrication de produits à valeur-ajouté tels les polymères. Cependant, leur production actuelle repose sur des technologies inefficaces et énergivores utilisant des combustibles fossiles comme matière première. Comme alternatif, la conversion du méthanol en oléfines (MTO) en utilisant des acides solides microporeux comme catalyseur représente une approche majeure pour la réduction de la demande énergétique et leur empreinte de carbone. En outre, le méthanol peut être fabriqué grâce à la gazéification de sources durables, ouvrant ainsi la possibilité de développer des alternatives « *vertes* ». Dans l'industrie, la SAPO-34 est utilisée pour la production d'oléfines de qualité polymère en raison de sa sélectivité exceptionnelle. Cependant, le catalyseur subit une désactivation à cause du dépôt de coke, se formant à une cadence relativement rapide. Cette porte, donc, sur la fabrication et les essais pour la réaction de MTO d'une SAPO-34 de type hiérarchique, composée d'une structure micro- et mésoporeuse. Dans la littérature, cette nouvelle configuration améliore la sélectivité vis-à-vis des oléfines légères, car elle réduit le temps de séjour des produits et leurs réactions secondaires

Tout d'abord, un traitement alcalin utilisant du NaOH a été exploré pour la formation d'une structure secondaire dans une SAPO-34 commerciale, qui présentait une structure microporeuse conventionnelle. L'effet du traitement sur les propriétés physico-chimiques a été étudié et des échantillons ont été testés dans l'accumulation de coke en utilisant le DME comme source de carbone. Ensuite, les effets de la température (300 et 500°C) pour la réaction MTO ont été étudiés en utilisant une SAPO-34 extrudée comme catalyseur. Un processus d'extrusion a été adapté pour permettre le test de différents catalyseurs dans un réacteur à lit-fixe. Les réactions ont été effectuées dans des conditions similaires soit une teneur en eau (80% en poids), une vitesse spatiale en poids d'heure (WHSV, 1.21-1.40 h^{-1}) et une masse de catalyseur extrudée (30 g par expérience). Ensuite, une SAPO-34 a été synthétisée en utilisant une méthode basée sur les organosilanes et teste pour la réaction MTO. Cette dernière méthode a conduit à des résultats positifs pour la fabrication d'une SAPO-34 hiérarchique, contrairement à la méthode de traitement alcalin, et son test à la température optimale (450°C) a conduit à une sélectivité remarquable pour les oléfines légères de 79.1% (sur une base de carbone), tout en minimisant la formation de coke (7.7%) et de propane (1.6%). La sélectivité plus élevée a été attribuée à la suppression des réactions secondaires, en particulier celles impliquant le propylène. En fin, autres paramètres tels que l'incorporation de métaux et le gaz de dilution sont suggérés pour stimuler davantage la sélectivité en oléfines légères.

Mots clés: MTO, SAPO-34, hierarchization, temperature effect, coke deposition, catalyst extrusion, organosilane method.

ACKNOWLEDGEMENTS

I want to start by thanking the organisms and institutions that provided me the opportunity to develop myself as researcher. This includes the University of Sherbrooke, the CRIEC-B and Enerkem Inc. I also want to thank those who help sponsored this endeavour: The Ministère de l'Énergie et des Ressources Naturelles du Québec (MERNQ), CRB Innovations, Enerkem Inc. and Éthanol Greenfield. It is important to emphasize that without their support, students would not be able to pursuit the "*art*" of research.

I would like to deeply express my gratitude to the people of the CRIEC-B, starting with my supervisor Prof. Jean-Michel Lavoie, for always helping me find reassurance that the goal was going to be met. Also, my two close advisers, Dr. Palla Assima and Dr. Bruna Rego, for sharing with me their wisdom and experience, not to mention the opportunity to see them at work.

Also, I would like to thank the people of Enerkem, Dr. Esteban Chornet, Dr. Stéphane Marie-Rose, Dr. Jennifer Gil and Dr. Ariadna Fuentes, for participating in my training and supporting my Ph.D. project.

Finally, I want to thank my parents and siblings for their support and apologize for the time I could not spend with them due to my goals in research.

I deeply appreciate the opportunity of working with the CRIEC-B and Enerkem, and the experience along acquired. I can only wish to Jean-Michel and his team success in the futures endeavours.

Ignacio Jorge Castellanos-Beltran

TABLE OF CONTENT

LIST OF FIGURES

LIST OF TABLES

INTRODUCTION

Ethylene and propylene (light olefins) are specially valued by the petrochemical industry, as they are compulsory building blocks in the fabrication of some of the most common items, most notably plastics [1]. However, the current methods (paraffin steam cracking) used to supply the ever-growing demand of these chemicals are energy-intensive, fossil-fueled technologies that may induce environmental and economic issues [2]. An alternative, the MTO (Methanol-to-Olefins) reaction was developed by Mobil scientists in the 70s for the production of olefins and other hydrocarbons using methanol as the starting molecule. This technique has demonstrated multiples advantages over steam cracking, including a higher carbon-based conversion to light olefins, in addition to a wider flexibility on the selectivity to ethylene and propylene. More remarkably, this route allows the diversification of the source from which methanol can be produced, permitting the development of a carbon-neutral route [3].

One possible approach to produce methanol is from refused derived fuel (RDF), a fraction recovered from municipal solid wastes (MSW) that includes materials such as paper, plastic, leather, wood, textile and rubber [4]. This feedstock is of great interest because it addresses two important concerns: waste management and the dependence on fossil fuels. In North America, waste management commonly involves landfilling and incineration. Such procedures, however, cause the release of large amounts of greenhouse gases (CH_4, CO_2, dioxins, furans, NO_X, SO_X, etc.) and other residues harmful to human health and the environment, which consequently has led some researchers to deem these procedures inadequate [5]. Furthermore, oil, gas and coal are by-far the most common materials powering industrialized countries, and not less important, the main source for the synthesis of a large number of man-made items including petrochemical and chemical products. To counter this dependence, it has been suggested that a "methanol economy", in which methanol and dimethyl ether (DME) were to replace fossil fuels, could be capable of providing the means for energy storage, ground transportation, and most remarkably, the raw material for the synthesis of the aforementioned hydrocarbons and corresponding derivatives [6].

To estimate the potential production of methanol from MSW in Canada, a straightforward mathematical exercise is demonstrated in the following lines. First, the amount of carbon available in MSW must be determined, and second, a conversion factor from the carbon atom in the RDF into the methanol (as product). To determine the amount of carbon in MSW, three values were required: the estimated production of MSW in Canada (i.e. 25 million metric tons in 2010 [7]), a standard RDF fraction found in MSW (i.e. 55% [8]) and a common carbon content found in RDF (i.e. 45.4% [9]). According to these values, the amount of carbon available in Canada from MSW in 2010 should be around 6.24 million metric tons (MT).

For the conversion of carbon to methanol, two parameters were taken from literature: a representative conversion of carbon to carbon monoxide (CO), and another from CO to methanol. For the latter, the conversion of syngas to methanol is a well-developed craft with close to full conversion of the carbon in the CO molecule into methanol [10]. However, for the generation of syngas suitable for methanol production via RDF gasification, this may lead to a certain loss in carbon conversion due to CO_2 and minor light alkane (CH_4, C_2H_6…) production.

Under a "conservative" assumption of 10% conversion [11], the potential amount of methanol produced should be around 1.67 million MT per year or 2,136 million liters per year (LPY) on a national scale.

To put the former value into the current context in Canada, the production of two commercial methanol plants are underscored. First, between 2001 and 2006 ***Methanex Corp.***, the largest methanol producer in Canada, shut down their plants as result of the volatility of natural gas prices [12]. Their methanol production was around 560,000 MT per year, which equated to around 800 million LPY, namely, 34.5% of 2,136 million LPY. On a smaller scale, ***Enerkem Inc.***, a company involved in the production of biofuels, has completed the construction of a methanol plant in Alberta (Canada), using MSW as feedstock with a capacity of 38 million LPY (1.78%) [13]. When comparing the production capacity of these two plants to that hypothesized from MSW in Canada (paragraph above), one may realize of the opportunity Canada has for developing an industry in which added-value products issue from "*neutral-carbon*" methanol, were to capable of competing evenly against the current oil-based infrastructure.

The present Ph.D. project is a collaboration between the University of Sherbrooke (CRIEC-B) and ***Enerkem Inc.***, in which the selective conversion of methanol to light olefins is investigated to provide an alternative route for the synthesis of ethanol. Currently, ***Enerkem Inc***. owns a functional process for the synthesis of ethanol from methanol [14]. However, by developing an alternative route, ***Enerkem Inc.*** production could become more flexible and add new value-added products to their repertoire, in this case ethylene and propylene.

The new route would have its basis on the MTO reaction using a SAPO-34, for which the major drawback found in current industrial systems is the fast deactivation this catalyst undergoes during reaction, forcing them to rely on complex fluidized reactors. However, in recent years there has been advances on the optimization of the catalyst, and so, it has been demonstrated that coke deposition can be substantially reduced by creating a hierarchical-type SAPO-34 through the incorporation of mesopores (pores 2 – 50 nm in dia.) into the innate microporous structure of the zeo-type (pores < 0.4 nm in dia.). The higher resistance to deactivation originates from the additional channels connecting the inner layers of the catalyst to the external surface, which facilitates the exit of product molecules, and thus, mitigates secondary reactions leading to coke deposition.

The goals of the thesis are the development of a catalyst and process efficient in the conversion of methanol to light olefins. The work included multiple steps such as catalyst synthesis/modification, extrusion process, characterization, MTO testing and characterization of the spent catalyst. The novelty of this work relied on the synthesis of a hierarchical-type SAPO-34 following an organosilane-directed method, which should render the catalyst resistant to coke deactivation, and the application of an extrusion step for testing different catalysts in the MTO reaction in a bench-scale, fixed-bed reactor.

The present manuscript starts off with a literature review (**Chapter 1**) addressing the context in which this project was built on. For that, statistics on the evolution of light olefin production and an examination on the technologies supplying it were presented. Then, the document focuses on the MTO reaction, a process being developed by Mobil since the 70s and whose

higher performance over conventional method has led to much interest. Furthermore, the most relevant studies (milestones) that have led to our current understanding of the MTO reaction are highlighted. Finally, the review centers on the *how* and *where* coke is formed, as well as the factors contributing to its formation.

In **Chapter 2**, the manuscript addresses the experimental work and different characterization techniques employed. The experimental work included two procedures that were attempted in the development of a hierarchical-type SAPO-34. First, the project focused on the alkaline treatment of a microporous SAPO-34 to incorporate intra-particle mesopores, referred as top-bottom approach. The targeted SAPO-34 was also developed following a bottom-top approach, in which the metal precursors were mixed and treated in an autoclave at high temperature to induce the nucleation of the catalyst. This section also included the extrusion process, which is a common technique used for the preparation of a "*macroscopic*" version (cylindrical pellets) of the powder catalyst. The extrusion was shown to be compulsory for our work, and so, a methodology developed at ***Enerkem Inc.*** was employed [15]. The experimental work was also complemented with the catalyst (extruded form) testing in the MTO reaction in a bench-scale, fixed-bed reactor, in which the temperature was varied from 300 to 500°C.

The characterization, which is also part of **Chapter 2**, included the analysis of the physicochemical properties measured for the pure and extruded catalysts via X-ray diffraction patterns (XRD), nitrogen adsorption-desorption isotherm (N_2 isotherm) and ammonia-temperature program desorption (NH_3-TPD). In addition, the spent catalyst recovered after reaction was examined for determining the quantitative (content) and qualitative (H/C ratio) analysis of the coke, as well as carbon.

Our first attempt on the development of a hierarchical-type SAPO-34 involved the alkaline treatment of a commercial SAPO-34 [16] (**Chapter 3**). This study demonstrated the limitations of such technique when applied to this zeo-type. However, a coke deposition study using DME as carbon source underscored the tendency of coke molecules to accumulate on the outer layer of the particle. Hence, the importance of creating a secondary intra-particle mesoporous structure in the SAPO-34.

The effect of temperature (300 to 500°C) on the MTO reaction was investigated using an extruded SAPO-34 (microporous-type SAPO-34) as catalyst (**Chapter 4**). This analysis paved the way for evaluating the influence of temperature on the selectivity towards light olefins, light alkanes, coke accumulation and coke quality. The results allowed us to determine the temperature at which the highest selectivity towards ethylene and propylene are consistently attained, as well as assessing the variation of ethylene-to-propylene ratio in the temperature range under study.

A hierarchical-type SAPO-34 was synthesized following an organosilane-directed method, a novel procedure recently introduced in microporous materials such as SAPO-34 (**Chapter 5**). The selection of this was based on the fact that it is easy to implement for large batches as required in our bench-scale study. The synthesized catalyst showed a higher performance, and so, the suppression of propane formation and carbon deposition (coke) was linked to the presence of physico-chemicals properties limiting secondary reactions.

Finally, the concluding remarks and recommendation of the present work are transmitted in **Chapter 6**. Furthermore, an outlook on the following steps to enhance the selectivity towards light olefins is presented.

Chapter 1. Literature review

1.1. Ethylene (C_2H_4) and propylene (C_3H_6)

Olefins can be defined as linear hydrocarbons having a double bond (C = C) and following general chemical formula C_nH_{2n}, where *n* indicates the number of carbon atoms. More importantly, the double bond confers to these species an ability to undergo a wide range of reactions. Consequently, olefins are key components in the modern petrochemical industry, in particular ethylene and propylene. They are required in the fabrication of a variety of polymers including PVC, polycarbonates, low-density (LD) and high-density (HD) polyethylene, polyurethane, nylon, polypropylene. They are also used to produce other commodities such as ethylene dichloride, ethylene oxide, propylene oxide, oxo-alcohol, acrylic acid and acrylonitrile [6,17,18].

Due to their wide range of applications, ethylene and propylene production has had a steady increase in the last decades. According to **Figure 1**, the average annual growth (worldwide) of ethylene production from 1995 to 2004 and from 2004 to 2010 were 5.15 and 4.71% respectively [1,19,20]. Similarly, propylene production increased by 4.40 and 9.05% from 1995 to 2004 and from 2004 to 2010, respectively [1,19,20]. Ethylene production displays an even evolution in the period under analysis, however, in the case of propylene, the larger olefin shows a drastic jump in the later period.

Eramo and co-workers [6] predicted that ethylene and propylene production would increase to 200 and 140 MMT/y, respectively by 2020. When analyzing the period from 2010 (record) to 2020 (predicted), ethylene production is expected to grow at a 3.27% annual rate, while that of propylene is expected to be at 3.42%. The lower values of growth rate obtained in this period are probably related to the slowdown of the world's economy. Nonetheless, the fact that these values maintain a positive balance indicates the expected expansion of the installed capacity for light olefins production.

According to the IHS (Information Handing Service) [21], an agency in the business of data collection, the raise in demand for ethylene and propylene are mainly driven by the polymer industry. Indeed, the ethylene demand in 2017 is expected to grow due to the use of polyethylene

as consumables, polyethylene terephthalate resins in fibers and packing items, and ethylene dichloride for PVC, which together account for 72% of the worldwide ethylene consumption [22]. Meanwhile in the case of propylene, polypropylene and its derivatives accounted for 64% of the total demand in 2014, and yet, these items are expected to consolidate their impact on the demand in the following years [23].

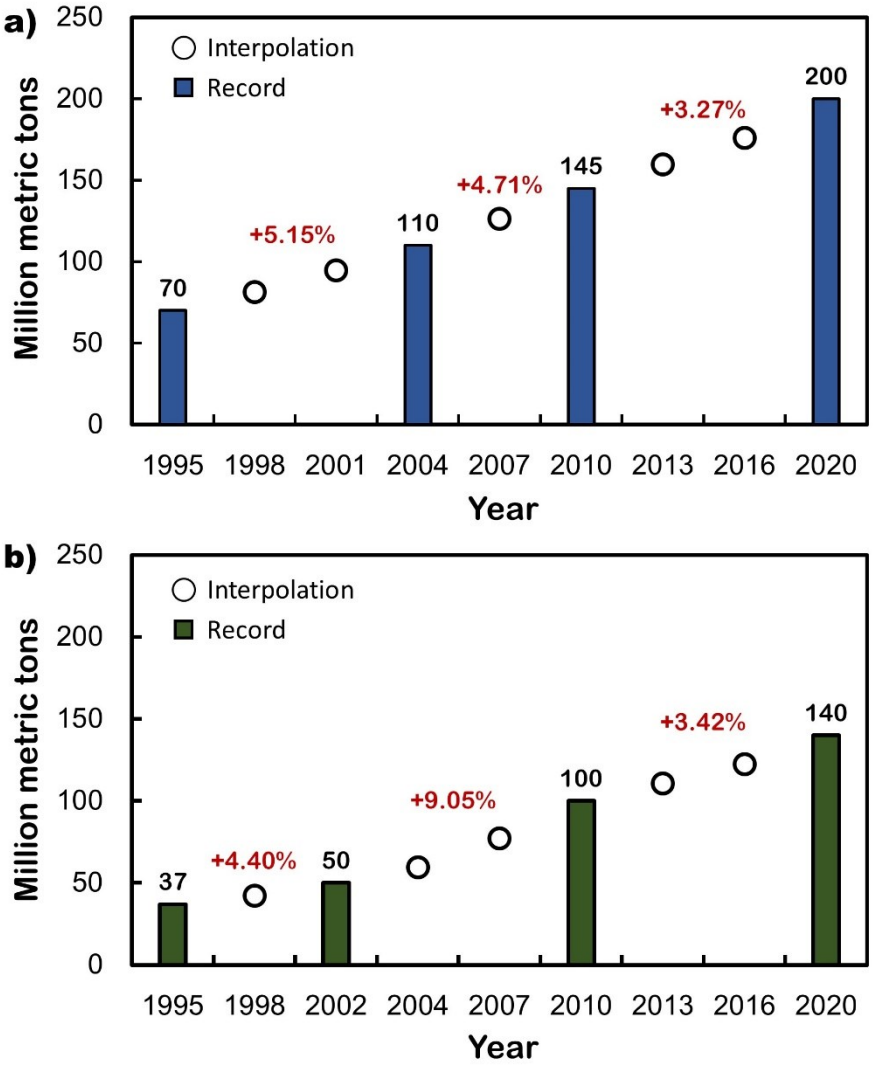

Figure 1. Annual production of ethylene (a) and propylene (b) in million metric Tons (MMT). The olefin production depicted in bar format corresponds to record values, while hollow points correspond to the interpolation between two record values. Out of the four record values presented for each olefin, those occurring before the year 2013 are past values, while the value in 2020 is a forecasted one.

1.2. Olefin production

Nowadays, ethylene and propylene are mainly produced by steam cracking of hydrocarbons (naphtha, ethane, gas oil and LPG) and fluid catalytic cracking (FCC) in oil refineries, and a to a lesser extent, via paraffin dehydrogenation [2]. These technologies however, present multiple disadvantages including low conversion of the feedstock to light olefins, a low flexibility on the ethylene-to-propylene ratio for a specific feedstock, and the generation of large amounts of carbon dioxide associated to the energy expenditure [2]. In a more detailed analysis, the ethylene present in the market originates basically from steam cracking, meanwhile, in the case of propylene, its production is divided in 60 to 65% steam cracking, followed by 30% FCC, and the rest is commonly distributed in metathesis and propane dehydrogenations processes [2].

Furthermore, one recurrent concern on the forecast of light olefins is that propylene cannot be produced in the amounts required to fulfill the demand without generating in parallel a surplus of ethylene, which ultimately could have a negative effect on price [2]. This disparity is largely caused by the booming of shale gas, which has increased ethane availability and, as shown in **Table 1**, this feedstock favors the production of ethylene over propylene 38-to-1 in a molar basis.

Table 1. Summary of the products yield distribution (wt.%) and ethylene-to-propylene ratio (EPR) resulting from the steam cracking of a particular feedstock [2]

Products yield, (Distribution in wt. %)	**Feedstock used**			
	Ethane	**Propane**	**Naphtha**	**Gas oil**
Ethylene	76	42	31	23
Propylene	3	16	16	14
C_4	2	5	9	9
Hydrogen	9	2	2	1
Methane	6	28	17	11
EPR* (molar)	38	4	3	2

*Ethylene to propylene ratio are based on molar values

To counter the overproduction of ethylene, different technological upgrades have been devised with the sole purpose of boosting the propylene production such as the Olefin Conversion Technology (OCT) developed by ABB Lummus [24]. In this technology, special units are implemented downstream of steam crackers and FCC reactors to transform ethylene, butenes and pentenes to propylene. A similar example is the Prolypur process created by Lurgi, while employing a catalyst developed by Sud-Chemie [25]. This process makes use of a fixed-bed reactor in which an olefin-rich stream is converted to propylene in the presence of steam. This technology has a propylene yield of up to 60% with regard to the feedstock weight, when integrated to an ethane steam cracking system.

Both technologies are based on the metathesis reaction, which involves the conversion of one molecule of ethylene and one of butene into two molecules of propylene (**Reaction 1**) [2].

$$C_2H_4 + C_4H_8 \rightarrow 2C_3H_8 \qquad \textbf{Reaction 1}$$

The most commonly used technologies for olefins production will be detailed in the following sections.

1.2.1. Steam cracking of paraffins

Steam cracking is a non-catalytic reaction in which high temperatures are employed to drive the break-down of saturated hydrocarbons (paraffins or alkanes) to smaller components. In the process, the high temperature cause the rupture of C–C and C–H bonds, which leads to the formation of unsaturated hydrocarbons (olefins or alkenes), and so, the selectivity towards ethylene, propylene and butenes can be tuned by adjusting the temperature and resident time [26]. A summary of the selectivity obtained in paraffin steam cracking using different feedstocks is presented in **Table 1**.

Originally, the process was developed for the use of a feedstock composed mainly of ethane and propane, similar to what is available in natural gas. However, due to price volatility, other fractions issued from petroleum oil have been employed, such as naphtha and gas oil [27]. In fact, naphtha has become the most important source for olefin production, accounting for up to

55% of the worldwide input in 2007, which is more than twice the amount produced from ethane (25%), the second most used alkane for olefins production [2].

Steam cracking is an energy-intensive process due to the highly endothermic reactions occurring inside the cracking unit and the high pressures required to favor the product yield. So, an important portion of the paraffin fed in the reactor is partially oxidized to deliver the thermal energy [28]. As example, an ethylene plant using ethane as feedstock traditionally exhibits a partial conversion of ethane to product around 50%, and so, the rest of the feedstock is consumed as fuel and released in the form of carbon dioxide [29]. Furthermore, high temperatures ranging between 750 and 900°C in the furnace, and up to 1100°C on the tube skin, lead to the generation of NO_X species, which causes the enforcement of environmental regulations [26].

1.2.2. **Fluidized catalytic cracking (FCC)**

The main goal of this process is the conversion of vacuum gas oil into gasolines. Nevertheless, olefins such as ethylene and propylene are produced as by-product, which explains the low selectivity for these species. In fact, the combined selectivity (C_2= + C_3=) is usually below 6.0 % with regard the feedstock weight (see **Table 2**) [2].

The FCC process uses a fluidized bed in which the catalyst particles are airborne by a high speed gas flow containing the feedstock. After deactivation, the catalysts particles must be recovered for combustion in a nearby regeneration unit [2]. Similarly to steam cracking, the process is energy intensive, requiring temperatures between 670 and 700°C [2]. In order to reduce energy consumption the FCC unit has been designed to reutilize part of the energy released in the regeneration chamber as a pre-heating source for the feedstock, as well as for the riser on top of the FCC reactor [2].

To increase the yield to olefins in the product stream, there have been two developments surrounding the FCC process. The first case is the Deep Catalytic Cracking process (DCC), which was crafted by the Research Institute of Petroleum Processing (RIPP) of SINOPEC to break heavy oils, such as atmospheric residues and vacuum gas oil, into olefins having three to five carbons in length. The process was developed in 1997 in Thailand, where the first

commercial unit was built after which multiple units have been put in operation in the following years. To enhance the selectivity for propylene, the process uses a zeolite H-ZSM-5 (*ZRP* in the patent [30]) as catalyst and employs milder conditions to those reported in FCC. A second technology is the Catalytic Pyrolysis Process (CPP), which is a second generation of the DCC (SINOPEC), which allows the reaction to take place at lower temperatures (< 450°C), and most importantly, the yield for ethylene was increased while keeping propylene at reasonable rates [2].

Table 2. Comparison of the product yield distribution obtained with the Deep Catalytic Cracking process (DPCC) and a conventional fluidization catalytic cracking (FCC) process [2]

Product yield (Distribution in wt. %)	**FCC**	**DCC**
Alkanes	7.3	12.7
Ethylene	0.8	6.1
Propylene	4.9	21.0
Butenes	8.1	14.3
Others*	74.3	39.3
Coke	4.3	6.0
Loss	0.3	0.6

[+]Includes: methane, ethane, propane and butanes
*Includes Naphtha, C_{5+}, light cycle oil and decanted oil

1.2.3. **Propane dehydrogenation (PDH)**

In this process, propane is selectively dehydrogenated to develop polymer-grade propylene gas. This technology has received much attention due to its simplicity as a single feed/single product feature. Nevertheless, despite its relatively simple chemistry, its industrial application has been limited in great part due to the side reactions occurring such as deep dehydrogenation, hydrogenolysis, cracking, polymerization and coke formation. Another limiting aspect in PDH is the low conversion associated with the thermodynamic equilibrium, which is combined with the necessity to minimize side reactions [31].

Despite the limitations stated above, the continuous breakthrough on catalyst design and process configuration has allowed the development of three commercialized PDH technologies: the CATOFIN PDH process licensed by Limmus Technology, the Oleflex PHD process licensed by UOP and the STAR PHD process with oxydehydrogenation licensed by ThyssenKrupp Uhde [31].

The dehydrogenation process can also be applied to ethane, however, because of the abundant production capacity and lower capital investment in ethane steam cracking, commercial systems are currently not available. However, Union Carbide has investigated a process for the catalytic oxidative dehydrogenation of ethane to ethylene, called *Ethoxene*, which also produces a substantial amount of acetic acid, which ultimately could render the process economically competitive [32].

1.2.4. The methanol route (MTH and MTO)

The technology behind the conversion of methanol to hydrocarbons was originally conceived to produce gasolines from coal or natural gas, the latter known as Gas-to-Liquid (GTL) process [1]. The application of methanol in the synthesis of fuels was in part triggered by the ban imposed on methyl tert-butyl ether (MTBE) as gasoline additive in the US, which caused a surge in methanol availability in the market [33]. The industry saw this scenario as an opportunity to explore new alternatives, since methanol had previously shown to be convenient as building block in the manufacture of known commodities, including formaldehyde and acetic acid [33].

The production of light olefins from methanol started in 1977 at a Mobil's research facility, where, according to Chang and Silvestri [34], Mobil scientists working on unrelated projects discovered accidently the generation of hydrocarbons from methanol (MTH) over a recently developed synthetic zeolite, ZSM-5 (*Zeolite Socony Mobil*). Later studies using pure methanol demonstrated that the catalyst was capable of achieving a full methanol conversion with an overall reaction stoichiometry as follow:

$$2\,CH_3OH \leftrightarrow CH_3OCH_3 + H_2O \rightarrow light\ olefins$$
$$\rightarrow higher\ olefins + paraffins + aromatics + naphthalenes + H_2O$$

Moreover, researchers discovered that by lowering the contact time, it was possible to limit the formation of gasolines, and instead light olefins could be favored (see **Figure 2**).

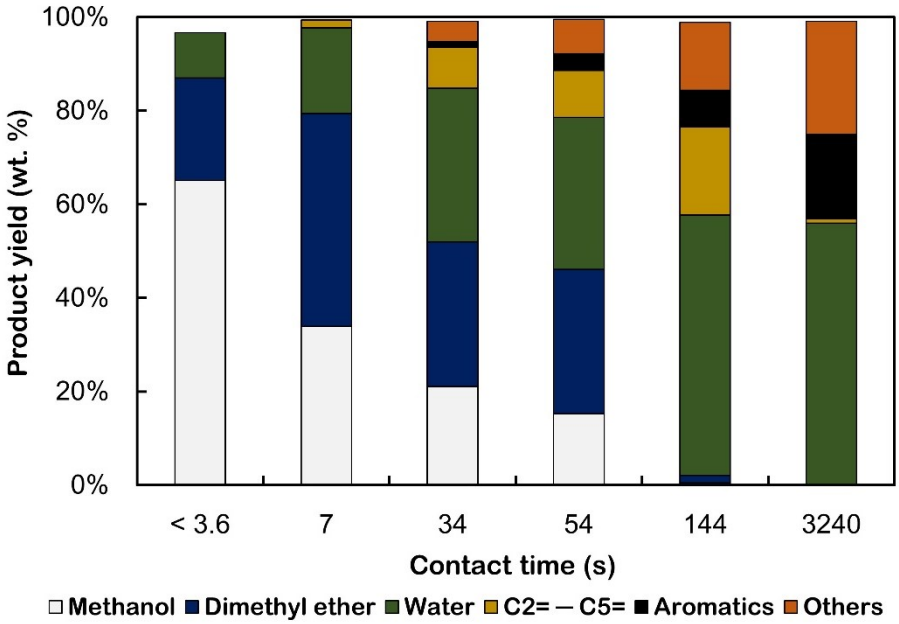

Figure 2. Effect of the contact time on the product yield distribution (wt. %) in the conversion of methanol to hydrocarbons (MTH) over a conventional H-ZSM-5 [3]. Products include oxygenated molecules (methanol and DME), olefins with 2 to 5 carbons and aromatic molecules, while saturated hydrocarbons (alkanes) and large olefins having six or more carbon atoms are presented as "others".

The oil crisis in 1973 and 1978 triggered the development of Methanol-to-Gasoline units in different parts of the world. For instance, Mobil worked with the government of New Zealand in the development of a pilot-scale plant for the production of gasolines from natural gas (Gas-to-Gasoline), using a fixed-bed reactor with a production capacity of 640 L/day. In 1980, they developed the ICI low-pressure methanol process (commercial scale). The plant converted natural gas to methanol, which was then transformed to gasolines at a rate of 570,000 Tons/day. This technology as well relied on a fixed-bed reactor system, and the generated fuel did not require further refining since the quality obtained was comparable to that seen in unleaded gasoline. From 1981 to 1984, Mobil, Union RBK and Uhde developed the first fluidized-bed MTG demonstration plant in one of RBK facilities in Germany. In 1986, Union Carbide developed its own process (fluidization system) using a silicoaluminophosphate (SAPO) as catalyst, and olefins yield could reach 90% in weight.

The drop in oil prices during the 80s reduced the interest in further investigation and the launching of other industrial-scale plants, though bench scales studies continued as part of research which led to a booming in patent submissions [33].

1.2.4.1. Fixed-bed and fluidized-bed MTG (Mobil)

The first version of the MTG (methanol-to-gasoline) reaction developed by Mobil relied on reactors presenting a fixed-bed configuration (see **Figure 3**) [33]. This choice caused complications in the control of the temperature due to the exothermal nature of the reaction. To overcome this problem, the process was split in two stages: one in which methanol was transformed into DME and water, releasing between 15 and 20% of the reaction heat, and a second stage, where a solution of methanol, DME and water was converted into hydrocarbons. For the first stage, alumina was employed as catalyst between 310 and 320°C, and the DME effluent stream was mixed with a recycle gas to regulate the temperature, which was then fed to the second reactor. The latter was packed with a zeolite (ZSM-5) and the inlet temperature fluctuated between 350 and 370°C. After reaction, the stream was separated into three phases: gas, liquid water and liquid hydrocarbons. The liquid water contained traces of unreacted methanol and DME, and so, it was sent for biological treatment. The liquid hydrocarbon was composed of gasolines, dissolved hydrogen, carbon dioxide and light hydrocarbons (C_1-C_4). Finally, the gas phase, which was constituted of light hydrocarbons, was recycled to the second stage to produce more gasolines. During reaction, the catalyst underwent aging, which caused changes in product distribution over time-on-stream, in addition to a loss of activity related to temperature degradation induced by the regeneration cycles [33].

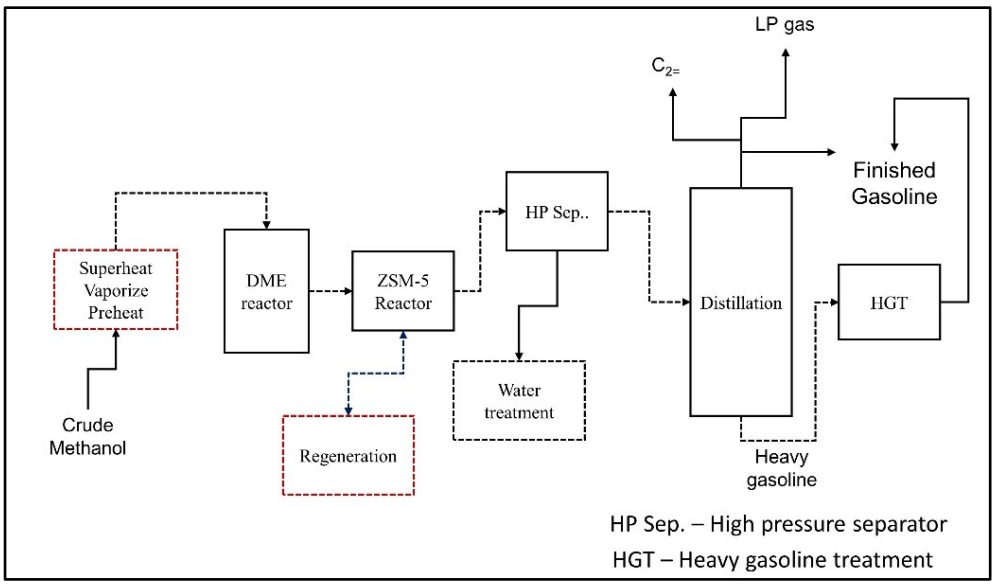

Figure 3. Block diagram of the fixed-bed MTG process developed by Mobil [33].

With the experience obtained in the first version, Mobil developed the fluidized-bed MTG process (see **Figure 4**) having as positives features the reuse of the heat in the reactor for steam generation, continuous regeneration of the catalyst, uniform bed temperature, uniform and stable temperature transition associated to the heating and cooling of the reactor, a higher specific feedstock input, a higher octane and a higher gasoline yield [33].

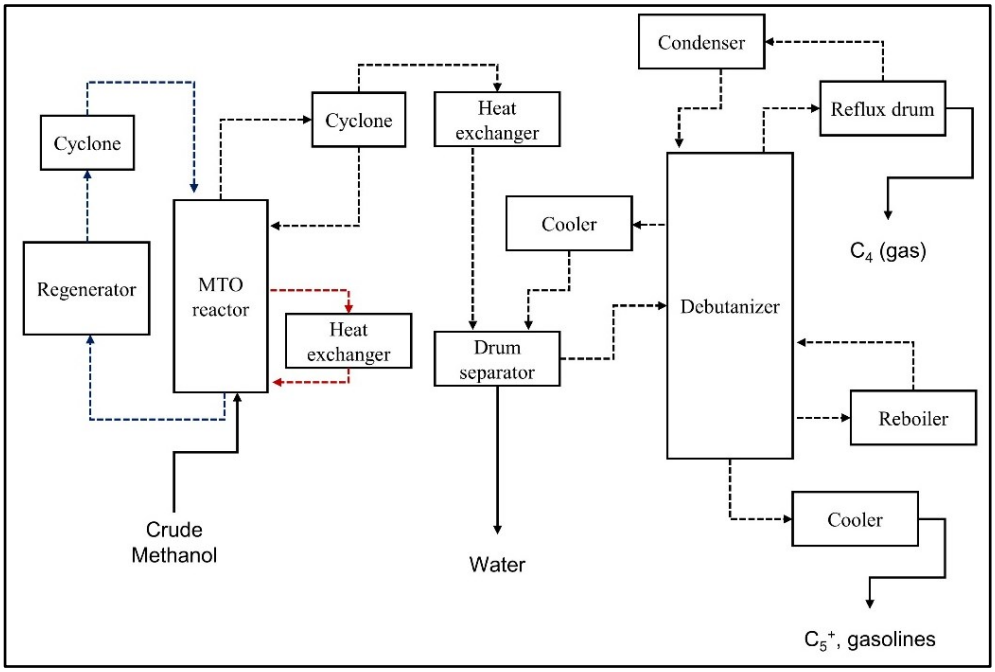

Figure 4 . Scheme of the Mobil MTG demonstration plant (2nd generation) using a fluidized-bed reactor [33].

The aqueous solution fed in both Mobil systems consisted of a synthetic crude methanol blend containing 83 wt% methanol (commercial, pure) and 17 wt% distilled water. This is a typical water content found in crude methanol made from natural gas, so by using this solution as feedstock, the purification process could be avoided to reduce capital and operational costs [33].

1.2.4.2. UOP/Hydro MTO process

This process has a high yield in ethylene (48%) and propylene (33%) while using an attrition-resistant SAPO-34. The flowchart of the process is presented in **Figure 5** [33]. The process uses two fluidized-bed reactors, one for the MTO reaction and another for the regeneration of the catalyst. In the latter, coke is burned out to generate steam for heat integration. The effluent gas goes through a purification train that includes a CO_2 caustic scrubber, a de-methanizer, a de-ethanizer, a C_2 splitter, a C_3 splitter, and a de-propanizer. The purification process delivered a gas mixture composed of ethylene and propylene appropriate for polymer synthesis.

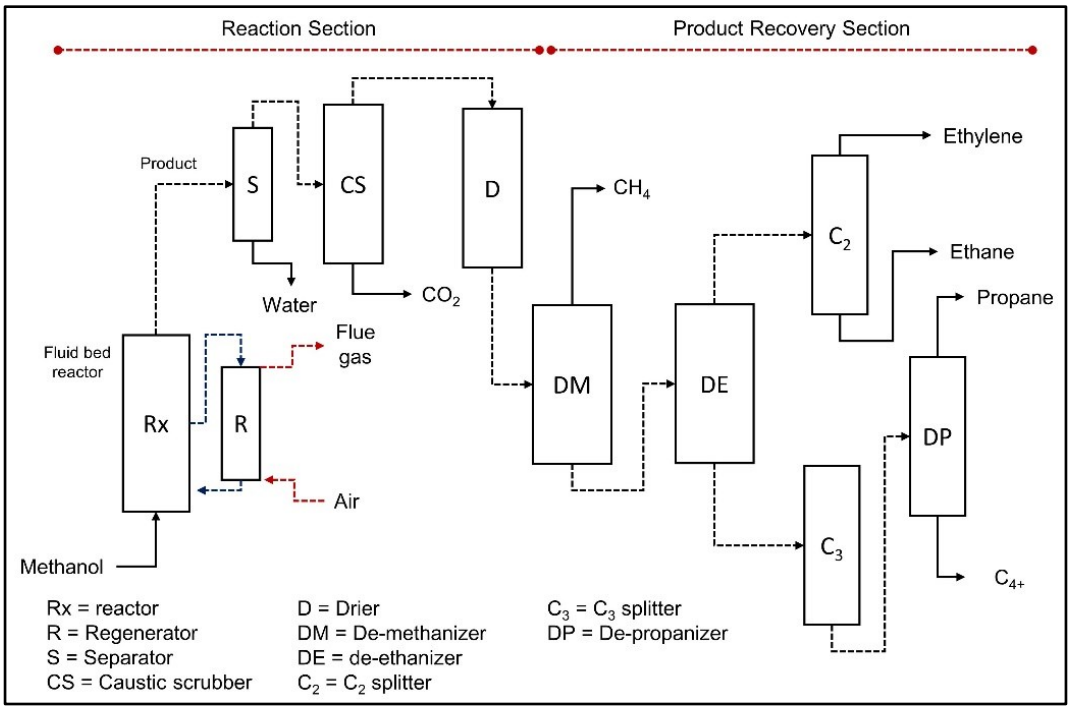

Figure 5. Scheme of the UPO/Hydro MTO process for the production of polymer-grade olefins [33].

In a subsequent paper about the recent advancements on this technology, the carbon selectivity for ethylene and propylene was said to have been enhanced by introducing an olefin cracking (OC) unit [35]. This unit targeted the cracking of heavier olefins and achieved an 80% reduction

in C_4 by-products and 20% increase in light olefins. The combined processes, MTO and OC, presented a great flexibility, and so, the propylene/ethylene ratio was possible to be enhanced to values above 2.

1.2.4.3. Shenhua group MTO process

This process is the last MTO system developed in recent years and was accomplished by the Shenhua group in Baotou, North China. Multiple research centers helped develop this process, including the National Engineering Laboratory for Methanol to Olefins, the Dalian National Laboratory for Clean Energy and the State Key Laboratory of catalysis, residing in Dalian China. (see **Figure 6**) [36]. The process presents many similarities with that of UOP/Hydro since both look to produce polymer grade olefins using a similar feedstock. It is composed of an MTO reactor, a regeneration chamber and a purification train that allows the recovery of larger hydrocarbons to be sent to a cracking unit to further enhance the yield of light olefins.

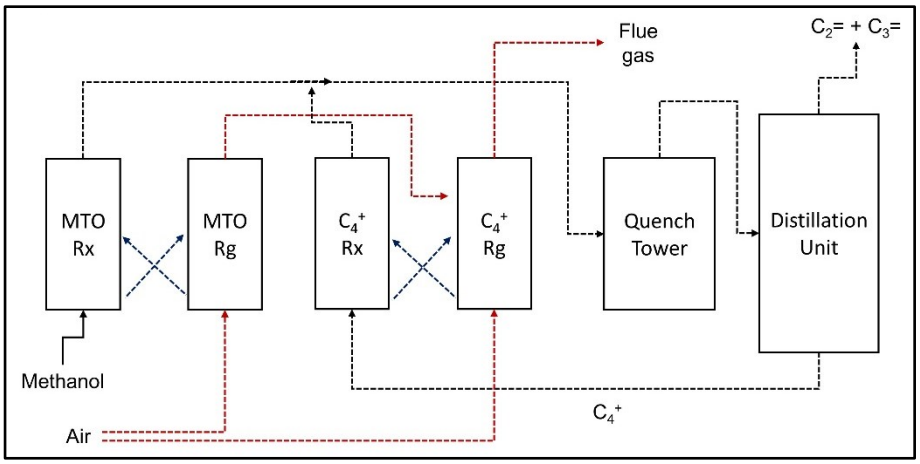

Figure 6. Scheme of the MTO demonstration plant developed by the Shenhua group in China [36].

1.3. Catalysts in the MTO reaction.

The conversion of methanol to olefins relies mainly on microporous acid catalysts including zeolites and silicoaluminophosphates (SAPO). Zeolites, for the most part, were first tested following a trial-error procedures, seeking to identify the characteristics and conditions required for developing processes stable during long periods [37].

Zeolites (from Greek, *zein* "to boil" and *lithos* "a stone") are solid acid used as catalysts and composed solely of Aluminum (Al) and Silicon (Si) assembled in a tetrahedral configuration

TO_4 (T represents the metal atom). In this crystal organization, the oxygen atoms surrounding the metal atoms work as bridges linking different tetrahedral units (TO_4). The latter creates a periodic complex porous structure displaying openings and cages with diameters ranging between 3 and 14 Å (framework density < 20 T/1000 $Å^{-3}$). Their activity stems from the Bronsted acid sites (Si-OH-Al) which result from the charge unbalanced residing on the oxygen atom connecting the Al (3^+) and Si (4^+) atoms. The synthesis of zeolites at laboratory scale was first achieved during the 40s and 50s, creating initially low Si/Al ratio zeolites (high acidity), followed by high Si/Al ratio zeolites (low acidity), and lastly pure SiO_2 molecules sieves (neutral) [37].

In the case of SAPOs, their fabrication started with the development of aluminophosphate molecules sieves ($AlPO_4$), which provided a new set of intrinsic properties. Nonetheless, they were deprived of acidity thus unable to undergo any type of reaction. To this purpose, researchers integrated a silicon substitution procedure, where phosphorus atoms (5^+) were exchanged with Si atoms (4^+), leaving behind a negatively charged framework. The latter was passivated by an organic molecule (usually an amine) and the recovered precipitate was calcined to generate a Bronsted acid site, as in zeolites. This new synthesis method added flexibility to the composition and properties of the catalyst, as other metals including Co, Ni, Mg, Fe, etc., in addition to Si, could be used (MeAPO) [38].

About 176 framework types are reported in the International Zeolite Association (IZA) database. The following sections will describe the two catalysts that have shown the best catalytic performance in the conversion of methanol to hydrocarbons: SAPO-34 and ZSM-5 [17,39].

1.3.1. **ZSM-5**

ZSM-5 (standing for *Zeolite Sonony Mobil-5*) is largely the most versatile zeolite employed in the transformation industry nowadays. Indeed, Tanabe and co-workers reported that out of the 71 industrial processes that employ zeolites, 31 had ZSM-5 as the main component of their catalyst [40]. ZSM-5 is composed solely of Silicon and Aluminum atoms (aluminosilicate) and displays an orthorhombic structure, characteristic in MFI. The ideal chemical formula is $Na_nAl_nSi_{96-n}O_{192} \times 16H_2O$, where n ranges between 0 and 27 (but typically close to 3). As in

other zeolites, the Si/Al ratio plays an important role in the physico-chemical properties of ZSM-5, which govern its reactivity and performance [15].

ZSM-5 is constituted by two perpendicularly-interconnected channels system: one displaying a zig-zag pattern, running along the crystal plane [100] and having semi-circular openings with dimensions *5.4 × 5.6 Å*; while a second system displays straight channels, with elliptical opening and with dimensions *5.1 ×5.5 Å*. A graphical description is shown in **Figure 7**. It has been suggested by Froment and co-workers that Bronsted acid sites reside at those intersections characterized by square openings ca. 9 Å [41].

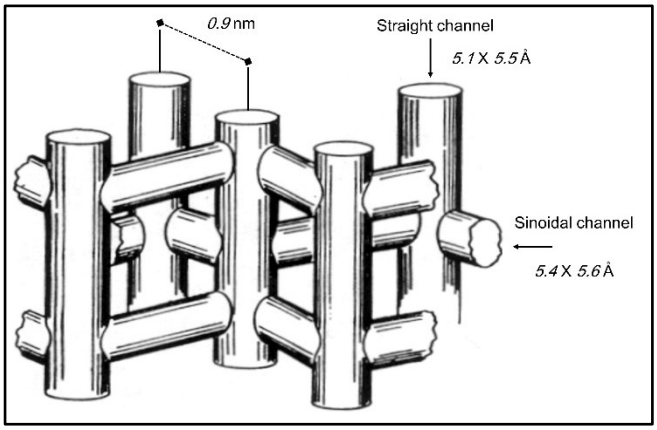

Figure 7. View of the ZSM-5 pore dimensions and channel system configuration [42].

1.3.2. **SAPO-34**

This zeo-type was developed and first reported in literature by Union Carbide Corporation in the 80s [43]. SAPO-34 is a cage-type, small-pore solid crystal, presenting a rhombohedral symmetry which induces the formation of cubic-like particles, as shown in **Figure 8A**. Its chemical formula is $(0\text{-}0.3)R \times (Si_xAl_yP_z)O_2$, where *R* represents the tetra-ethyl ammonium ion template, and *x*, *y* and *z* are parameters with values ranging from 0.01 to 0.98, 0.01 to 0.60 and 0.01 to 0.52 respectively, according to the equation x +z +y = 1 [43]. Its internal structural display a Chabazite (CHA) framework composed of double six-membered rings stacked in an ABCABC configuration (see **Figure 8B**). This arrangement leads to the formation of semi-circular pore openings *3.8 X 3.8 Å* in dimension and cages around *11.0 X 6.5 Å* (see **Figure 8C**). The latter are interconnected to each other through six elliptical eight-membered rings (see **Figure 8D**), which ultimately leads to the assembly of a three-dimensional channel system [44].

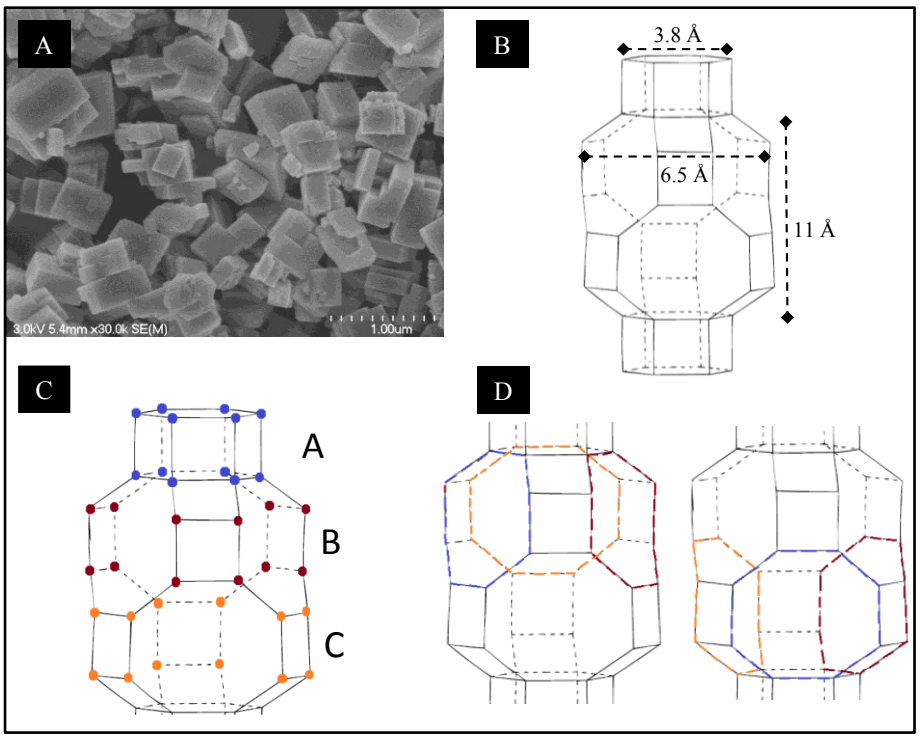

Figure 8. SAPO-34 crystal structure: Scanning Electron Microscope (SEM) of SAPO-34 (A), SAPO-34 pore and cage dimensions (B), SAPO-34 plane stacking ABCABC (C), and cage interconnection (D).

1.4. Methanol-To-Olefins (MTO) mechanism.

The study of the mechanism governing the MTO reaction can be separated historically in two stages. One corresponding to the early stage consecrated to elucidating the formation of the first C-C bond, also referred as direct mechanism. A second stage originated from the identification of polymethylbenzenes as the molecules responsible of the indirect conversion of methanol to olefins. The latter is referred as the "*hydrocarbon pool mechanism*", which is considered as the most valid explanation for the MTO reaction nowadays. The two mechanisms will be discussed in the following sections.

1.4.1. The direct mechanism: formation of the first C-C bond.

The mechanism involved in the conversion of methanol to olefins over zeolite and zeo-type catalysts has been extensively investigated over the past 30 years. It is believed that the reaction starts with the conversion of methanol to dimethyl ether, as show in **Figure 9**.

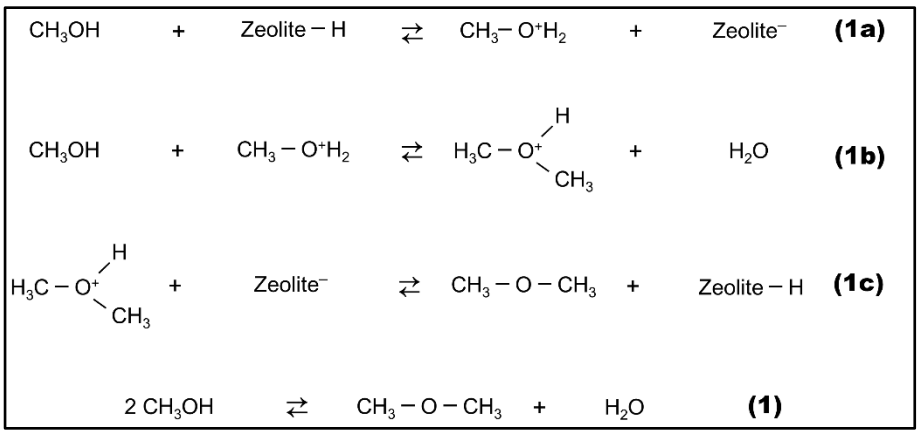

Figure 9. Reaction steps on the dehydration of methanol to dimethyl ether over zeolites

According to this mechanism, dimethyl ether (DME) of formula CH_3-O-CH_3 is formed through a successive set of reactions (driven by thermodynamic equilibrium) involving the protonation of a methanol molecule by a Bronsted acid site (1a) followed by the formation of a binary transition-state molecule (1b). This reaction also causes the release of a water molecule. Finally, DME is formed in parallel with the re-protonation of the acid site (1c).

In zeolites presenting medium-size (i.e. H-ZSM-5, d_{pore} = *5.5* Å) and large-size cavities (i.e. Faujasite, d_{pore} = *12.0* Å), thermodynamic equilibrium is reported to be attained. However, in the case of SAPO-34, the narrow dimensions and fast accumulation of coke have been found to restrict the diffusion of DME, which instead leads to a low conversions to DME [45]. It is important to emphasize that the dehydration reaction does not lead to the first C-C bond. Nonetheless, its occurrence illustrates that both molecules (methanol and DME) can be considered equally valid as the initial molecule for the formation of olefins and other hydrocarbons.

With this knowledge, extensive efforts were made to determine the mechanism to form the first C-C bond using methanol or DME as precursor. More than twenty mechanisms have been proposed, such as carbene mechanism, oxysonium ylide mechanism, carbon-cation mechanism, free radical mechanism, etc. However, in later theoretical calculation studies, these hypothesis were shown to be substantially restricted by high energy barriers, and so, a consensus was never reached [3,18].

1.4.2. The "*autocatalytic*" mechanism

The transition from direct to indirect mechanism required a set of milestones that revealed the existence of an autocatalytic process operating within the catalyst pores. For instance, Dessau and co-workers [46], based on experiments using isotope labelling, proposed a mechanism for H-ZSM-5 indicating that direct mechanism could be relevant in the early stage. However the formation of light and heavy olefins was deduced to result from the combination of chain growth and cracking processes. More importantly, aromatics were considered to be formed in series from olefins composed of six carbons, as a final product with no participation in any catalytic cycle (see **Figure 10**) [46].

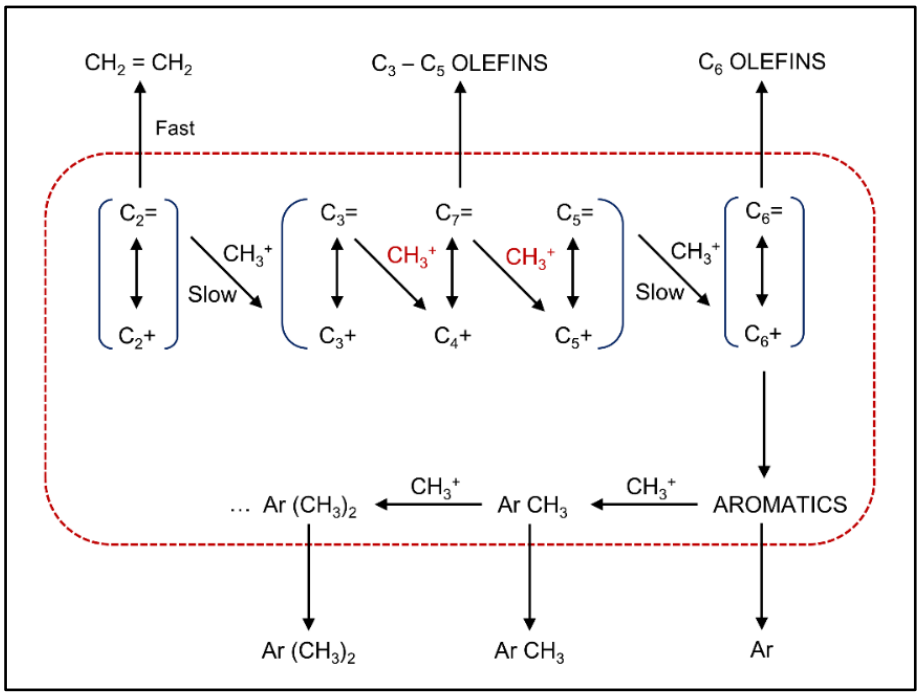

Figure 10. Scheme of the autocatalytic MTO mechanism based on successive methylation and cracking reactions as proposed by Dessau and co-workers [46]. Methyl groups (CH_3^+) are fed into the system via a methanol dehydration process occurring in parallel.

The first attempt to depict the molecules responsible for this autocatalytic behavior came from the work of Mole and co-workers [47]. In their work, methanol was fed in parallel with toluene and cyclohexene, and so, they discovered that both aromatic molecules reduced the induction period, indicating a possible co-catalyst effect caused by these cyclic species. Moreover, this finding suggested that the direct mechanism was not relevant in the late period, where the steady

and fast formation of hydrocarbons was attained. Hence, their conclusions partially supported those obtained by Dessau's research group.

1.4.3. The "*hydrocarbon pool*" mechanism.

In the 90s, Dahl and Kolbe co-fed methanol with isotope-labelled ethylene (co-feeding ethanol) and propylene (co-feeding propanol) to evaluate the importance of olefin chain growth and cracking in the MTO/SAPO-34 system [48,49]. Their results revealed that these processes were not relevant in the formation of ethylene, propylene and butenes, and so, they concluded that a pool of adsorbed species (mainly aromatic-like molecules based on its CH_2 composition) underwent a catalytic cycle in which methanol was being consumed and hydrocarbons, including olefins, paraffins and aromatics were being released (see **Figure 11**).

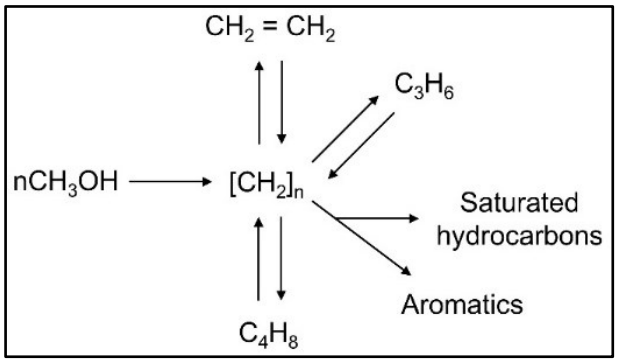

Figure 11. Scheme of the MTO "*hydrocarbon pool*" mechanism as proposed by Dahl and Kolbe [3]. In parallel to the MTO reaction, water is produced from the dehydration of methanol.

These findings led Dahl and Kolbe to propose the "hydrocarbon pool" mechanism as a new experimental and theoretical framework that considered that both oxygenated species, methanol and dimethyl ether, underwent transformation through aromatic molecules trapped within the solid cages and channels. They hypothesized that these aromatic molecules behaved as a scaffolding for the synthesis of light olefins to avoid the unfavorable energy intermediates required in "direct" mechanisms [3].

In subsequent studies, Kolboe and Arstad identified polymethylbenzenes as the "*reaction centers*" orchestrating the indirect mechanism in H-SAPO-34 [50,51], which was later supported by Song and co-workers who used NMR spectroscopy [52]. Other molecules, including polymethylnaphtalenes, were also identified as hydrocarbon pool species (HCP), and

so, researchers concluded that the nature of the molecule depended on multiple factors such as acidity, pore dimensions, as well as reaction conditions [36,53,54].

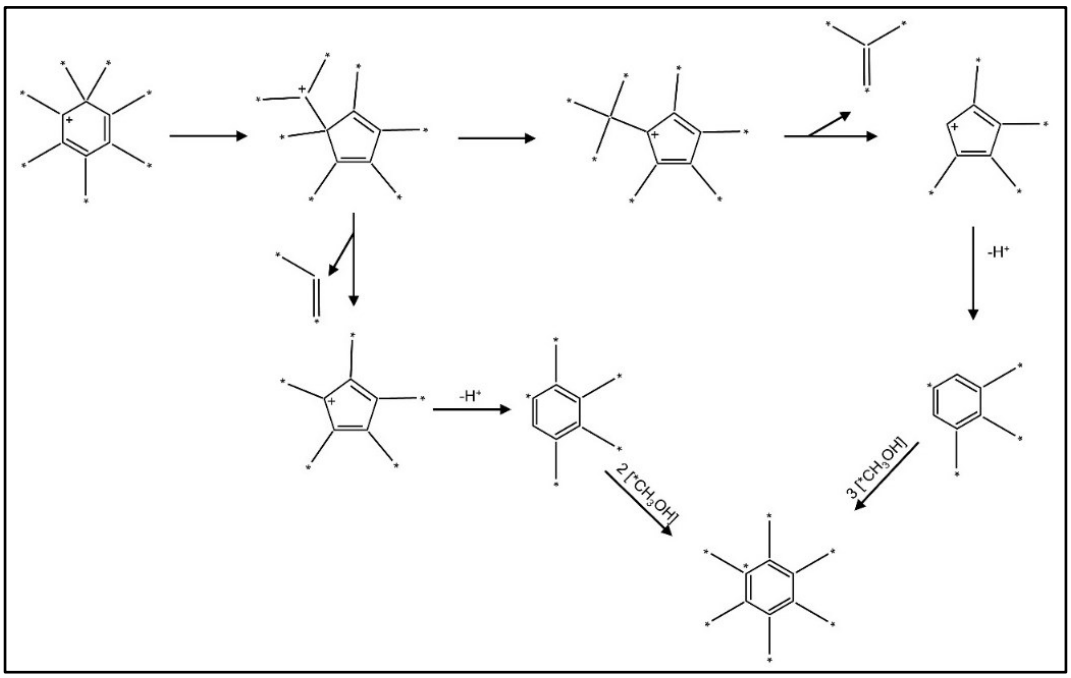

Figure 12. Scheme of the paring reaction leading to the formation of propylene and/or isobutylene from hexamethylbenzenium cation by a ring contraction [55].

Two polymethylbenzene-mediated mechanisms were suggested for the production of olefins. The first was a combination of ring contraction and expansion, leading to methyl exocyclic growth (growth of a methyl chain attached to a cyclic molecule). This process was called "*paring*" and was first reported by Sullivan and co-workers for explaining the release of isobutene from hexamethylbenzenium cations (see **Figure 12**) [56]. A second process, referred as "*side chain*" growth, originated from the work of Mole and Haw, in which olefins such as ethylene and propylene were explained to be formed from the exocyclic alkylation of heptamethylbenzenium cation (see **Figure 13**) [57].

The main difference between the early-conceived autocatalytic mechanism by Dessau and the "*Hydrocarbon pool*" was that the former considered aromatic species as reaction products and coke precursor, occurring in successive steps, while the latter considered polymethylbenzenes

as intermediates trapped in the micropores of the zeolite, undergoing a "*regenerative*" catalytic cycle to produce olefins.

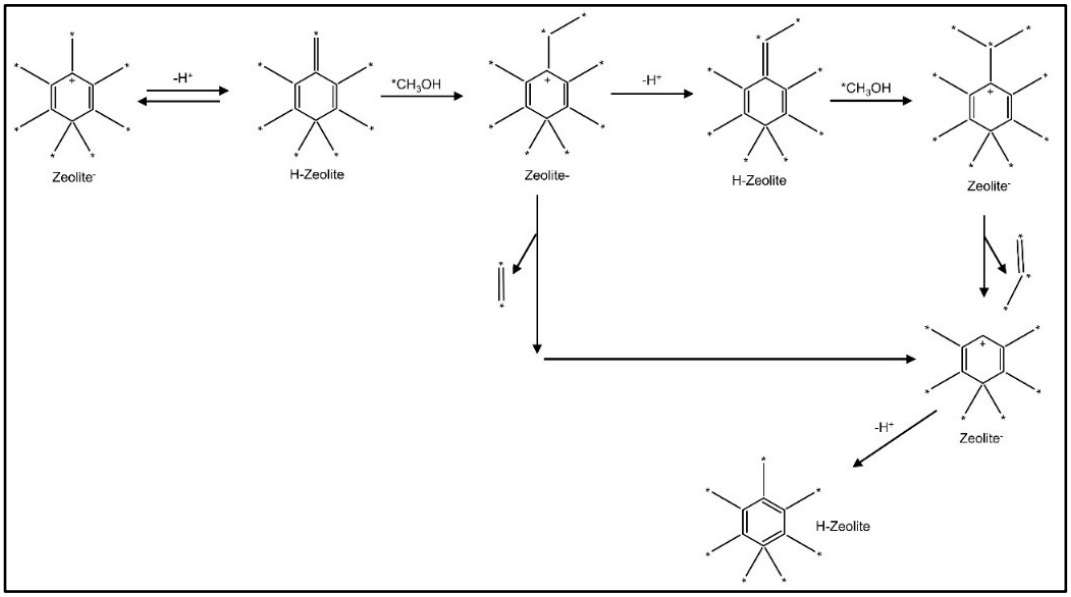

Figure 13. Scheme of the exocyclic methylation reaction forming ethylene or propene from a Heptamethylbenzenium cation [55].

With the arrival of more powerful computers and software on transition-state theory simulation, research groups have enriched their respective work with DFT calculation to compare the theoretical work with experimental data. For instance, experimental work combining different techniques such as pulse methanol injections, low temperature and isotopic methanol switching (^{12}C to ^{13}C) have identified pentamethylbenzenium and hexamethylbenzenium cations as the most "active" trapped molecules in H-SAPO-34 [50–52]. Different research groups have used these molecules as reference to conceive low-energy reaction paths to explain observables values such as ethylene and propylene selectivity, as well as the fast swap of labelled carbon [58].

1.4.4. The "*dual cycle*" mechanism.

The dual mechanism is a recent concept, enclosing former studies, that considers that the MTO/MTH process is influenced by two type of reaction mechanisms: aromatic and olefin types [36, 131].

Aromatic-based reactions corresponds to those involved in the "*hydrocarbon pool*" mechanism, in which methyl groups, from methanol, cause the full methylation of the benzene ring (aromatic methylation) and lead to the release of olefins either by "*paring*" or "*side-chain*" cycles (aromatic de-alkylation). Concurrently, olefins-based reactions are considered to be relevant and these include: olefin methylation (via methanol), olefin cracking and cyclization. Hydrogen transfer reactions occurs as well and they lead to the formation of hydrogen-poor components such as aromatics and hydrogen-rich molecules such as light alkanes [36, 131].

The advent of the dual cycle has improved the understanding of the relation between the internal topology (dimension and shape) of the catalyst and the dominant reactions (aromatic and/or olefin type) occurring in the catalyst. For instance, SAPO-34, which presents a CHA framework with 8-membered atoms pore (8-MR), is known to hinder the diffusion of molecules larger than four carbon atoms (linear case, n-butane). These molecules are formed in the 12-MR cages, and so, aromatic reactions are well-known to be the dominant ones. Meanwhile, ZSM-5, which displays an even 10-MR structure along its internal topology, allows both aromatic and olefin reactions to occur [36, 131]. Nevertheless, the active aromatic molecules in ZSM-5 differ from those in SAPO-34 and H-Beta, which present large cages (12-MR). For these two, hexamethylbenzenium cation (benzene with six methyl groups) has been identified as the most active molecule for the production of ethylene and propylene. Meanwhile, trimethylbenzene or smaller aromatic molecules (i.e. Toluene) are the ones active leading to the formation of the ethylene in ZSM-5 [45].

1.5. The MTO reaction network and formation of coke

The conversion of methanol to olefins in SAPO-34 leads to the production of different species including olefins, saturated hydrocarbons and aromatics. The olefin mixture is mainly constituted of ethylene and propylene, followed by butenes, and to a minor extend, pentenes and hexenes (less than 5% of the carbon input) [59]. The saturated mixture may include methane, ethane, propane and butanes, nonetheless, methane and propane are usually the only paraffins reported by researchers due to their high concentration which may be comparable to those of light olefins, depending of the reaction conditions. Finally, aromatic molecules are

retained within the narrow pores of the catalyst and whose mixture composition includes polymethylbenzenes and polycyclic aromatics.

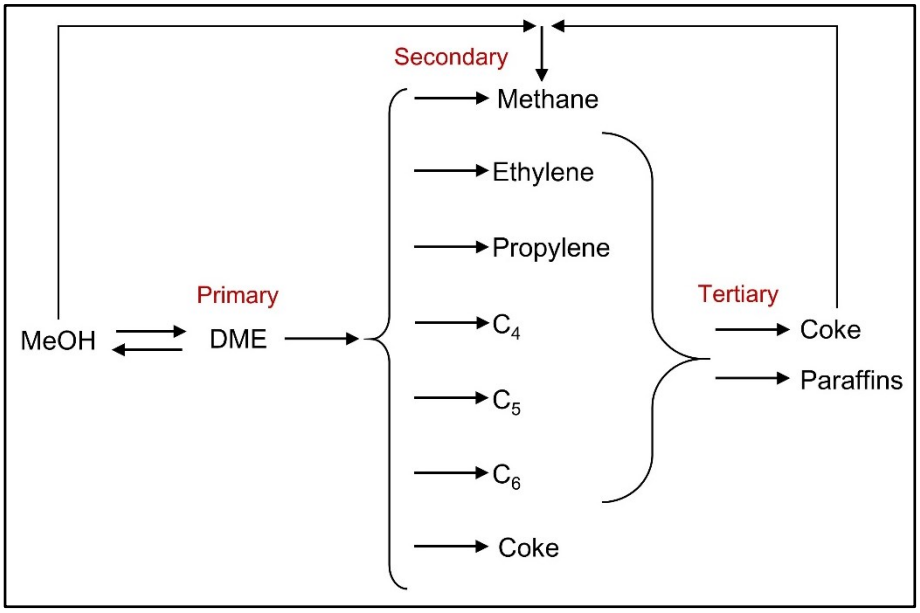

Figure 14. Reaction network of the MTO reaction over SAPO-34 as proposed by Chen and co-workers [60].

The "*order*" of the species listed above was investigated by Chen and co-workers [60–62]. The "*order*" determines whether a species results from the direct conversion of methanol or from the conversion of primary and/or secondary products, and to this purpose, the authors used an oscillating microbalance catalytic reactor in which methanol was injected in pulses to control its conversion.

A summary of the identification of the order is presented in **Figure 14**. As shown, olefins (C_2-C_6) were found to be stable products, in which reactions such as methylation and cracking were not relevant for their formation once the reaction had overcome the induction period (formation of HCP species). Moreover, the limited amount of olefin produced at low methanol conversion was indicative that these species were secondary in *"order*". In contrast, saturated hydrocarbons such as ethane and propane were observed only at high methanol conversion, and so, these were categorized as tertiary products stemming from olefin secondary reactions. In the case of coke and methane, the authors found that these were observed in a wide range of methanol conversion, still far from conversions close to zero, and so, these were considered to behave as secondary and tertiary products. In the study, DME was the only species detected at conversions

close to zero, and so, it was identified as a primary product that originated from the direct dehydration of methanol.

In a more recent review on the MTO reaction over SAPO-34, Tian and co-workers reported a brief reaction network indicating that the reactions leading to coke could be categorized as driven by aromatic or olefins molecules (see **Figure 15**) [36]. Luo and co-workers studied the MTO reaction in a catalyst bed, which was divided in multiple sections with the objective to correlate the qualitative analysis of the coke and bed position [63]. Their results showed the presence of two types of coke, one capable to produce olefins residing close to the reactor entrance, and an inactive one accumulating in the posterior sections of the catalyst bed.

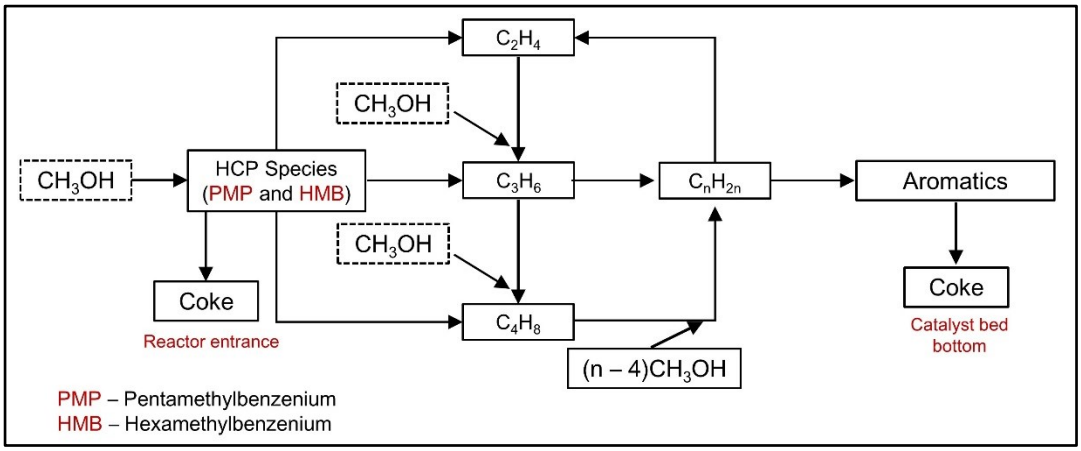

Figure 15. Reaction network of the MTO reaction over SAPO-34 as proposed by Tian and co-workers [36].

1.5.1. **Shape selectivity due to coke accumulation**

As described previously, the conversion of methanol to olefins also involves (and requires) the formation of carbonaceous species referred as "*coke*". For SAPO-34, these carbonaceous species include active molecules in the MTO reaction such as polymethylbenzenes [52], less active ones like polymethylnaphthalenes [64], and inactive polycyclic aromatics (i.e. anthracene, phenanthrene and pyrene) [63,65]. More importantly, coke molecules play a key role in both selectivity and deactivation, not only because polymethylbenzenes catalyze the reaction, but also due to the physical constrains these voluminous molecules can impose on species mobility within the catalyst pores [66,67].

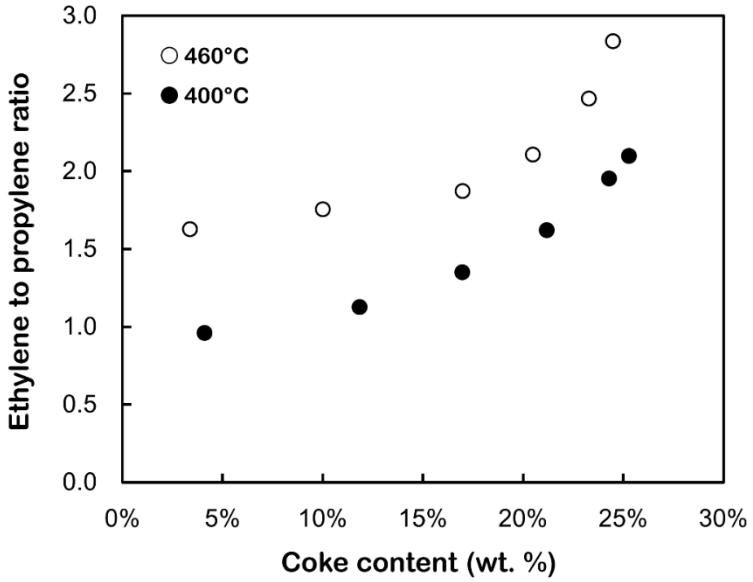

Figure 16. Effect of coke content on the ethylene-to-propylene ratio during the conversion of methanol to olefins over a SAPO-34 [65].

Changes in selectivity arising from this physical constraint are referred as "*shape*" selectivity, and can be categorized as reactant, intermediate (transition-state) or product type, depending on the molecule being affected [68]. For instance, reactant selectivity happens when the pore dimension limits the entrance of certain species. An intermediate type occurs when the geometry and dimension within the pores restrict the formation of a particular transition-state species (prior to the formation of the products). A product selectivity takes place when molecules formed within the pores are not capable of diffusing out of the catalyst [61]. There has been a controversy regarding the type of shape selectivity governing the MTO reaction over SAPO-34. Nonetheless, product selectivity has been considered more adequate to explain the surge of selectivity to ethylene as coke content is increased, and so, limiting the exit of other larger hydrocarbons (see **Figure 16**).

Since the selectivity to light olefins can be enhanced due to coke obstruction, some MTO systems are operated to maintain a relatively "*high*" coke content in their catalyst, by adjusting the residence time in the MTO reactor and regeneration unit. For instance, Tian and co-workers showed that the highest combined selectivity towards ethylene, propylene and butenes was achieved at a coke content close to 8.0%, which was only a couple of percentage less before observing a sudden drop in the catalyst activity (≈10.0%) [36].

1.5.2. Factors influencing the rate of coke deposition

The following section focuses on those parameters affecting the catalytic formation of coke, namely, aromatic molecules stemming from the "*hydrocarbon pool*" mechanism. The non-catalytic formation of coke molecules is not envisioned, since they require higher temperatures to occur, and also, are not thermodynamically favored at MTO conditions.

1.5.2.1. Residence time: crystal size and hierarchization

Decreasing the residence time of products within the catalyst pores is a direct way for limiting the occurrence of olefins secondary reactions in a system restricted by slow molecular diffusion. In literature, two strategies are well documented to achieve this goal: 1) decreasing the total size of the SAPO-34 particle or at least one of the domains, and 2) introducing a meso-scale secondary structure to the innate SAPO-34 microporous structure.

The effect of the particle size on coke deposition was first demonstrated by Chen and co-workers, who studied the MTO reaction using SAPO-34 particles with similar acid strength and composition, but with sizes ranging between 250 and 2,500 nm [61,66]. They concluded that olefins were produced from the consecutive reaction: *MeOH → DME → Olefins*. DME diffusion was identified as the limiting step based on the high MeOH-to-DME ratio which ranged between 1 and 9, far from the equilibrium value of 0.47 at the temperature set. When investigating the smallest SAPO-34 particles, they found that the ratio of the effective diffusivity of DME and the intrinsic rate constant decreased from 0.95 to 0.80 when coke content increased from 4.0 to 15.0 wt.%. This variation indicated a transition from a kinetically-controlled to a diffusion-controlled regime caused by coke deposition. Furthermore, this effect was observed at lower values of coke content when larger SAPO-34 particles were used, therefore resulting in catalyst fast deactivation.

Likewise, Wang and co-workers developed a two-step synthesis procedure, allowing tuning the crystallite size between 160 and 1,100 nm [69]. Their results further corroborated the positive effect of small crystals, which exhibited the highest conversion to olefins (up to 90%) while coke accumulated at the lowest rate.

Recently, different research groups have investigated the development of two-dimensional SAPO-34 nanostructures referred as nanosheets [70,71]. Their performance in the MTO reaction has shown a positive effect, however, their synthesis still present some substantial limitations due to the use of expensive chemicals and low conversion from the precursors into the SAPO-34 nanosheets (ca. 15%).

The positive effect of the incorporation of a mesoporous structure to the SAPO-34 was early reported by Schmidt and co-workers, who added different graphene nanostructures including (nano)spheres and (nano)tubes to the SAPO-34 gel, prior to crystallization [72]. By doing so, the authors realized that carbon nanostructures could be trapped within the crystallized solid and, after calcination, they could be consumed thus creating a complex web of channels connecting to the external surface. Prior to MTO testing, Schmidt and co-workers studied the diffusivity of n-butane, a molecule larger than methanol but small enough to diffuse through the SAPO-34 openings. Their results showed that the calculated characteristic diffusion times [L^2/D] (average diffusion length over diffusivity) for un-modified SAPO-34 and SAPO-34 templated with carbon nanotubes were 9.8×10^4 and 4.7×10^2 s, respectively. The lower diffusion time found in the carbon-templated SAPO-34 was concluded to arise from the mesopores created by the combustion of the carbon nanostructures, a proposition that was later supported by the catalytic studies in the MTO reaction, as this catalyst displayed a significantly longer lifetime.

The experiment performed by Schmidt and co-workers for assessing the effect of the mesopores is simple and could help support MTO testing [72]. The experiment consisted in the analysis of the up-take of n-butane in a SAPO-34 sample placed in micro-balance (B111, Seratam) at 298 K and atmospheric pressure. N-butane was chosen due to its kinetic diameter (4.3 Å), which barely fits through SAPO-34 micropore openings. A plot of the weight gain $\frac{g_{n-butane}}{g_{SAPO-34}}$ over time (minutes) over samples presenting similar microporous volume would allow assessing the rate of saturation visually. In addition, numerical analysis can be done by plotting the normalized loading ($\frac{Weight\ gain\ (t)}{Weight\ gain\ (\infty)}$) over the square of time and, from the slope in the first minutes, calculate the characteristic diffusion time (L^2/D), according to the following equation:

$$\frac{Weight\ gain\ (t)}{Weight\ gain\ (\infty)} = \frac{2}{\sqrt{\pi}}\sqrt{\frac{D}{L^2}}\sqrt{t} \qquad \textbf{Eq. 1.1}$$

The L is the characteristic length of diffusion and D is the diffusivity from Fick's second law:

$$\frac{\partial C}{\partial t} = D\left(\frac{\partial^2 C}{\partial x^2}\right) \qquad \textbf{Eq. 1.2}$$

A lower L^2/D translate into a faster diffusion rate, and hence, a lower residence time inside the particle.

More recently, organosilane molecules have been applied for the synthesis of hierarchical-type SAPO-34 [73,74], following a similar conception in which these molecules were trapped within the crystallized particle and removed upon calcination. Similarly to carbon-templated SAPO-34, their performance displayed a stronger resistance to coke deposition, in parallel with a higher selectivity to light olefins.

A less recurred technique for adding mesopores is through chemical treatment of SAPO-34 with hydrofluoric acid (HF). This treatment was shown effective in slowing down the deactivation related to coke, however, the handling of such a dangerous compound (HF) restrict some laboratories from applying such technique, since special safety measures should then be taken into consideration. Moreover, the creation of mesopores by carving out part of the framework has a major impact on the acidity of the catalyst, and so, it becomes difficult to pinpoint the effect of the treatment to one feature in the catalyst [36].

1.5.2.2. Reaction temperature and nature of the coke molecules

Temperature plays a major role in the selectivity of olefins, since it affects the rates at which the most relevant reactions are occurring, including MTO catalytic cycles, cracking, oligomerization, fusion/condensation, hydrogen transfers and others related to coke formation. In literature, the evolution of the MTO reaction as a function of temperature has been described as follow [36].

Below 300°C, methanol conversion is generally limited to dehydration into dimethyl ether and water, with no important concentrations of hydrocarbons in the tail gas. Between 300 and

350°C, methanol undergoes an induction period that is quickly reduced with the temperature rising. In this temperature range, olefins and saturated species evolve into a more stable product distribution in the gas phase, which still involves a relatively low methanol conversions (< 50%). Meanwhile coke accumulation is significant due to the favorable formation of diamondoid hydrocarbons (methyladamantanes) over HCP species [75]. The former have been recently identified to be formed in the MTO reaction over SAPO-34 at low temperatures, and unlike polymethylbenzenes, these are inactive species in the conversion of methanol to olefins (see **Figure 17**). Their formation, however, is reduced as the temperature shifts from 300 to 350°C, at which point polymethylbenzenes and polycyclic aromatics are the only species found in the catalyst. Furthermore, in this temperature range, oligomerization and condensation reactions are strongly favored which explains the poor conversion to hydrocarbons reported in the literature [76,77].

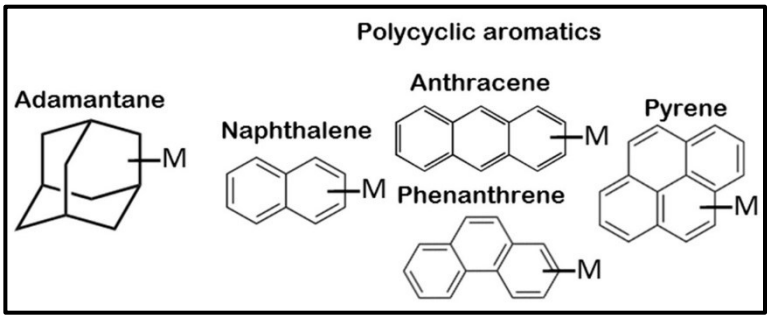

Figure 17. Organic molecules commonly found in SAPO-34 after reaction (spent catalyst). Species presented are categorized as diamondoid molecules (left) and polycyclic aromatics (right) [65,75].

Between 400 and 450°C, the conversion of methanol to olefins reaches the highest value along with the lowest rate of coke accumulation. This optimal effect has been attributed to the enhancement of the cracking of coke precursors such as oligomers [45]. Increasing the temperature above 450°C has a negative effect on the reaction, and so, coke deposition once more increases causing the accumulation of large polycyclic aromatics and graphitic material referred as "*insoluble coke*". Different research groups have consistently identified naphthalenes, anthracene, phenanthrene and pyrene as the most common species found in the deactivated catalyst at temperatures above 400°C (see **Figure 17**) [63,65]. Experiments at 500°C are scarce, nevertheless results indicate that selectivity towards olefins decreases though with a higher ethylene-to-propylene ratio, occurring in parallel with a strong production of methane, carbon dioxide and hydrogen [78–80].

One element that remains still not fully understood on the nature of the coke is how an active coke molecule (or cation) such as heptamethylbenzenium (intermediate) transforms into an inactive one such naphthalene. Bjorgen and co-workers reported the conversion of the former to a naphthalene precursor (dihydrotrimethylnapthalene). This link was suggested on the fact that both species present the same number of carbon atoms, and so, multiple hydrogen transfer reaction (4 hydrogen simultaneously) were hypothesized to occur to induce the transformation [53]. Multiple studies have been done on the chemistry of coke molecules but little work has been done on the matter of deactivation occurs [77].

1.5.2.3. Acidity

The concentration and strength of the acid sites present in the SAPO-34 are well known to have an impact in the catalyst lifetime. Different studies on zeolites and SAPOs have shown that a large concentration of strong acid sites favors reactions leading to coke deposition, such as oligomerization, cyclization and hydrogen transfer [45].

The acidity in SAPO-34 results from the incorporation (or substitution) of silicon atoms (Si) into the neutral aluminophosphate ($AlPO_4$) during the hydrothermal treatment, also referred as crystallization. This substitution can occur following two known mechanisms denominated as SM2 and SM3. SM2 mechanism corresponds to the single substitution of a phosphorus (P) atom by a Si atom, while the SM3 corresponds to the double substitution of neighboring aluminum and phosphorus (Al--P) atoms by two Si atoms. It has been suggested that SM2 takes place during the early stages of Si incorporation, when the Si content in the formed crystal is still low. This substitution creates a charge unbalance in the framework, which is passivated by an organic template (amine) and, upon calcination, it is turned into a Brønsted acid site [81].

In contrast, SM3 occurs in the late period of the crystallization stage and causes significant changes in the Si distribution along the crystal framework, inducing in some cases the formation of Si patches. The latter is relevant given that the strength of the acid site is influenced by the Si environment [82]. The unequal distribution of Si produces a variety of Si environments including [Si(*0*Al)], [Si(*1*Al)], [Si(*2*Al)], [Si(*3*Al)] and [Si(*4*Al)]. Studies on the effect of the Si incorporation in SAPO-34 has shown that a homogenous distribution of Si atoms [Si(*4*Al)] leads to a higher selectivity to olefins, in addition to a longer catalyst lifetime [83]. Meanwhile Si

patches [Si(*0*Al)], which are usually observed in the outer layers of the SAPO-34 particle, enhance secondary reactions and cause deactivation at relatively low coke content [82]. The latter was concluded to arise from strong acid sites located close to the pore opening connecting to the external surface [45].

This phenomena has also been pointed out by Liu and co-workers, who studied the MTO reaction over SAPO-34 treated with oxalic acid [84]. Their results indicated that the acid treatment removed Si-rich domains from the catalyst framework, thus reducing the presence of "*unwanted*" strong acid sites. During testing, the latter was found to enhance the catalyst selectivity towards olefins, while also prolonging the accumulated time-on-stream before observing any drop in methanol conversion.

1.5.2.4. Diluting gas

In literature, the MTO reaction over SAPO-34 has only been executed using nitrogen and/or water as diluting gases, probably due to their availability and non-toxicity. Moreover, diluting methanol with an inert gas (i.e. N_2 at low temperatures and He) is known to prolong the catalyst lifetime. However, this effect is not as strong when using nitrogen as compared to water. As example, Chen and co-workers used a methanol pulse method over SAPO-34 to study the effect of temperature, partial pressure and WHSV on the product selectivity. Methanol was injected intermittently while a nitrogen flow was added to ensure the transport of the oxygenated species through the reactor [66]. Their results indicated the importance of temperature on the selectivity toward olefins and saturated species, nonetheless, partial pressure, hence nitrogen dilution, had no significant effect on the product selectivity at similar coke content.

Conversely, Wu and co-workers performed a detailed study on the effect of water on light olefins secondary reactions over SAPO-34 [85]. The authors co-fed ethylene (ethanol), propylene (propanol) and/or water to methanol over a fresh SAPO-34 and calculated the changes in ethylene, propylene and butene concentrations in the tail gas. Their results indicated that for experiments in which water was not included, ethylene and propylene were strongly consumed to form other olefins, such as, propylene and butenes from an ethylene/methanol mixture, and ethylene and butenes from a propylene/methanol mixture. The results also indicated that propylene was substantially more reactive than ethylene, to the extent that it was

capable of completely suppressing ethylene consumption when both olefins were co-fed. When water was fed in the reaction system, ethylene and propylene consumption was substantially suppressed.

Furthermore, Wu and co-workers studied the MTO reaction (no olefin added) by varying the water content in the methanol aqueous solution [85]. The authors found that a water content between 73 and 80% was optimal for converting up to eight times the amount of methanol that would be converted when using a pure methanol input. The authors concluded that strong acid sites were responsible for the consumption of light olefins, which occurred in parallel with a fast accumulation of coke. Water, being more polar than olefins, was able to compete for such type of sites, and therefore, mitigated olefin secondary reactions.

As mentioned before, nitrogen and water have only been reported in the MTO reaction over SAPO-34. Nevertheless, in the case of the MFI (ZSM-5), carbon dioxide, syngas and hydrogen have been used as well as diluting gases, though in the conversion of dimethyl ether to olefins (DTO). For instance, Sardesai and co-workers studied the effect of nitrogen and carbon dioxide as vector gases over an unmodified H-ZSM-5 [86]. Their results showed that the diluting gas had no effect on the product selectivity, and so, carbon dioxide and nitrogen were considered inert in the reaction.

Man and co-workers studied the "*atmosphere*" effect by using hydrogen, syngas (H_2 and CO) and carbon dioxide as vector gas over a modified MFI, Ca-ZSM-5 [87]. Their results indicated that the presence of calcium turned all these gases reactive, and so, the hydrogen (pure hydrogen or syngas) was found to enhance the formation of light alkanes at the expense of olefins. Indeed, propylene and ethylene were consumed to form propane and ethane, respectively, and in the case of carbon dioxide, the authors observed that carbon monoxide was produced during the reaction which incidentally increased the catalyst lifetime. The latter was attributed to the consumption of coke molecules through the reverse Boudouard reaction ($C+CO_2 \rightarrow 2CO$).

1.5.2.5. Incorporation of metal on the catalyst framework

The following metals have been incorporated and tested in SAPO-34 for the MTO reaction: Co, Mn, Fe, Cu, Ti, Cr, C, Zn, Mg, Ca, Sr ,Ba and Ce [80,88,89]. The effect of the metal on the

SAPO-34 framework were rather inconsistent since they did not always lead to better performances. However, in some cases, their presence were found to increase the selectivity to both light olefins (ethylene and propylene), which allowed prolonging the catalyst lifetime.

Nickel (Ni) incorporation to SAPO-34 showed exceptional results, which were characterized by a particular increase in selectivity to ethylene [81,90,91]. The effect of Ni on the MTO reaction was first investigated by Inui and Kang during the early 90s. They co-authored multiple scientific papers on Ni-SAPO-34 and eventually patented a Methanol-to-Ethylene process (MTE), in collaboration with Shell (Japan) [92].

Understanding the causes behind the higher performance of the metal-incorporated SAPO-34 (over the pure SAPO-34) is still under debate, as the cited studies here relied on "*shallow*" analysis of the physico-chemical properties, in particular acidity, with no mechanistic study involving NMR spectroscopy and/or isotopic labelling that could potentially provide important insights. Instead, a reduction in acidity has been pointed out as main cause. However, the same reduction could be obtained with metals different from Nickel, yet the performances achieved were not the same [80][89].

1.6. Strategy of the research work

To achieve the development of a catalyst and process for the production of light olefins, an optimization strategy was followed in which two elements were investigated: the creation of an intra-particle mesoporosity in the SAPO-34 and the effect of the temperature.

For the development of a mesoporous structure, two lines of research were followed: a post-synthesis modification and a synthesis study. For the former, the alkaline treatment using NaOH was selected since such procedure has demonstrated positive results in multiple Zeolites, such as the ZMS-5 and Mordenite. For the latter, an organosilane-directed method was chosen for the creation of a hierarchical-type SAPO-34 from the initial metal precursors. The organosilane procedure applied on a SAPO-34 catalyst is recent and has reported positive results in the formation of mesopores and increasing the selectivity to light olefins during the MTO reaction.

In parallel, the effect of the temperature on the MTO reaction was investigated using first a commercial SAPO-34, previously extruded. For testing, the MTO reaction was performed in a bench-scale, fixed-bed reactor, which allowed a fast optimization process. Due to the dimensions of the reactor, the catalyst (purchased and synthesized) was extruded to avoid clogging. The effect of the extrusion step on the catalyst properties was studied and incorporated in the results and discussion.

The optimization of the temperature was then followed by the study of the performance of a hierarchical-type SAPO-34 at different temperatures, which provided diverse coke accumulation regimes. The strategy sought to maximize the production of light olefins while reducing the formation of coke (and light alkanes), which is well-known to be the main cause of catalyst deactivation.

Chapter 2. Methodology

The experimental procedures and characterization techniques used in the course of the Ph.D. were executed following protocols supported on literature. A detailed description of the actions taken on the preparation of the catalyst from precursors to the extruded form, characterization including pre-treatment and analysis, experimental testing from catalyst activation to experimentation, and validation of the experiment by carbon mass balance and data evaluation are provided below.

2.1. Procedures and characterization techniques. Post-synthesis modification of a commercial SAPO-34

2.1.1. Chemicals

Microporous SAPO-34 was acquired from **Advanced Chemical Suppliers** under the product name: *ACS Material Molecular Sieve SAPO-34* (see **Figure 18a)**. For the treatment of the catalyst, sodium hydroxide (NaOH, ACS reagent >97%) and ammonium nitrate (NH_4NO_3, 99.99%) used were purchased from Sigma-Aldrich. According to the supplier, the purchased catalyst had been calcined at 600°C.

2.1.2. Catalyst preparation

The preparation of the samples included three steps: alkaline treatment, ion-exchange and calcination. For highlighting the effect of the alkaline treatment, an untreated SAPO-34 (as received from the provider) and an ion-exchanged SAPO-34 (H-SAPO-34) were also included in the analysis. Samples treated with NaOH also underwent three steps of ion-exchange and calcination to eliminate any accumulation of sodium atoms (Na), as this may affect the results of the characterization techniques. A full description of the sequence for alkaline treatment is presented in **Figure 18b**.

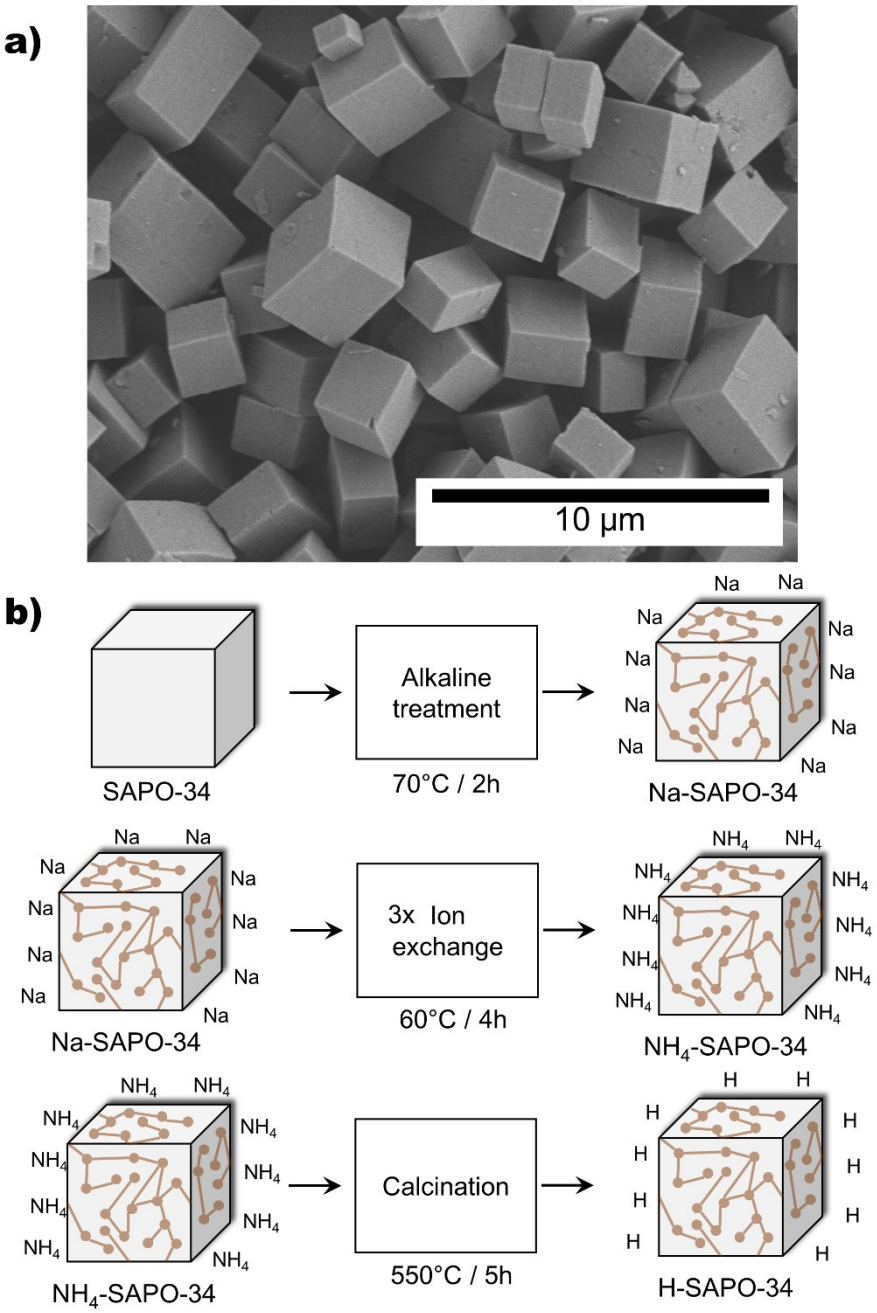

Figure 18. Scanning Electron Microscope (SEM) images of the SAPO-34 (a), and the scheme of the procedure performed for the preparation of the alkaline-treated SAPO-34 (b).

2.1.2.1. Chemical treatment via an alkaline solution

Three grams of the acquired SAPO-34 were placed in 60.0 mL of a NaOH solution previously heated to 70°C. Treatment took place with continuous stirring at a constant temperature for 2 hours. Afterward, the solid was recovered by centrifuging at 9,000 RPM during 5 minutes. The liquid was discarded and the precipitate was again re-suspended in deionized (DI) water and

centrifuged following the same conditions. The procedure was done several times until the equivalent of 100 mL of DI water have been used. The solid was then placed in a crystal beaker and dried overnight in an oven set at 105°C.

2.1.2.2. Ion exchange via an ammonia nitrate solution

Sixty millilitres of an ammonium nitrate (NH_4NO_3) solution with a 2.0 N concentration was poured in a beaker and heated to a temperature of 60°C. Afterward, a SAPO-34 or an alkaline-treated sample was added to the solution and stirred continuously for 4 h. The recovery of the solid followed a similar procedure to what was explained in the previous section (centrifuging and drying overnight).

2.1.2.3. Calcination

Calcination of the samples was done in a temperature-controlled, static furnace (air atmosphere), in which samples were placed in a quartz container. The temperature of the furnace was increased to 550°C at a rate of 1°C/min and maintained for 5 h.

2.1.3. Characterization

2.1.3.1. Nitrogen adsorption-desorption isotherm

The texture properties of the catalysts were measured using a Micrometrics 2020 ASAP apparatus. Samples (60 –100 mg) were placed inside a glass cell and put under vacuum at 100°C for 1 h, and subsequently heated up to 350°C and kept there for six more hours prior to characterization. The Brunauer-Emmet-Teller (BET) surface area was calculated from the adsorption isotherm values obtained in the relative pressure (P/P_o) range between 0.05 and 0.15. The total pore volume was determined using the nitrogen amount adsorbed at a P/P_o of 0.98. In addition, the external surface area and microporous volume were calculated using the t-Plot method as reported by Leofanti and co-workers [93].

2.1.3.2. X-ray diffraction patterns (XRD)

XRD diffraction was employed for the identification of the crystal phases present in the different catalysts studied. XRD patterns were recorded with a Miniflex RIGAKU diffractometer using a CuKα (λ=1.54 Å) radiation with a 40 kV voltage and 40 mA current. The step width and

scanning speed settings were 0.017° and 1.05°/min, and the range recorded by the equipment was from 5 to 40°. For identification, the XRD readings were compared to those reported by the International Zeolite Association (IZA) for a CHA-type SAPO-34 [39].

2.1.3.3. Ammonia temperature program desorption (NH_3-TPD)

Acidity was measured using a Micrometrics Chemisorption analyzer (Model AutoChem II 2920), which was operated automatically. The sample preparation was the following. A wool quartz patch was first placed inside a quartz U-tube micro-reactor. Then, a sample with a known mass (150–200 mg) was added and secured with a second patch fixed on top. Prior to the adsorption and desorption steps, the sample was placed in a oxidizing atmosphere at 450°C for 1 h to remove water and any other organic residue. The oxidizing atmosphere was then exchanged by a He flow, and the system temperature was lowered to 50°C and maintained for 1 hour. Afterward, the sample was exposed to a NH_3/He flow for 30 minutes. Upon NH_3 exposure, the gas stream was switched back to He, and temperature was raised to 100°C and maintained for 2 hours, as this was the time required to fully stabilize the TCD signal. After stabilization, the temperature of the system was raised to 700°C using a temperature ramp of 10°C per minute.

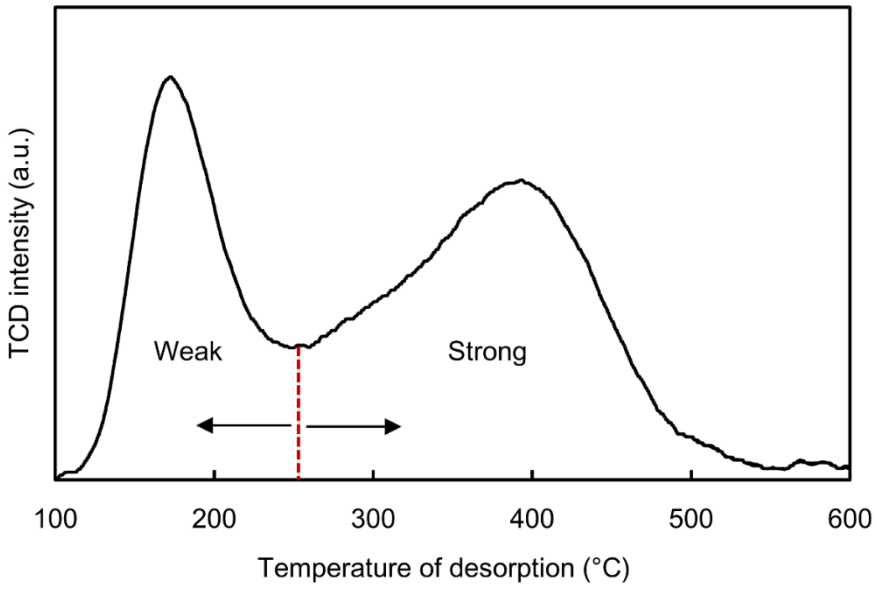

Figure 19. TCD reading of the NH_3-TPD performed on the SAPO-34 (*as-received*). The TCD signal is separated in two areas, a weak and a strong one, according to the temperature of inflection of the NH_3 desorption as indicated by the red dashed line.

This technique allows measuring the total acid sites in the catalyst, as well as classifying these sites as weak or strong depending on the desorption temperature. For this, the classification of the acid sites strength was determined based on the temperature of inflection between the two desorption peaks (see **Figure 19**), as reported by Al-Dughaither and co-workers [42].

2.1.4. Coke deposition test

Samples were exposed to DME to induce the accumulation of coke. The procedure involved two steps: catalyst preparation followed by the conversion of DME to coke molecules.

The procedure was performed in a customized apparatus equipped with a quartz cell enclosed in a portable temperature-controlled oven. A basket-shaped quartz microbalance with was placed inside the quartz cell that was connected to a gas manifold system that allowed the introduction of different atmospheric conditions such as vacuum, air or pure DME. The microbalance reactor was capable of achieving mass measurements with an accuracy down to microgram (μg).

For each experiment, a known amount of catalyst (~50 mg) was placed in the microbalance sample port. The preparation of the catalyst was done by pulling vacuum slowly while temperature was increased to 350°C and maintained for 24 h. Afterward, the deposition of coke was done by injecting a DME gas flow into the "hot" system while the pressure was set between 760 and 770 Torr. The mass of the catalyst was recorded continuously on-line for the whole duration of the manipulation.

The weight gained due to coke deposition (*coke gain*) was calculated according to **Eq. 2.1**:

$$coke\ gain\ (\%\ at\ time\ t) = \frac{weight_t - weight_0}{weight_{initial}} \times 100 \qquad \textbf{Eq. 2.1}$$

, where $weight_0$ is the weight of the sample at time zero and $weight_t$ is the one measured after t minutes upon DME injection. The analysis demonstrated that after 8 minutes of DME exposure, the weight of the sample had become stable.

2.1.5. Spent catalyst analysis

Due to the limited amount of mass that could be placed in the microbalance reactor, around 1.0 g of sample was poured at the bottom of the glass cell. Upon experimentation, between 500 and 550 mg of this catalyst was used for characterization as described below.

2.1.5.1. Coke extraction by HF dissolution

This technique was done according to the procedure described by Magnoux and co-workers [94]. This produced included two steps: extraction of the external and internal coke. For the former, the spent catalyst was placed in a stainless steel autoclave and rinsed with a fixed volume of dichloromethane at high pressure using a *soxhlet* system. Results indicated that no coke was found in the outside of the spent catalyst, and hence, coke was concluded to form within the catalyst pores.

Extraction of the coke molecules within the pores was done as follow. Dissolution of the solid framework was done at room temperature using 10.0 mL of a hydrofluoric acid (HF) solution at a 51 wt% concentration. This step was done under continuous stirring and lasted for 1 h, after which the solution pH was first manipulated with a saturated boric acid (HB) solution followed by a saturated sodium carbonate (Na_2CO_3) solution. Addition of the latter was done until a pH between 3 and 4 was obtained. The coke molecules, which were initially trapped within the catalyst pore, were liberated and diluted with 10.0 mL of dichloromethane. The brown organic solution was separated from the water phase, and then passed through a cartridge equipped with a silica phase. The filtered solution was then analyzed with a gas-chromatographer (GC) coupled with a mass-spectrometer (MS). Analysis of the organic phase was done using a DB5ms column (30 m X 0.25 mm X 0.25 mm). The GC-MS temperature program had the following description: the initial column temperature was 40°C and, after 2 minutes, it was increased to a final temperature of 300°C using a temperature ramp of 6°C/min and. Upon reaching the target temperature, the system was maintained for 15 minutes.

2.1.6. **Data evaluation**

The following equations and procedures were employed for the analysis regarding the determination of the average molar weight of the coke molecules found in the spent catalyst. This value was later used for determining the acid site-to-coke molecule ratio.

2.1.6.1. Average molecular weight (MW_{ave})

For this parameter, the peaks obtained in the chromatographs were identified using a Mass Spectroscopy database, which was incorporated in the Software in charge of analyzing the MS readings (see **Figure 20**). After identification, the average molar weight (of the coke mixture) for each sample was determined using **Eq. 2.2**:

$$MW_{ave}\ \left(\frac{g}{mol}\right) = \frac{\sum_i^n Pk{-}Int._i(a.u) \times MW_i(\frac{g}{mol})}{\sum_i^n Pk{-}Int_i\ (a.u.)} \qquad \textbf{Eq. 2.2}$$

This formula is known in statistics as the "first momentum" of a data set and represents the average value of the cokes molecules weighted, in this case, by the intensity of the peak ($Pk\text{-}Int_i$), where the index i correspond to each coke molecule found.

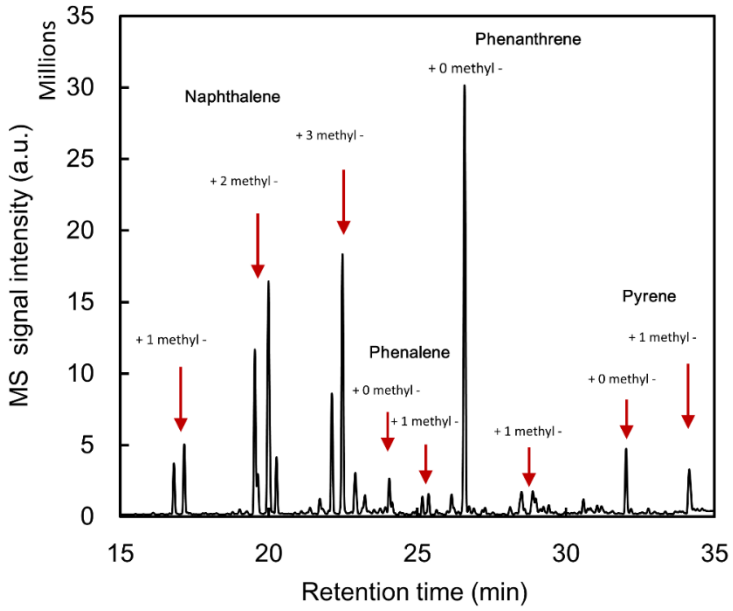

Figure 20. Example of an MS chromatograph obtained from the H-SAPO-34 spent catalyst. Peaks are indicative of polycyclic aromatics as highlighted by the red arrows, with the corresponding number of methyl groups presents in each component.

2.1.6.2. Acid site-to-coke molecule ratio

For this parameter, the $coke_{mole}$ (mass expressed in mole units) was determined according to **Eq. 2.3**:

$$coke_{mole}\ (\mu mol/g) = \frac{coke\ gain_8\ (\%) \times 1\ (g)}{MW_{ave}\ (\frac{g}{mol})} \times 10^6 (\frac{\mu mol}{mol}) \qquad \textbf{Eq. 2.3}$$

, where $wt\ gain_8$ is the weight gain after 8 minute of DME injection.

The *acid site-to-coke molecule ratio* was determined according to **Eq. 2.4**:

$$Acid\ site - to - coke\ molecule\ \ ratio = \frac{Coke_{mole}\ (\mu mol/g)}{Acid\ sites_{total} (\mu mol/g)} \qquad \textbf{Eq. 2.4}$$

, where $Acid\ sites_{total}$ is the sample acid concentration including both weak and strong acid sites.

2.2. Procedures and characterization techniques. MTO reaction: suppression of undesirables products with a SAPO-34 synthesized via an organosilane-directed method

2.2.1. Chemicals

ACS Material Molecular Sieve SAPO-34 (micro-type SAPO-34) was purchased from Advanced Chemical Suppliers. According to the supplier, the purchased SAPO-34 had been calcined at 600°C. For the synthesis of the hierarchical-type SAPO-34, phosphoric acid (H_3PO_4 85 wt% in water), fumed silica (SiO_2 98% purity), tetraethyl ammonium hydroxide (TEAOH 35 wt% in water) and dimethyloctadecyl[3-(trimethoxysilyl)propyl]ammonium chloride (TPOAC 42 wt% in methanol) were purchased from Sigma-Aldrich. The Aluminum precursor was provided by SASOL North America under the name Catapal-B (pseudoboehmite 72 wt% purity). For the extrusion process, the permanent (colloidal SiO_2 40 wt% in water) and temporal binder (hydroxyethylcellulose 99.9% purity) were purchased from Sigma-Aldrich and Fluka, respectively. Finally, the MTO catalytic study used methanol that was provided by Enerkem Inc. (IMPCA bio-methanol grade).

2.2.2. **Synthesis of Hierarchical-type SAPO-34**

Three batches of hierarchical-type SAPO-34 were synthesized according to the following procedure (**Figure 21**). First, a solution of 112.6 g of phosphoric acid and 121.7 g of deionized water (DI) were mixed and stirred. Then, 67.0 g of Catapal-B were slowly added while maintaining the agitation (300 ─ 400 RPM) as the solution underwent hydrolysis to form an amorphous aluminophosphate phase ($AlPO_4$). Then, 116.6 g of water were further added to ensure a complete dilution of the aluminum precursor. During this time, in a second beaker, 386.2 g of TEAOH were placed and 8.96 g of fumed Silica were slowly added while keeping the agitation between 300 ─ 400 RPM. An equivalent of 26.0 mL of TPAOC was also added and the solution was stirred for 30 minutes until a homogenous phase was obtained. In a third step, the second solution was slowly added to the first and the final solution was stirred for at least 12 h. After mixing, the final gel-solution presented the following molar composition:

1.0 Al_2O_3 : **1.0** P_2O_5 : **0.3** SiO_2 : **2.0** TEAOH : **0.02** TPAOC : **55.7** [MeOH+H_2O]

The gel was then placed inside a 1-L stainless steel autoclave, which was firmly closed and leak tested. The temperature of the autoclave was raised to 180°C and maintained for a defined crystallization time, either of 3, 5 or 7 days without stirring. The white mixture, product of the crystallization step, was extracted and mixed with 500 mL of DI water. The solid phase was precipitated by centrifugation at 5000 RPM for 5 min. The wet precipitate was then dried overnight at 105°C, and calcined at 550°C for a period of 5 h. The final powder was then finely ground and stored for characterization and extrusion.

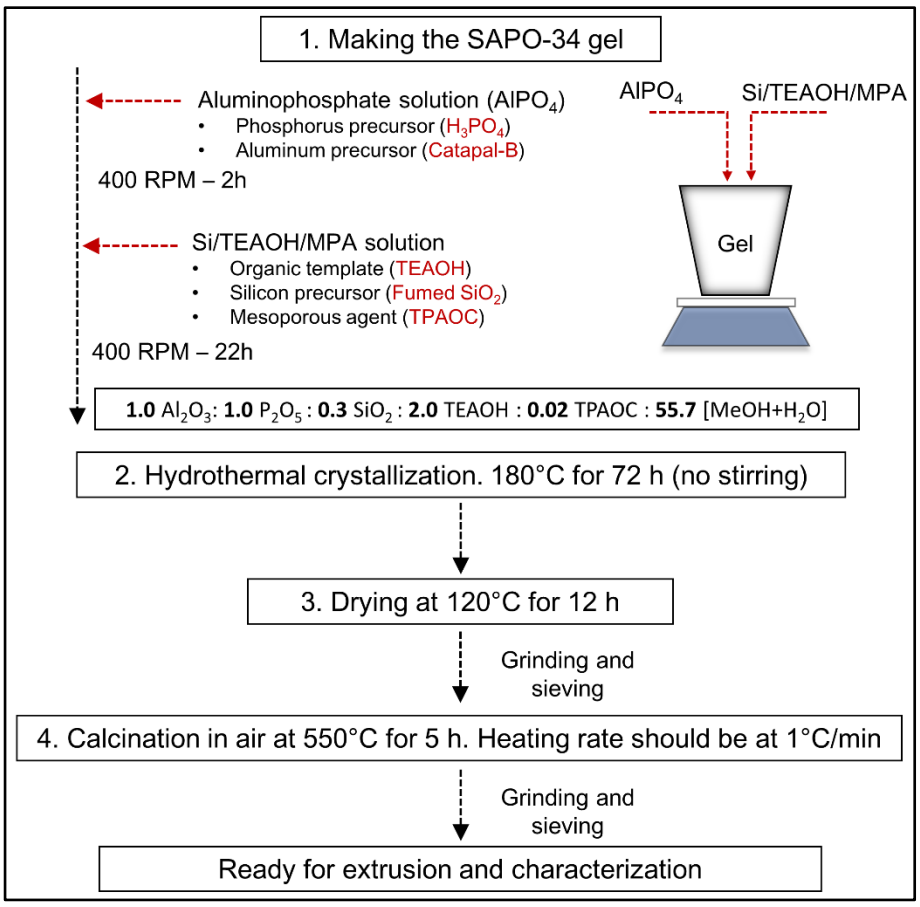

Figure 21. Scheme for the preparation of the hierarchical-type SAPO-34.

2.2.3. **Extrusion process**

The extrusion of the SAPO-34 was done with the objective of creating "macroscopic" forms of the catalyst to avoid pressure drops within the reactor as a consequence of clogging [95–97]. The extruded catalyst was prepared following the procedure reported by Gil and co-workers [15]. A summary indicating the relevant parts of the extrusion process is presented in **Figure 22**.

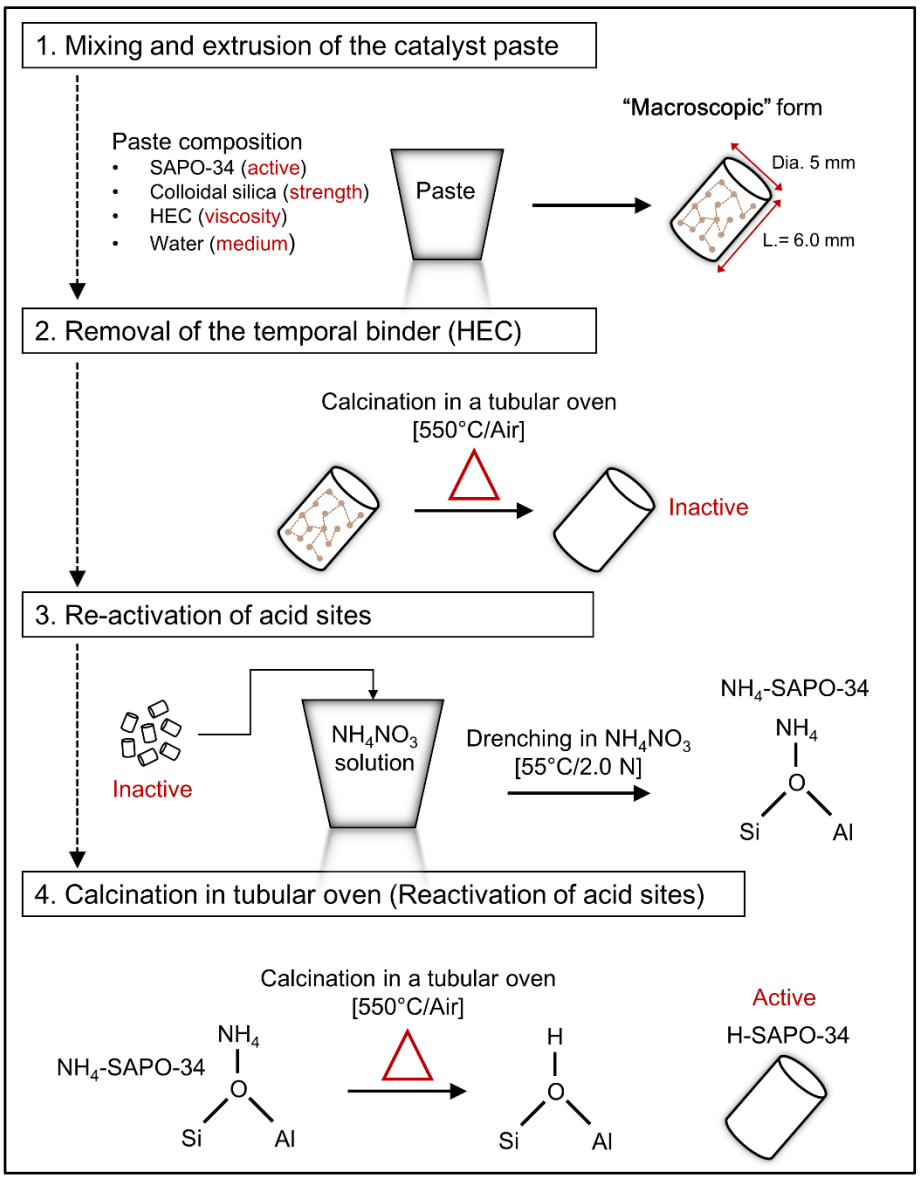

Figure 22. Scheme indicating the steps involved in the extrusion process.

The micro-type extruded catalyst was prepared from a reactive paste composed of 65% (*w/w*) SAPO-34 and 35% (*w/w*) colloidal silica, whereas for the hierarchical-type, the extruded catalysts used a loading of 55% (*w/w*) of the native SAPO-34 to ensure mechanical strength at the highest possible loading. Other compositions presenting higher active-part content (i.e. 70 and 70%) were also tested, however, they were shown unable to sustain mechanical strength, which from our experience, could be determined by pressing individual pellets with the fingers (wearing nitrile gloves) with the objective of breaking or crushing the pellet. If samples were capable of retaining their full physical integrity, the paste mixture was considered as satisfactory for withstanding any type of handling during catalytic testing. This method proved to be reliable

as, upon reaction, the spent catalyst was still presenting the initial cylindrical form. Nonetheless, it is important to mention that small amount of a gray powder residue was recovered with the bed supporting material, which could have been released by the catalyst.

2.2.4. Characterization

2.2.4.1. Nitrogen (N_2) adsorption-desorption isotherm

The texture properties of the catalysts were analyzed using the N_2 adsorption-desorption isotherm method (at 77 K), and to this purpose, a Micrometrics 2020 ASAP apparatus was employed. A sample mass between 60 and 100 mg was placed inside a glass cell and subjected to low vacuum at 100°C for 1 h. Subsequently, the intensity of the vacuum was increased and in parallel the temperature in the cell was raised to 350°C, at which point it was maintained for 8 h in order to remove any trace of water and/or organic molecule.

The Brunauer-Emmet-Teller (BET) surface area was computed from the adsorption isotherm at relative pressures (P/P_o) extracted between 0.05 and 0.15. In addition, the total pore volume was evaluated based on the amount of nitrogen adsorbed at a P/P_o of 0.98. The external surface area and the microporous volume were calculated using the t-Plot method as described by Leofanti and co-workers [93].

2.2.4.2. X-ray diffraction (XRD)

Analysis of the crystal structure was performed with a Panalytical X'Pert Pro Multipurpose Diffractometer (MPD), powered by a Philips PW3040/60 X-ray generator and fitted with a PIXel 1D detector. Diffraction data was acquired (2θ between 5 and 40°) by exposing the powder samples to a Cu-K_α X-ray radiation, which had a characteristic wavelength (λ) of 1.5418 Å. X-rays were generated from a Cu anode supplied with a voltage of 40 kV and a current of 50 mA.

The relative crystallinity of the extruded catalysts was calculated according to **Eq. 2.5**. The area of the crystal plane [101] was selected as reference because it showed the highest intensity.

Relative crystallinity (RC):

$$RC\ (\%) = \frac{AreaExtruded_{[101]}}{AreaPure_{[101]}} \times 100 \qquad \textbf{(Eq. 2.5)}$$

From **Eq. 2.5**, AreaExtruded$_{[101]}$ is the area under the peak of the crystal plane [101] computed from the extruded catalyst XRD, meanwhile, AreaPure$_{[101]}$ is the area under the peak for the corresponding catalyst in its pure form.

2.2.4.3. Ammonia temperature program desorption (NH_3-TPD)

Acidity was measured using a Chemisorption Analyzer operated manually. First, a sample between 150 and 200 mg in mass was subjected to an oxidizing atmosphere (He/O_2 mixture, 12.5 vol. % in O_2) at 450°C for a period of one hour to remove any trace of water and/or organic molecule. Afterward, the sample was cooled down to 50°C and a He/NH_3 mixture (15 vol. % in NH_3) was flushed in the system for 30 min. Then, the system was placed in a He atmosphere, then, temperature was raised to 100°C and maintained for 2 h, at which point the TCD signal became stable. Then, the TCD signal (NH_3 desorption) was recorded from 100 to 600°C at a heating rate of 5°C/min.

This technique allows measuring in the catalyst the amount of acid sites as well as their strength, which depends on the temperature of ammonia desorption. The separation of the signal into different acid strengths was done according to the temperature of inflection between the two desorption peaks (see **Figure 19**) [42]. The acid sites below the temperature of inflection were considered weak, while those related to ammonia desorption at temperatures higher than the inflection were considered strong. For comparison purposes, the temperature of inflection of the pure catalyst was applied to the extruded catalyst.

2.2.4.4. Carbon content in spent catalyst

After reaction, the unreacted white catalyst acquired different shade colors, including yellow, green, brown and black, which was indicative of coke deposition (see **Figure 23**) [65]. To obtain a representative sample for analysis, the spent catalyst had to be categorized by coloration and a sample was constructed by taking the mass from each portion forming the whole sample.

Coke content in the spent catalyst was obtained by thermogravimetric analysis (TGA) using a TA instrument TGA model Q500. The samples (20 – 30 mg) were heated up from room

temperature to 900°C at 10°C/min under air atmosphere. Coke content was then calculated based on the sample weight difference at 220°C (water-free) and 900°C (water-/coke-free). The total carbon (C) content in the spent catalyst was measured using a ThermoFischer Scientific Flash 2000 CHS/O analyzer. The analyzer was calibrated using standards at different concentrations, while the temperature of the analyzer was set at 960°C.

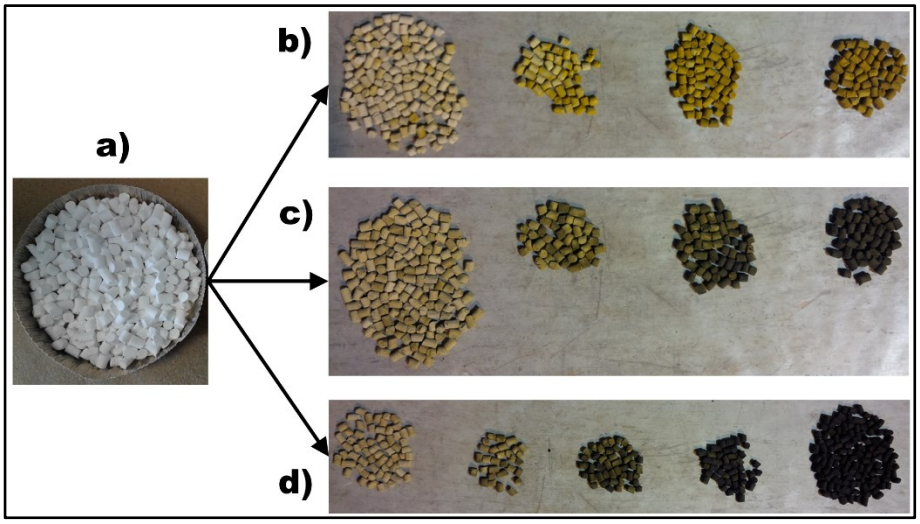

Figure 23. Images of the extruded catalyst, prior to reaction (a), and after reaction at 350° (b), 450° (c) and 500° (d).

2.2.5. Catalytic testing (MTO)

2.2.5.1. Description

Catalytic reactions were carried out in a stainless steel fixed bed reactor (I.D. =2.03 cm, L=100 cm) placed in a tubular furnace equipped with a temperature controller. Silicon carbide (SiC) was placed above and below the catalyst bed to serve both as a support and fluid distributor (supporting material). Prior to each experiment, the extruded catalyst (30 g) was activated overnight by flushing nitrogen gas (0.5 LPM) while the temperature was set to 500°C. The procedure was done by increasing gradually the temperature (< 3°C/min) to ensure a homogenous temperature along the catalyst bed. After activation, the temperature was set to the experimental temperature (350 and 450°C) while the methanol aqueous solution was fed using a HPLC pump and evaporated before entering the reactor. The experimental apparatus is shown in **Figure 24**.

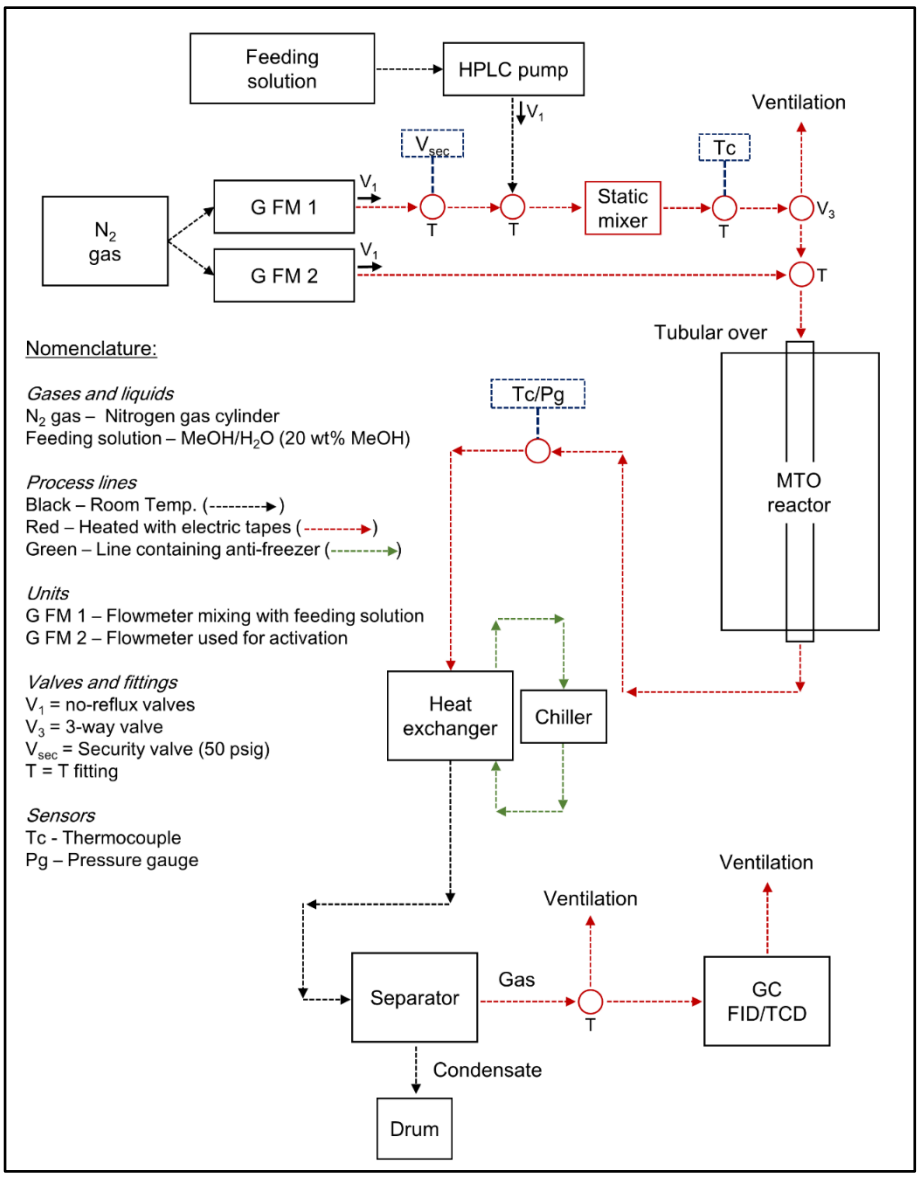

Figure 24. Scheme of the bench-scale experimental setup used for testing the MTO reaction at Enerkem Inc. research lab

The reactor outlet stream was cooled down to 18°C with a chiller, allowing the separation of gas from the condensable phase. The gas products were analyzed and quantified using an on-line GC (Agilent Technologies, model 7820A) equipped with flame ionization (FID), a thermal conductivity detectors (TCD) and an Agilent HP-Plot Q capillary column (30 m×0.25 mm×1.4 µm). Gas analysis was performed using the following temperature program: isothermal at 40°C for 2 min, heating at 20°C/min up to 120°C (maintained for 1 min), then heating at 30°C/min to 220°C (maintained for 5 min).

2.2.5.2. Validations of the experiment through the C-mass balance

The carbon mass balance of each experiment was calculated based on the sum of three independent outputs: gas (GC), liquid (GC) and solid phases (TGA & elemental analysis). Then, the difference of carbon (missing carbon) was calculated by subtracting the carbon fed (methanol input) and the obtained sum of products.

2.2.5.3. Data evaluation

The performance parameters detailed in **Eq. 2.8 – 2.10** were used for analyzing the effect of the temperature and other variables on the performance of the catalysts.

Weight Hour Space Velocity (WHSV):

$$WHSV\ (h^{-1}) = \frac{Massic\ flow\ rate\ of\ feed\ (^{g}/_{h})}{Mass\ of\ SAPO{-}34\ in\ extruded\ catalyst\ (g)} \qquad \textbf{(Eq. 2.8)}$$

Conversion of methanol to hydrocarbons (MCH):

$$MCH\ (\%) = \frac{mass\ of\ carbon\ atoms\ in\ hydrocarbons\ (^{g}/_{h})}{mass\ of\ carbon\ atoms\ in\ methanol\ fed\ (^{g}/_{h})} \times 100 \qquad \textbf{(Eq. 2.9)}$$

Selectivity (Sel.):

$$Sel.(\%) = \frac{mass\ of\ carbon\ atoms\ in\ species_i\ (^{g}/_{h})}{mass\ of\ carbon\ atoms\ in\ hydrocarbons\ (^{g}/_{h})} \times 100 \qquad \textbf{(Eq. 2.10)}$$

Chapter 3. Post-synthesis modification of a commercial SAPO-34 via an alkaline treatment

Abstract

The effect of an alkaline treatment on a commercial SAPO-34 using multiple NaOH concentrations was investigated, focusing on the modifications induced on the texture properties, acidity and crystal structure of the catalyst. Also, samples underwent a coke deposition test using dimethyl ether (DME) as carbon source. Characterization results indicated that the treatment was unable to achieve a positive trade-off between the loss of microporous volume (internal structure) and the formation of an intra-particle mesoporous structure in the SAPO-34. The negative effect of the treatment was further supported by the lower coke gain obtained and it was concluded that such procedure was not suitable for SAPO-34 hierarchization. The deposition of coke, however, did emphasize on the importance of creating an intra-particle secondary structure, as the calculations of the acid site-to-coke molecule ratio for the untreated samples (3.50 and 3.68) suggested that coke preferentially formed on the outer layers of the particle, restricting the access of DME to the deeper layers. Hence, it was concluded that by adding a secondary system of channels, the lifetime of the catalyst could be increased more than three times.

Keyword: SAPO-34, hierarchization, intra-particle mesopores, alkaline treatment, coke deposition.

Modification post-synthèse d’une SAPO-34 commercial en utilisant un traitement alcalin

Résumé

L'effet d'un traitement alcalin sous une SAPO-34 commerciale en utilisant plusieurs concentrations de NaOH a été étudié, en se concentrant sur les modifications induites sur les propriétés de texture, la concentration en acide et la structure cristalline. De plus, les échantillons ont subis un essai de dépôt de coke en utilisant de l'éther diméthylique (DME) comme source de carbone. Les résultats de caractérisation ont indiqué que le traitement ne permettait pas d'obtenir un compromis positif entre la perte de volume microporeux (structure interne) et la formation d'une structure mésoporeuse intra-particulaire dans la SAPO-34. L'effet négatif du traitement a été en outre soutenu par un gain de coke inférieur et il a été conclu qu'une telle procédure ne convenait pas à la hiérarchisation de la SAPO-34. Le dépôt de coke a cependant démontré l'importance de créer une structure secondaire intra-particulaire, car les calculs du rapport molécule site acide-coke pour les échantillons non traités (3.50 et 3.68) suggèrent que le coke se forme préférentiellement dans les couches externes de la particule, limitant l'accès du DME aux couches plus profondes. Par conséquent, il a été conclu qu'en ajoutant un système secondaire de canaux, la durée de vie du catalyseur pourrait être augmentée d’un facteur trois.

Mots clés: SAPO-34, hierarchization, intra-particle mesopores, alkaline treatment, coke deposition.

3.1. Introduction

Solid acids, including zeolites and silicoaluminosilicates (SAPO), are the results of an extensive quest in the development of crystalline materials adequate in the fields of adsorption and catalysis [98]. The evolution from the conception of zeolites to SAPO-n involved multiple milestones. For instance, after the synthesis of zeolites (alumino-silicates) at laboratory conditions, the partial substitution of P^{5+} for Si^{4+} in zeolites with high Al content was achieved [99]. Then, followed the conception of aluminophosphate ($AlPO_4$), a novel material that displayed an unseen set of texture properties, nonetheless, these were deprived of an acid or basic quality, making them inactive for applications such as catalysis [100]. In the ensuing years, the partial substitution of Si^{4+} for P^{5+} in $AlPO_4$ led to the conception and fabrication of SAPO-n zeo-types, a material that embodied features seen in zeolites, such as hydrothermal stability combined to an accessible microporous structure, a shape selectivity influenced by the internal topology and a weak-to-moderate acidity adequate for catalysis [43].

In particular, zeolites and silicoaluminophosphates are highly praised for their selectivity, which originates from their unique internal topology and configuration [40]. However, this "*superior*" selectivity comes along with a penalty in diffusion limitations, pore blocking, and quite often, catalyst deactivation [45]. Shortening the products diffusion path has been pointed out as the most convenient strategy for limiting the aforementioned effects, and so, two approaches are found in the literature. The first consists in decreasing the particle size to a nanometer scale as observed in novel morphologies such as nanosheets, in which one of the sides is restricted to grow while the others follow normal crystallization rates [70]. This option creates materials highly resistance to coke deposition, however such complex structures are expensive to synthesize because their formation occurs at low crystallization conditions and, as consequence, a large amount of precursor is wasted. The second option is the introduction of a mesoporous structure (intra-particle type) into the microporous SAPO-34, a process referred as hierarchization [101].

The introduction of mesopores can be done using a "bottom-top" approach, for instance, employing a sacrificial molecule (i.e. mesoporous agent) which becomes trapped during crystallization, and upon calcination, a secondary channel network is formed on top of the

microporous structure [102]. This procedure is flexible and suitable to many zeolites, nonetheless the combustion of the mesoporous agent leads to a large emission of heat and water which may negatively impact the stability of the solid and cause a crystallinity loss. A more common approach is the post-synthesis modification of the catalyst via alkaline and/or acid treatment [103]. While this procedure has been widely applied and demonstrated to have a positive effect in zeolites such as H-ZSM-5 [104–107] and Mordenite [108,109], other microporous materials such as aluminophosphate ($AlPO_4$) and silicoaluminophosphates (SAPOs) have seen a limited number of publications which for some did not report of a higher performance [84,110].

In particular, the preparation of hierarchical-type SAPO-34 is of great interest because such material has shown potential in multiple applications such as gas separation (CO_2/CH_4) [111], thermos-chemical heat storage [112], and hydrogen purification [113]. More importantly, this material has achieved industrial status in the Methanol-To-Olefin (MTO) process, due to its exceptional selectivity towards light olefins, which originates from its cage-type framework configuration and dimensions (3.8 × 3.8 Å pore openings and 11.0 × 6.5 Å cages) [44]. Conversely, the latter is also responsible for the fast deactivation associated with the prolonged retention of products (olefins and other hydrocarbons), and condensation of the active organic molecules (polymethylbenzenes) into inactive polycyclic aromatics [66,73,114–116]. As consequence, industrial MTO systems employ fluidization reactors that allow the recovery of the spent catalyst for its regeneration [33,36].

In catalytic processes, fixed-bed reactors are preferred because of their simplicity, in addition to the lower capital and operational cost when compared to fluidization systems [1]. In this chapter, we investigated the application of an alkaline treatment of a commercial SAPO-34 (ACS) for customizing the physico-chemical properties of the catalyst, more notably, the formation of an intra-particle mesoporosity. Great emphasis was given to the physico-chemical properties since they play a major role in the performance of solid acids in a wide range of reaction. To this purpose, a SAPO-34 composed only of a microporous structure was treated with different NaOH solutions and underwent characterization with traditional techniques, such as X-ray diffraction pattern (XRD), nitrogen isotherm analysis (N_2 isotherms) and ammonia temperature desorption (NH_3-TPD). In addition, the accumulation of coke in the original and

treated samples was studied in a microbalance reactor, in which dimethyl ether (DME) was used as carbon source. Upon coke deposition, the spent catalyst was recovered and dissolved in a HF solution for the extraction and identification of the coke molecules formed within the catalyst pores. Finally, the results obtained exhibit the limitations of this technique when applied to a SAPO-34 and the importance of a secondary structure for increasing the accessibility of the catalyst inner layers to enhance its lifetime.

3.2. Results and discussion

3.2.1. Effect of alkaline treatment on the physico-chemical properties

The texture properties of the samples studied and their corresponding treatment conditions are summarized in **Table 3**.

Table 3. Treatment conditions and texture properties obtained via N_2 adsorption-desorption isotherm

	Preparation		Area ($m^2/g_{SAPO-34}$)		Volume ($m^3/g\text{-}_{SAPO-34}$)	
Catalyst	**Conc.***	**Steps$^+$**	**BET**	**External**	**Micro**	**Total**
SAPO-34	–	–	748	0	0.297	0.297
H-SAPO-34	–	B/C	772	0	0.308	0.308
0.2 NaOH	0.2	A/B/C	450	0	0.177	0.179
0.4 NaOH	0.4	A/B/C	70	0	0.029	0.029
0.6 NaOH	0.6	A/B/C	139	130	0.005	0.151
0.8 NaOH	0.8	A/B/C	156	180	0.000	0.295
1.0 NaOH	1.0	A/B/C	169	176	0.000	0.403

*Concentration of alkaline solution in Normality (N), $^+$ Nomenclature A: [Alkaline treatment] B: [3 × ion-exchange with ammonia nitrate] C: [calcination]

The results showed that samples that did not undergo alkaline treatment, SAPO-34 and H-SAPO-34, exhibited a similar BET surface and microporous volume, which suggests that the ion-exchange step did not have any effect on the internal structure of the catalyst. In contrast, samples that underwent alkaline treatment showed a drop in their respective BET area (internal and external area) and microporous volume values, and moreover, such effect was noticed to be stronger as the concentration of sodium hydroxide used was increased.

The pristine SAPO-34 (*as-received*) exhibited a microporous volume of 0.297 $cm^3/g_{SAPO-34}$, and upon alkaline treatment, this value lowered to 0.177, 0.029 and 0.005 for NaOH solutions with a concentration of 0.2, 0.4 and 0.6 N, respectively (see **Table 3**). For samples treated with a concentration of 0.8 and 1.0 N, the microporous volume was non-existent, though nitrogen was still condensed in the solid. The latter was attributed to pockets formed between adjacent SAPO-34 particles (inter-particle mesoporosity). It is assumed that these pockets originated due to a

change in the SAPO-34 morphology, which implied that the particles no longer presented a regular rhombohedral form as observed in **Figure 18a**.

Furthermore, comparison of the total and microporous volume indicated that intra-particle mesopores were not formed in parallel with the loss of the internal structure. This observation was unexpected but could be indicative of particles becoming amorphous due to the dissolution of parts of the SAPO-34 framework. This process could cause the liberation of material that blocked the access of nitrogen to the deeper layers in the particle, therefore explaining the decrease in microporous volume. This hypothesized liberation of material, however, did not have any significant effect on the external surface as this value remained zero. It was once that the microporous structure was practically loss that the onset of the external surface and inter-particle mesoporosity occurred.

A similar result was reported by Verboekend and co-workers, who performed a less "aggressive" alkaline treatment (65°C and 30 minutes) in a SAPO-34 acquired from the same source (ACS [101]. Their results showed that the alkaline treatment led to a decrease in the microporous volume from 0.30 to 0.15 $cm^3/g_{SAPO-34}$, while the mesoporous volume increased to 0.02 $cm^3/g_{SAPO-34}$ and the external surface increased 19 $m^2/g_{SAPO-34}$. Similar to our results, the drastic loss of microporous volume did not translate into the formation of a significant amount of intra-particle mesoporous structure.

The inability to develop intra-particle mesopores in SAPO-34 using basic solutions was pointed out by Verboekend and co-workers, who discovered that such zeo-type had a particularly low resistance to inorganic solutions (i.e. NaOH) [101]. According to the authors, the alkaline treatment led to a preferential destruction of Al – O – P bonds. This is unwanted as the formation of intra-particle mesopores, as it has been underscored by other researchers [117], should induce an even elimination of multiple metals to avoid the formation of patches rich in one element. Verboekend and co-workers deduced that in basic media, the stability of the bond was as follow: [Al – O – Si] >> [Si – O – Si] > [Al – O – P].

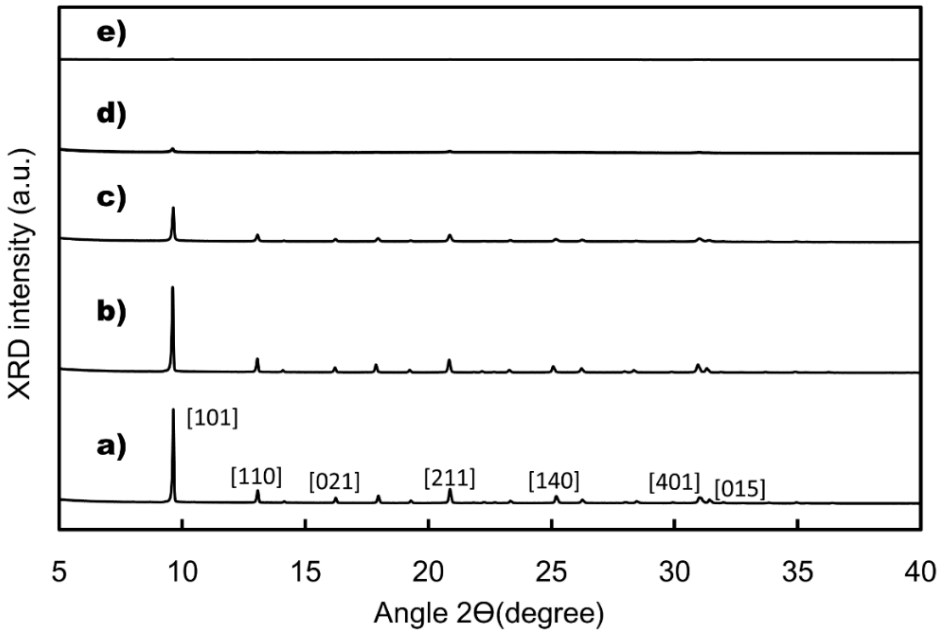

Figure 25. X-ray diffraction patterns analysis of SAPO-34 (a), H-SAPO-34 (b), and alkaline-treated samples 0.2 NaOH (c), 0.4 NaOH (d) and 0.6 NaOH (e).

The analysis of the crystal structure via XRD is presented in **Figure 25**. When comparing the evolution of the intensity of the peak [101], which was noticed to be the most prominent, it was observed that the ion-exchange step did not change its magnitude (**Figure 25b**). However, alkaline treatment lowered the intensity causing to drop close to zero when the concentration of NaOH used was 0.4 N or above. These results, in conjunction with those regarding the texture properties, further support that a process rendering the crystal structure amorphous was occurring as result of the alkaline treatment.

Measurements of the acid site concentration was done using NH_3-TPD and the results are presented in **Table 4**. The readings obtained were characterized by the presence of two distinct peaks: one at 175°C and a second around 400°C (see **Figure 19)**. In the literature, the first peak (weak) has been attributed to surface hydroxyl groups while the second (strong) has been related to the structural acidity (Lewis and Brönsted acid sites) [118].

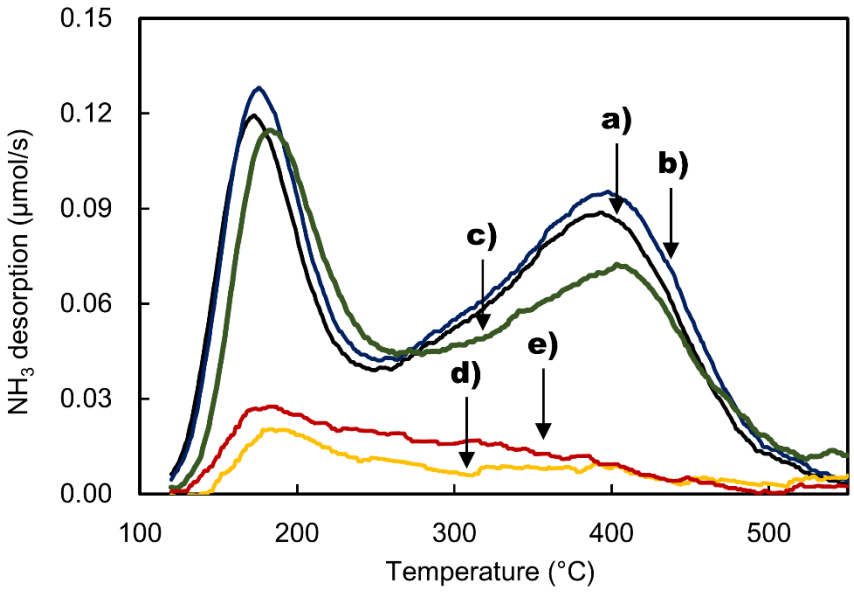

Figure 26. NH_3-TPD of samples SAPO-34 (a) and H-SAPO-34 (b); and alkaline-treated samples 0.2 NaOH (c), 0.4 NaOH (d) and 0.6 NaOH (e).

Similar to the results observed in the texture properties and crystal structure, the ion-exchange step did not have any significant effect on the acidity. Moreover, when analyzing the effect of the alkaline treatment, it was noticed that this step decreased the acid concentration, and in the case of samples treated with a NaOH concentration of 0.4 and 0.6 N, the characteristic two peaks were no longer observed (see **Figure 26**), while an irregular signal was obtained from which it was not possible to distinguish a point of inflection. It was concluded that the process could have led to an uncontrolled de-metallization of the catalyst (likely Al and P) which in turned caused the elimination of acid sites [101].

Table 4. Summary of the acid concentration measured via NH_3-TPD

Catalysts	**Concentration of acid sites (µmol/$g_{SAPO-34}$)**		**Ratio**
	Weak (W)	**Strong (S)**	**W/S**
SAPO-34	1064	1809	0.59
H-SAPO-34	1072	1830	0.59
0.2 NaOH	1106	1427	0.78
0.4 NaOH (total)	459*	–	–
0.6 NaOH (total)	613*	–	–

*Distinction between weak and strong acid sites was not possible

3.2.2. **Coke deposition test**

As described in the experimental section, the prepared samples were subjected to coke accumulation using dimethyl ether (DME) as carbon source. The weight gain related to coke deposition was recorded (see **Figure 27)** and the coke in the spent catalyst was extracted using GC-MS as shown in **Figure 28**.

As observed in **Figure 27**, the deposition of coke in the untreated samples, SAPO-34 and H-SAPO-34, displayed similar behavior over time-on-stream, reaching both coke gain values of 12.32 and 12.33% respectively, after 8 minutes of DME exposure (see **Table 5**). In contrast, samples treated with NaOH showed lower coke gains in the same time frame. For instance, an alkaline treatment of 0.2 N led to a coke gain of 7.52% while treatments of 0.4 and 0.6 N led to values of 2.10 and 1.56%, respectively.

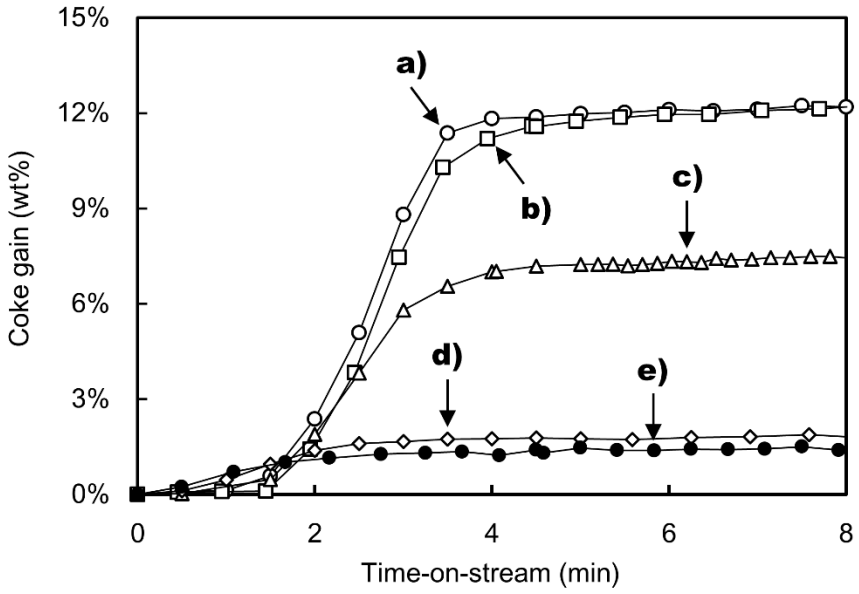

Figure 27. Evolution of the coke gain over time-on-stream for un-treated samples SAPO-34 (a) and H-SAPO-34, and alkaline-treated samples, 0.2 NaOH (c), 0.4 NaOH (d) and, 0.6 NaOH (e).

The identification of coke molecules via MS indicated that polycyclic aromatics were the only species found, though each sample presented a different peak distribution which led to small variations in the coke average molecular weight (see **Table 5**). No correlation was possible to determine between the treatment conditions and the type of molecules preferentially formed. Three main groups were identified in the spent catalyst. Group 1 corresponded to naphthalene

molecules presenting one or multiple methyl groups, saturated molecules were not seen. Group 2 was composed of species having three benzene rings in different configurations such as phenanthrene, phenalene and anthracene. Moreover, these species were identified in their saturated forms or presenting one or two methyl groups. Finally, group 3 was composed of pyrene molecules, saturated or having just one methyl group.

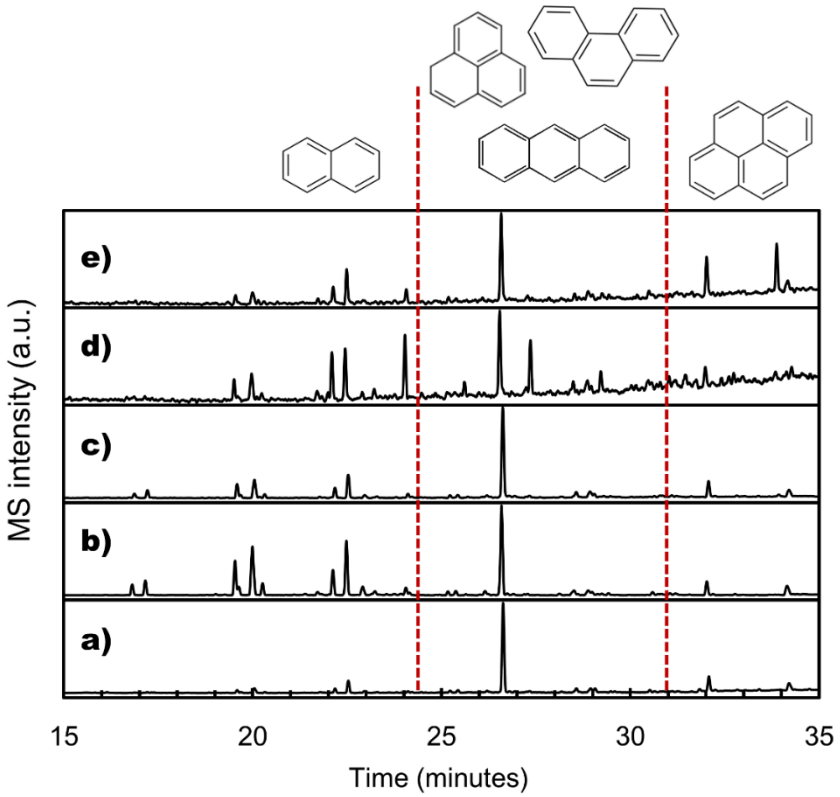

Figure 28. GC-MS chromatographs of the coke molecules extracted from the spent catalyst including SAPO-34 (a) H-SAPO-34 (b), and alkaline-treated samples 0.2 NaOH (c), 0.4 NaOH (d) and 0.6 NaOH (e). Coke molecules were identified mainly in three families: naphthalene, phenanthrene/anthracene/phenalene and pyrene; each group also included also their respective methylated forms.

The formation of polycyclic aromatics from methanol and DME is widely believed to originate from a combination of oligomerization and condensation reactions involving said oxygenated molecules and light olefins [119,120]. The system under study, however, presented strong diffusion limitations, for instance, DME is well-known to slowdown the mobility of molecules inside SAPO-34 due to a hindrance effect [61]. In addition, it is thought that said effect could have been accentuated because the system employed was a static type, in which no flow was taking place on the particle external surface, and so, this could have favored species build-up. Based on these two observations, it can be deduced that molecule retention led to a straight

conversion of DME to oligomer and aromatic molecules with an insignificant release of light olefins or paraffins in the process. The growth process reached a maximum size of four benzene rings (pyrene), as such species has been suggested to be the largest molecule to mature inside SAPO-34 cages [63,65].

Further analysis was done with the objective of quantifying the effect of the coke molecules on the availability of the acid sites. A summary of the weight gain during coke accumulation, time of deactivation, average coke molecular weight and the acid sites-to-coke molecule ratio are presented in **Table 5**.

Table 5. Summary of the catalyst performance obtained from the coke deposition testing using DME as carbon source over different untreated and treated catalysts

Catalysts	Coke gain (%)	Deactivation time (min)[a]	Coke MW_{ave} (g/mol)	Acid site/coke molecule
SAPO-34	12.32	3.20	179.8	3.68
H-SAPO-34	12.33	3.37	169.6	3.50
0.2 NaOH	7.52	3.14	173.5	5.4
0.4 NaOH	2.10	2.29	172.2	6.6
0.6 NaOH	1.56	2.64	185.7	10.9

[a] Deactivation time was considered as time span required to achieve 90% of the final coke gain.

Overall, results indicated that the treatment had a negative effect on the load capacity of the catalyst, which is to say that the catalyst was left with a lower number of acid sites capable of undergoing deposition. Moreover, the time of deactivation was found to be reduced accordingly to the values computed. Indeed, SAPO-34 and H-SAPO-34 required no less than 3.2 minutes to achieve 90% of the final coke gain, meanwhile, alkaline-treated samples, 0.2, 0.4 and 0.6 N, required 3.17, 2.29 and 2.64 minutes respectively. Should a longer time was required to achieve 90% of the coke gain in alkaline-treated samples, despite the lower acidity, it could be possible to consider an enhancement in the performance. However, the results pointed out clearly that the treatment did not achieve the desired goal.

Furthermore, the computing of the acid site-to-coke molecule ratio illustrated on the negative effect of coke on the accessibility of acid sites (see **Table 5**). As observed, all values were above

one, suggesting that the formation of coke caused the blocking of multiple acid sites. The way in which coke accumulated in SAPO-34 has been underscored by More and co-workers, who studied the time and space evolution of coke in a SAPO-34 crystal grain using a combination of UV-Vis microscopy and a confocal fluorescence microscope [121]. Their results indicated that the wave of coke formation started on the outer layers of the grain, and so, the volume comprised in the inner layers presented a significant less crowded population of aromatic molecules. A description of the account is represented in **Figure 29**.

The obstruction generated by the coke molecules revealed the potential of increasing the catalyst lifetime by introducing a secondary mesoporous structure. If it is assumed that the addition of an intra-particle mesoporous structure to the microporous SAPO-34 were done with a minimum destruction of the framework (i.e. < 10%), thus, maintaining a similar number of acid sites; then, the extra channels added could lower the ratio (coke-to-acid site) from 3.68 and 3.5 closer to 1. The latter value would correspond to a coke molecule affecting only one acid site, and thus, achieving the best possible use of the catalyst. If such value were reached, this would imply that the catalyst lifetime could be increased close to threefold.

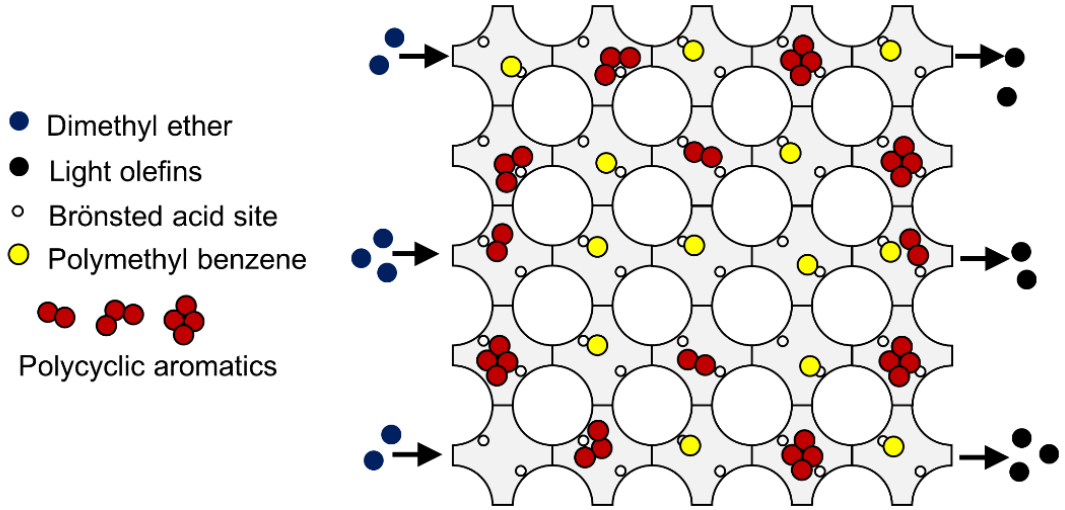

Figure 29. Hypothetical two-dimensional representation of the conversion of DME to coke. Polycyclic aromatics are formed in the outer layers of the catalyst, restricting the access of DME to the still active sites in the inner layers.

3.3. Conclusions

In this chapter, the effect of the alkaline treatment on the physico-chemical properties of a SAPO-34 composed solely of a microporous structure was investigated, as well as, their performance in the conversion of DME to coke molecules. And so, the following conclusions were obtained:

Physico-chemical properties

- The original SAPO-34 and H-SAPO-34 (ion-exchanged sample) displayed texture, crystal structure and acid properties consistent with a SAPO-34 crystal phase. However, after samples were treated with an alkaline solution, the original said properties were reduced as supported by XRD and NH_3-TPD measurements. More importantly, the alkaline treatment did not lead to a positive trade-off between the loss of the microporous volume and the onset of an intra-particle mesoporous structure, a feature commonly seen in zeolites with successful results (i.e. MFI and MOR).

Coke deposition test

- Analysis of the spent catalyst through HF dissolution and GC-MS identification showed that polycyclic aromatics including naphthalene, phenanthrene, phenalene and anthracene, pyrene, and un-substituted forms thereof, were the common species found in coke.
- The analysis of the coke gain and deactivation time, which is the time required to achieve 90% of the final coke gain, demonstrated that the alkaline treatment did not have any benefit, and in fact, it was concluded that this only reduced the efficacy of the catalyst.
- The analysis of the acid site-to-coke molecule ratio suggested that DME turned rapidly into large polycyclic aromatics in the outer layers of the particle, which restricted the access of DME to the inner layer of the particle. Based on the ratio value obtained in SAPO-34 and H-SAPO-34, 3.68 and 3.50 respectively, it was concluded that by providing a mesoporous structure to the microporous volume, it could be possible to lower this value which would imply an increase in catalyst lifetime.

Chapter 4. Effect of temperature in the conversion of methanol to olefins (MTO) using an extruded SAPO-34 catalyst

Effet de la température pour la conversion du méthanol en oléfines (MTO) en utilisant un catalyseur de SAPO-34 extrudé

Résumé:

La réaction de MTO a été étudiée dans un réacteur à lit fixe en utilisant un catalyseur extrudé composé d'une SAPO-34 commercial (65% pourcentage en poids, wt%) incorporé dans une matrice amorphe de $Si0_2$ (35 wt%). Les propriétés de texture, l'acidité et la structure cristalline de la SAPO-34 pure ainsi que sa forme extrudée (E-SAPO-34) ont été analysées et les résultats ont indiqué que l'étape d'extrusion n'affectait pas les propriétés du catalyseur. Ensuite, l'E-SAPO-34 a été testée dans une plage de température variée entre 300 et 500°C, en utilisant un mélange de méthanol aqueux (teneur en eau de 80 wt %) alimenté à une vitesse volumique de 1.21 h^{-1}. A 300°C, une faible conversion a été observée le tout combiné avec une désactivation du catalyseur, ayant été attribuée aux réactions d'oligomérisation et condensation. L'analyse du coke a montré la présence d'hydrocarbures diamandoïdes, reconnus comme étant des molécules inactives dans le procédé MTO. A des températures plus élevées, un état quasi stationnaire a été atteint pendant une réaction de 6 h, où la température optimale a été identifiée à 450°C, ayant conduit au dépôt de coke le plus bas combiné au rapport H/C le plus élevé. Au-dessus de 450°C, des abruptes poussées d'éthylène et de méthane ont été associées à une combinaison de réactions de transfert d'hydrogène et de craquage protolytique. Enfin, le présent travail a permis de mettre en évidence l'efficacité de la technique d'extrusion pour tester les catalyseurs dans des conditions de banc d'essais.

Auteurs et affiliations:

Castellanos-Beltran, Ignacio J:

Département de génie chimique et de génie biotechnologique, Faculté de Génie, Université de Sherbrooke. La Chaire de Recherche Industrielle sur l'Éthanol Cellulosique et les Biocommodités (CRIEC-B)

Palla Assima, Gnouyaro:

Département de génie chimique et de génie biotechnologique, Faculté de Génie, Université de Sherbrooke. La Chaire de Recherche Industrielle sur l'Éthanol Cellulosique et les Biocommodités (CRIEC-B)

Lavoie, Jean-Michel:

Département de génie chimique et de génie biotechnologique, Faculté de Génie, Université de Sherbrooke. La Chaire de Recherche Industrielle sur l'Éthanol Cellulosique et les Biocommodités (CRIEC-B)

Date de submissions: 13-Sep-2017

Revue Scientifique: Frontiers of Chemical Science and Engineering

Effect of temperature in the conversion of methanol to olefins (MTO) using an extruded SAPO-34 catalyst

Ignacio Jorge Castellanos-Beltran[1], Gnouyaro Palla Assima[1], Jean-Michel Lavoie[1*]

[1]Université de Sherbrooke, Chaire de Recherche Industrielle sur l'Éthanol Cellulosique et les Biocommodities (CRIEC-B). 4070, boul. de Portland, Sherbrooke, QC, Canada, J1L 2Y4

*Corresponding author: Jean-Michel.Lavoie2@usherbrooke.ca

Abstract

The MTO reaction was investigated in a bench-scale, fixed-bed reactor using an extruded catalyst composed of a commercial SAPO-34 (65 weight percentage, wt%) embedded in an amorphous SiO_2 matrix (35 wt%). The texture properties, acidity and crystal structure of the pure SAPO-34 and its extruded form (E-SAPO-34) were analyzed and results indicated that the extrusion step did not affect the properties of the catalyst. Subsequently, E-SAPO-34 was tested in a temperature range between 300 and 500°C, using an aqueous methanol mixture (80 wt% water content) fed at a weight hour space velocity (WHSV) of 1.21 h^{-1}. At 300°C, a low conversion was observed combined with catalyst deactivation, which was ascribed to oligomerization and condensation reactions. The coke analysis showed the presence of diamandoid hydrocarbons, which are known to be inactive molecules in the MTO process. At higher temperatures, a quasi-steady state was reached during a 6 h reaction where the optimal temperature was identified at 450°C, which incidentally led to the lowest coke deposition combined with the highest H/C ratio. Above 450°C, surges of ethylene and methane were associated to a combination of H-transfer and protolytic cracking reactions. Finally, the present work underscored the convenience of the extrusion technique for testing catalysts at simulated scale-up conditions.

Keywords: MTO, SAPO-34, temperature, extrusion, coke, light alkanes.

Graphical abstract:

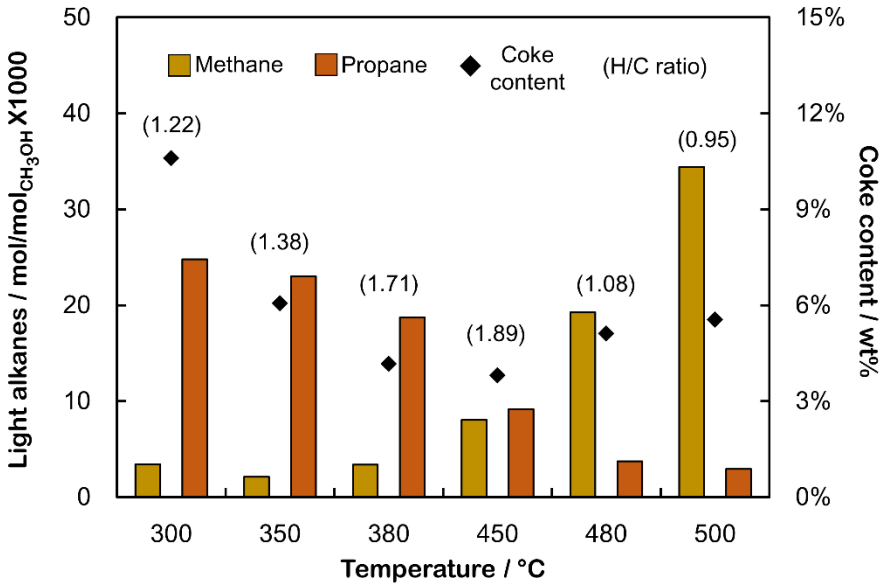

Acronyms:

MTO: Methanol to olefins

P-SAPO/E-SAPO: Pure SAPO-34/Extruded SAPO-34

WHSV: Weight hour space velocity

PMB: Polymethylbenzenes

DME: Dimethyl ether

C_{4-6}: Large hydrocarbons including alkanes and alkenes

MHC: Methanol conversion to hydrocarbons (alkanes and alkenes)

EPR: Ethylene-to-propylene ratio

H/C: Atomic hydrogen-to-carbon ratio measured in the coke retained in the spent catalyst

wt%: Weight percentage

RC: Relative crystallinity

CS: Crystallite size

HTI: Hydrogen transfer index

Δ_R: Differences of consecutive EPR and their related temperature differences

4.1. Introduction

Ethylene (C_2H_4) and propylene (C_3H_6) are light olefins highly valued in the chemical industry, as they are compulsory in the fabrication of a wide variety of commodities including PVC, polycarbonates, LDPE and HDPE, polyurethane, nylon, motor fuels and others [17]. By 2016, ethylene and propylene global production were around 150 and 80 million metric tons respectively, and are expected to increase in the following years [122]. Accordingly, the propylene market is expected to grow at a faster relative pace which is mainly ascribed to the expansion of the polypropylene demand (and derivatives), accounting for 58% of the propylene use in 2000 [1,123]. This upsurge in propylene has created a strong disparity between the selectivity capable to accomplish the current production infrastructure and the market demand, which in turn has caused an increase in the propylene price. It is therefore expected that any new olefin technology should look to offset this gap by adjusting the ethylene-to-propylene ratio [1].

At the present moment, the production of light olefins originates mainly from energy-intensive and fossil fuel processes such as steam cracking of ethane and naphtha (predominantly), and fluidized catalytic cracking (FCC) and paraffin dehydrogenation [17,124]. Consequently, their production is strongly linked to the availability and cost of fossil fuels. However with the recent planetary resolutions resulting from the COP21 agreement and the increasing awareness of the public on global warming and climate change, the urgency of developing and implementing green alternatives has been emphasized prior to further increasing the existing production capacity. As such, the methanol-to-olefin (MTO) process, a chemical route discovered by Mobil scientists during the 70s, has demonstrated to be a viable (technically and economically) substitute for the production of light olefins [3]. The MTO process is an interesting alternative because methanol required for the reaction can be generated by thermochemical conversion of syngas, which in turn can be produced from natural gas reforming, and/or renewable resources such as biomass and municipal solid waste gasification [125]. Hence, one may realize that by diversifying the syngas source, it becomes feasible to implement green alternatives to the existing production infrastructure.

Catalysts typically used in the MTO process are microporous solid acids including zeolites and zeotype molecular sieves, among which H-ZSM-5 and SAPO-34 equipped with a MFI and CHA framework type respectively, provide the best performances as result of the combined effect of their internal topology and acid strength [33]. At industrial scale, SAPO-34 has been selected by UOP-Norsk Hydro and the Shenhua group for the production of polymer-grade olefins reaching similar performances in methanol conversion and light olefin selectivity [35,36]. In contrast, Shell developed a unique Methanol-to-Ethylene process (MTE) using a SAPO-34 in which nickel was incorporated in the native framework. The process is not disclosed, however the patent states an ethylene selectivity as high as 90% (carbon based) and full conversion of methanol are achieved [90,92].

The selection of SAPO-34 in the MTO reaction originates mainly from its high selectivity for ethylene and propylene combined with a full conversion of the methanol [44]. SAPO-34 is a small-pore crystal with mild acid strength, hydrothermal stability and a cage-type framework composed of double six-membered rings stacked in ABCABC configuration, leading to 3.8 × 3.8 Å pore openings and 11.0 × 6.5 Å cages [44]. The geometry combined with the small internal dimensions are responsible for the preferential formation of light olefins, nonetheless, they are also responsible for the fast deactivation associated with trapping and condensation of organic molecules into inactive polycyclic aromatics [45]. To avoid this, water has extensively been used and was shown to enhance both light olefin selectivity and catalyst lifetime by acting as a competitor for strong acid sites due to its polar nature [85]. Also, the dilution of methanol combined with the higher heat capacity of water allows the latter to behave as a “heat-sink” countering the exothermal nature of the MTO reaction (-100 to -300 cal/g depending on olefin selectivity) [45]. Furthermore, water has been reported to induce the hydration and conversion of Lewis acid sites to Brönsted types (BAS) [126]. The latter are well-known to catalyze the MTO reaction, while the former have been linked to enhancing secondary reactions leading to coke deposition [127].

The conversion of methanol to olefins is believed to start with the partial dehydration of methanol into dimethyl ether (DME) [66]. Conversely, the formation of the first C–C bond is not well-understood to date and more than 20 mechanisms have been proposed including oxonium ylide mechanism, carbene mechanism, free radical mechanism and carbocation

mechanism, etc. [3]. In the last years, a big leap in understanding the reaction occurred from the "Hydrocarbon pool" mechanism proposed by Dahl and Kolboe [48]. In this novel concept, the authors stated that methanol molecules initially undergo a set of reactions to produce polymethylbenzenes (PMB), which subsequently catalyze the conversion of methanol to olefins (and water). Later studies on MTO led to the conception of two (hypothesized) catalytic routes, pairing and/or side-chain [55]. Further support on the mechanism was obtained from isotopic studies underscoring the high activity and involvement of PMBs in the reaction, therefore reducing the interest in explaining the formation of the first C-C bond [128].

Generally, solid acids including zeolites and zeotypes are synthesized as powders. At laboratory scale, hundreds of milligrams of catalysts are compacted into tablets, crushed and sieved to produce micrometer to millimeter-size particle, which are then used in small reactors to avoid clogging. When scaling-up to pilot or medium-size (bench) scales, such method becomes inadequate and therefore catalyst (powder) must be mixed with binders to prepare "macroscopic forms" [96]. To this purpose, extrusion is one of the most commonly used method for the preparation of fixed-bed catalyst, which involves multiple steps including paste mixing, extrusion, drying, as well as thermal and chemical treatments [95]. The current trend of research on improving MTO technology aims at developing hierarchical type structures [72,73,129] or nanosheets [70,71] to counter the fast deactivation of SAPO-34. Nonetheless, little attention has been put on investigating the performance of SAPO-34 when embedded in a matrix structure simulating conditions closer to industrial scale.

Therefore, to enrich the existing body of work on the performance of extruded catalyst used for the MTO reaction, the present work focused on the preparation, characterization and catalytic testing of an extruded catalyst composed of 65 wt% SAPO-34 and 35 wt% silica. Various characterization techniques were used to assess the effect of the extrusion process on the properties of the original catalyst including texture, acidity and crystal structure. The catalytic testing was performed in a bench-scale, fixed-bed reactor, and focused on the effect of temperature on the selectivity of olefins and light alkanes, as well as the accumulation and characteristics of the coke deposited after reaction. Methanol was diluted with water up to 80 wt% to enhance both light olefin selectivity and catalyst lifetime. Finally, this work aimed at

demonstrating the convenience of the extrusion technique for testing catalyst at simulated scale-up conditions.

4.2. Materials and methods

4.2.1. Catalyst preparation

Zeotype SAPO-34 (P-SAPO-34) was purchased from Advanced Chemical Suppliers. P-SAPO-34 was used to prepare the extruded catalyst (E-SAPO-34) following the procedure reported by Gil and co-workers [15]. E-SAPO-34 was composed of 65 wt% P-SAPO-34 and 35 wt% colloidal silica (Ludox-HS-40 purchased from Sigma-Aldrich) to ensure mechanical strength at the highest possible loading. The viscosity of the initial paste was tuned by adding a temporal binder (hydroxyethylcellulose, HEC) purchased from Fluka. The extrusion process was carried out as follow. P-SAPO-34 was mixed with colloidal silica and vigorously blended for several minutes until a homogeneous phase was obtained. In parallel, HEC and water were mixed and stirred for 5 minutes in a different container, after which point both mixtures were combined into a paste and further kneaded with a large spatula. The paste was then placed in a 50-mL syringe and compressed with a caulk gun forming 5-mm thick cords, which were immediately cut into small cylinders (5-7 mm). The extruded cylinders were dried at low temperature (40°C) for 24 h to avoid fracturing, and then calcined in a tubular furnace to remove the temporal binder (HEC). Calcination was performed under a continuous air flow of 100 mLPM per gram of catalyst, while the temperature was increased 2°C/min from room temperature to 550°C and maintained for 3 h. The calcined solid was afterwards drenched (no agitation) in an ammonium nitrate solution (NH_4NO_3, 2.0 N) for 4 h at 55°C to reactivate acid sites that may have been passivated in previous steps. 10 mL of ammonium nitrate solution was used per each gram of solid. The treated solid was subsequently dried at 120°C for 2 h and re-calcined under conditions similar to the previously described calcination step.

The selection of the 65/35 composition was according to two "*rule of thumb techniques* employed by our industrial partner, Enerkem Inc., for evaluating the impact and crushing properties of the catalyst. For the former, multiple extruded pellets (ready for testing) were dropped from a 1 meter height and it was observed that the physical integrity of the pellets was preserved. As for the crushing resistance, individual samples were pressed with the fingers, wearing nitrile gloves, with the objective of breaking or crushing the pellet. Samples retained their full physical integrity, and so, it was considered that the selected paste mixture had a satisfactory active catalyst-to-permanent binder weight ratio for withstanding any type of

handling during catalytic testing. Higher loadings of active catalyst were also tested (i.e. 70 and 75 wt%), but these did not pass the crushing examination. Attrition resistance was not taken into consideration since the catalyst was not exposed to motion and/or high gas flow, as it would occur inside a fluidized reactor. These *"rules of thumb techniques"* proved to be reliable as, upon reaction, the spent catalyst was still presenting the initial cylindrical form. Nonetheless, it is important to mention that small amounts of a gray powder residue was recovered with the bed supporting material, which could have been released by the catalyst.

4.2.2. Catalyst characterization

4.2.2.1. Nitrogen adsorption-desorption isotherm

The nitrogen adsorption isotherm was obtained using a Micrometrics 2020 ASAP apparatus. Samples (60-100 mg) were placed inside a glass cell and put under vacuum at 100°C for 1h, and subsequently heated up to 350°C and kept for 8 h prior to characterization. The Brunauer-Emmet-Teller (BET) surface area was calculated from the adsorption isotherm at relative pressure (P/P_o) between 0.05 and 0.15. The total pore volume was determined from the nitrogen amount adsorbed at a P/P_o of 0.98. The external surface area and the microporous volume were calculated using the t-Plot method [93].

4.2.2.2. X-ray diffraction (XRD)

Analysis of the crystal structure was performed with a Panalytical X'Pert Pro Multipurpose Diffractometer (MPD), powered by a Philips PW3040/60 X-ray generator and fitted with a PIXel 1D detector. Diffraction data was acquired (2θ between 5 and 40°) by exposing the powder samples to a Cu-K_α X-ray radiation, which had a characteristic wavelength (λ) of 1.5418 Å. X-rays were generated from a Cu anode supplied with a voltage of 40 kV and a current of 50 mA. The relative crystallinity of the extruded catalyst was calculated according to **Eq 4.1** and the crystallite size by using the Scherrer equation (**Eq 4.2**):

Relative crystallinity (RC):

$$RC\ (\%) = \frac{E\text{-}SAPO\text{-}34\ Area_{[101]}}{P\text{-}SAPO\text{-}34\ Area_{[101]}} \times 100 \qquad \textbf{(Eq 4.1)}$$

The area of the crystal plane [101] was selected as reference because it showed the highest intensity.

Crystallite size (CS):

$$CS\ (\%) = \frac{K\lambda}{\beta \cos(\theta)} \qquad \textbf{(Eq 4.2)}$$

, where K is the dimensionless shape factor (0.9), λ is the X-ray wavelength (1.5418 Å), β is the line broadening at half the maximum intensity (FWHM) at the 2θ angle and θ is the Bragg angle.

4.2.2.3. Ammonia temperature program desorption (NH_3-TPD)

Acidity was measured using a chemisorption analyzer operated manually from 100 to 700°C using a 5°C/min temperature ramp. Prior to the adsorption and desorption of NH_3, samples (150-200 mg) were placed in a oxidizing atmosphere (He-O_2) at 450°C for 1 h to remove water and any other organic residue. This technique allows measuring the amount of acid sites in the catalyst, as well as to classify them as weak and strong depending on the desorption temperature of the peak. The separation of the signal into different acid strengths was done according to the temperature of inflection between the two desorption peaks [42]. For a representative comparison, the temperature of inflection of the pure catalyst was applied to the extruded catalyst.

4.2.2.4. Coke quantitative and qualitative analysis

The coke content in the spent catalyst was obtained by thermogravimetric analysis (TGA) using a TA instrument TGA model Q500. Samples (20 – 30 mg) were heated up from room temperature to 900°C at 10°C/min under an air atmosphere. The coke content was then calculated based on the sample weight difference between 220 (water-free) and 900°C (water-/coke-free). Total hydrogen (H), carbon (C), and oxygen (O) were measured using a ThermoFischer Scientific Flash 2000 CHS/O analyzer. The analyzer was calibrated using a set of 5 standards, each with a different concentration. The temperature of the analyzer was set at 960°C for measuring C and H content and at 1040°C for measuring O content.

The oxygen content measured by the elemental analyzer was assumed to originate from physisorbed water. It was thus used to calculate, via basic stoichiometric relationships, the

hydrogen contribution of water in the spent catalyst. Hydrogen present in the coke molecules was obtained by subtracting the hydrogen of water from the total hydrogen measured. The total carbon content measured did not require any further manipulation since unreacted catalyst showed no traces of organic molecules. Finally, both the hydrogen and carbon content of coke molecules were used to compute the H/C atomic ratios. For each, the following equation was used:

$$\frac{H}{C} = \frac{\frac{H_{Total} - H_{H_2O}}{AW_{H\ atom}\ (g/mol)}}{\frac{C_{Total}}{AW_{C\ atom}\ (g/mol)}} \qquad \textbf{(Eq 4.3)}$$

, where AW stands for atomic weight of the element.

4.2.2.5. Identification of coke molecules

The extraction and identification of coke molecules accumulated in the spent catalyst was done following the procedure reported by Magnoux and co-workers [94]. For each experiment, approximately one gram of spent catalyst was dissolved in a 51 wt% hydrofluoric acid (HF) solution. The organic phase was then extracted with dichloromethane (CH_2Cl_2) and then analyzed using a GC-MS (Agilent GC model 7890A and MS model 5975C) equipped with an Agilent DB-1 capillary column (60 m×0.32 mm×5.0 μm). The following temperature program was employed: isothermal at 40°C for 10 min, followed by heating at 2°C/min up to 130°C, then heating at 40°C/min up to 200°C, which was maintained for 35 min.

4.2.3. MTO bench-scale setup and procedures

Catalytic reactions were carried out in a fixed-bed stainless steel reactor (I.D. =2.03 cm, L=100 cm) placed in a tubular oven equipped with a temperature controller. Silicon carbide (SiC) was placed above and below the catalyst bed to serve as fluid distributor and support. Prior to each MTO experiment, the extruded catalyst (30 g) was activated overnight at 500°C with a constant flux of nitrogen (0.5 LPM). The procedure was done gradually (< 3°C) to ensure homogenous temperature along the catalyst bed. After activation, the temperature was set to the experimental temperature (300, 350, 380, 450, 480, 500°C), after which the aqueous mixture was fed at a WHSV of 1.21 h^{-1} for 6 h.

The methanol used was provided by **Enerkem Inc**. (99.7 wt%, IMPCA grade) and was mixed with distillate water to make up the feeding solution. The latter was then injected in the MTO system using a HPLC pump.

The reactor outlet stream was cooled down to 18°C with a chiller, allowing a gas separation from the condensable phase. The gas products were analyzed and quantified using an on-line GC (Agilent Technologies, model 7820A) equipped with flame ionization (FID), a thermal conductivity detectors (TCD) and an Agilent HP-Plot Q capillary column (30 m×0.25 mm×1.4 μm). The following temperature program was employed: isothermal at 40°C for 2 min, heating at 20°C/min up to 120°C (maintained for 1 min), then heating at 30°C/min to 220°C (maintained for 5 min).

The carbon content in the liquid was quantified by injecting 5-8 μL samples in the external port of the GC equipped with an FID. The GC peak areas were divided by the weight and compared to a methanol calibration curve also standardized by sample weight. Injections showed that the prominent residues in the liquid were methanol and DME. Only 0.84% of the initial carbon was found in the liquid phase, except in the case of the experiment performed at 300°C in which ca. 11.6% of carbon (as methanol) was measured.

The carbon mass balance of each experiment was calculated based on the sum of three independent outputs: gas (GC), liquid (GC) and solid phases (TGA & elemental analysis). Then, the difference of carbon (missing carbon) was calculated by subtracting the carbon fed (methanol input) and the obtained sum. Differences consistently showed less than 5.6% of missing carbon.

4.2.4. **Data evaluation**

Weight Hour Space Velocity (WHSV):

$$WHSV\ (h^{-1}) = \frac{Massic\ flow\ rate\ of\ feed\ (^{g}/_{h})}{Mass\ of\ SAPO{-}34\ in\ extruded\ catalyst\ (g)} \qquad \textbf{(Eq 4.4)}$$

Conversion of methanol to hydrocarbons (MCH):

$$MCH\ (C\ wt\%) = \frac{mass\ of\ carbon\ atoms\ in\ hydrocarbons\ (^{g}/_{h})}{mass\ of\ carbon\ atoms\ in\ methanol\ fed\ (^{g}/_{h})} \times 100 \qquad \textbf{(Eq 4.5)}$$

Ethylene-to-propylene ratio (EPR):

$$EPR\ (\%) = \frac{Ethylene\ [molar\ \%]}{Propylene\ [molar\ \%]} \times 100 \qquad \textbf{(Eq 4.6)}$$

Hydrogen transfer index (HTI):

$$HTI\ = \frac{Propane\ [molar\ \%]}{Propane\ [molar\ \%] + Propylene\ [molar\ \%]} \times 100 \qquad \textbf{(Eq 4.7)}$$

Differences of consecutive EPR and their related temperature difference (Δ_R):

$$\Delta_R = \frac{EPR_i - EPR_j}{T_i - T_j} \qquad \textbf{(Eq 4.8)}$$

4.3. Results and discussion

4.3.1. Physico-chemical properties

Micro-imaging of the native (P-SAPO-34) and extruded SAPO-34 (E-SAPO-34) are displayed in **Figure 30**. P-SAPO-34 shows a distinctive rhombohedral morphology in which the lattice constant of one of the three axis differs (a=b≠c). Dimension analysis using an imaging software (ImageJ) revealed that the SAPO-34 particles had an average size of 2.1 μm and presented a large standard deviation of 0.5 μm (≈ 25%). In the E-SAPO-34 catalyst, particles revealed an accumulation of permanent binder around the surface and edges. However, close analysis of the particles indicated that no changes in shape and dimension were observed, nor particles fusion as result of the extrusion process.

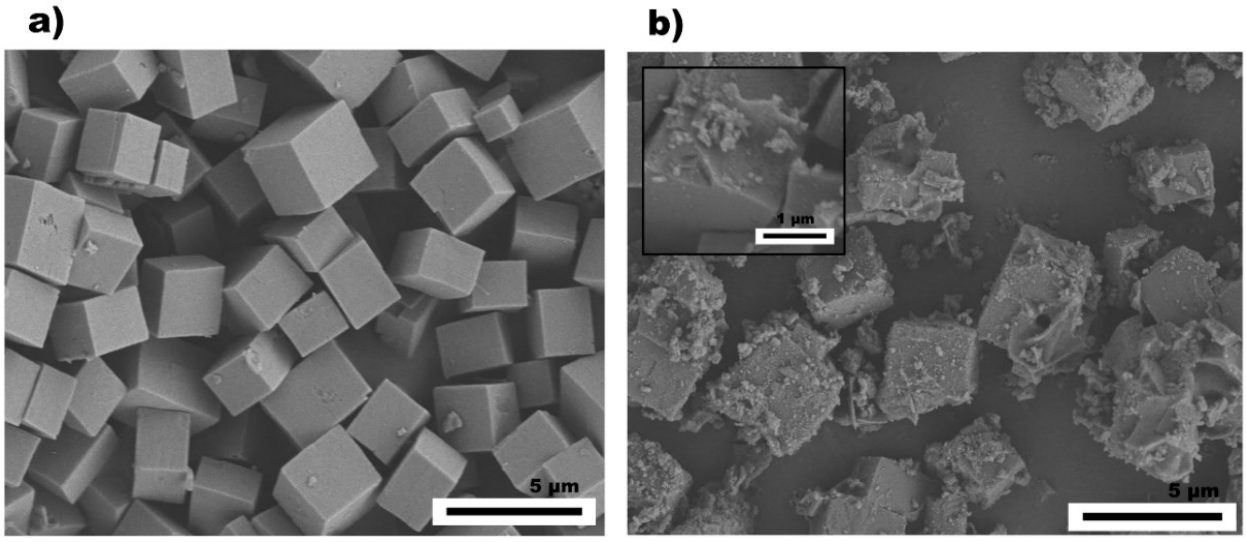

Figure 30. Scanning electron microscope images of (a) P-SAPO-34 (5,000x), (b) E-SAPO-34 (5,000x), and (b-inset) magnified E-SAPO-34 surface (30,000x)

Crystallinity and other related features were determined via XRD analysis, for which the patterns are presented in **Figure 31**. The characteristic crystal planes of SAPO-34 including [101] (Strongest signal), [110], [021], [211], [401] and [015] were observed in both P-SAPO-34 and E-SAPO-34. The permanent binder employed (amorphous silica) was not detected by XRD. Relative crystallinity and crystallite size are presented in **Table 6**. The calculated relative crystallinity of E-SAPO-34 was 68.5%, whose close proximity to the loading value (65%) indicated the presence of the permanent binder in the extruded catalyst. Both catalyst, pure and extruded, were analyzed using the same XRD conditions to ensure a reliable crystallinity

comparison. The variance (≈5.4%) could have been the result of handling and equipment uncertainty. Comparison of the crystallite size showed a difference of ca. 1.7% among samples, supporting that the crystal structure of the native SAPO-34 remained intact after extrusion.

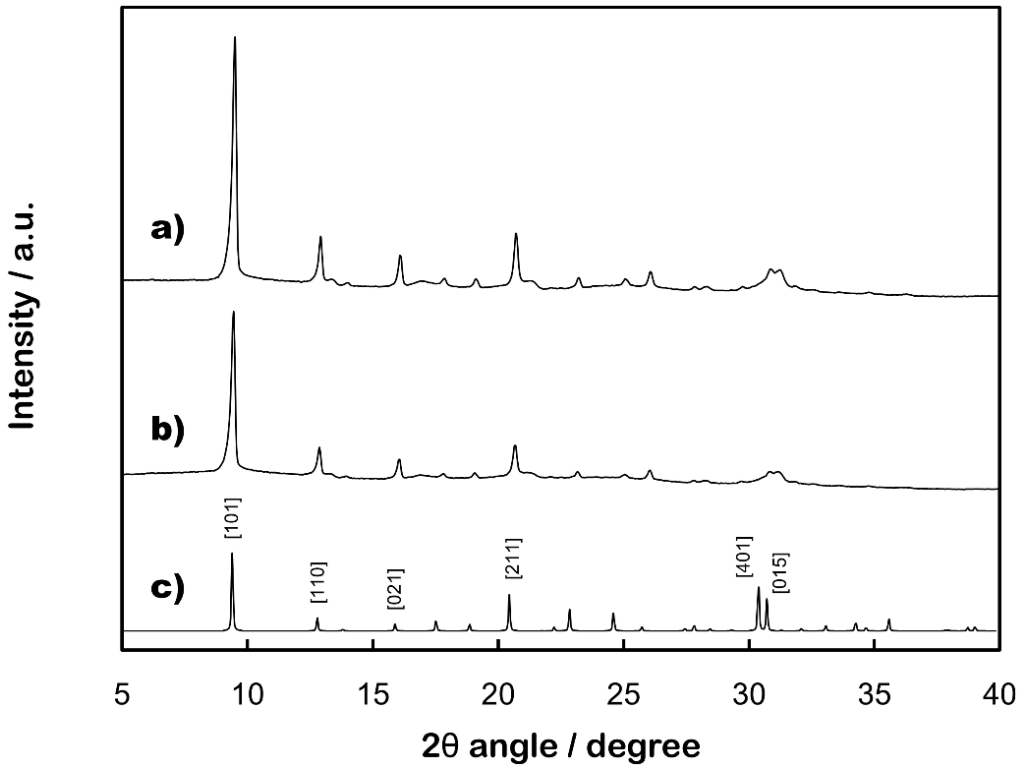

Figure 31. XRD patterns of (a) P-SAPO-34, (b) E-SAPO-34 and (c) SAPO-34 extracted from the IZA database

Texture properties evaluated by N_2 adsorption are summarized in **Table 7**. P-SAPO-34 was composed solely of a microporous structure (pores < 2 nm in diameter, Type I isotherm), whereas the E-SAPO-34 catalyst presented in addition to the microporous structure, a mesoporous one (pores 2-50 nm in diameter, IV isotherm) [93]. The mesoporous structure originated from the interaction of the permanent binder and the SAPO-34 framework. It is worth mentioning that the mesopores formed in E-SAPO-34 were inter- not intra-particle type, since the internal structure of the SAPO-34 particles was not modified. Comparison of the microporous volume showed a slight difference, 0.252 and 0.237 cm^3/g for P-SAPO-34 and E-SAPO-34, respectively. The difference could be ascribed to minor particle occlusion in the extruded catalyst, a feature reported by Gayubo and co-workers when using large amounts of binder (bentonite/alumina at 75%) [97].

Table 6. Crystal properties of the SAPO-34 in powder (P) and extruded (E) form

Samples		SAPO-34 content %	Relative crystallinity %	Cristallite size Nm
SAPO-34	(P)	100.0	100	41.3
	(E)	65.0	68.5	42.0

The results of acid site concentration measured by NH_3-TPD are reported in **Table 7**. Measurements showed the presence of two distinctive peaks. A peak at low temperature (~202°C) ascribed to weakly bonded hydroxyl groups (weak acid sites), and a peak at high temperature (~437°C) attributed to ammonia (NH_3) interacting with Brönsted and Lewis acid sites (strong acid sites) [118]. The overall acidity and weak-to-strong acid site ratio of the pure and the extruded catalysts showed discrepancies of less than 2%, which further supported the notion that the extrusion step did not affect the acidity of the active part.

Table 7 Physico-chemical properties of SAPO-34 in powder (P) and extruded (E) form

Samples		Pore volume $cm^3/g_{SAPO-34}$			NH_3-TPD $\mu mol/g_{SAPO-34}$		
		Total	V_{Micro*}	V_{Meso*}	Total	Weak	Strong
SAPO-34	P	0.252	0.252	0.000	1 348	528	820
	E	0.483	0.237	0.246	1 370	531	839

*V_{Micro} = Microporous volume V_{Meso} = Mesoporous volume

Table 8. Effect of temperature on the conversion of methanol to hydrocarbons (MCH), products molar distribution and performance parameters computed at 2 and 6 h of time-on-stream

		Initial /2 h						Final /6 h					
Temperature / °C		**300**	**350**	**380**	**450**	**480**	**500**	**300**	**350**	**380**	**450**	**480**	**500**
MCH / C wt%		61.8	74.4	85.6	83.5	83.3	84.9	15.8	72.2	80.2	86.1	89.1	91.5
Product molar distribution / %													
Olefins	**Ethylene**	31.0	37.3	48.3	59.9	66.6	64.4	10.1	38.1	49.2	62.4	67.8	66.4
	Propylene	32.8	31.7	29.7	25.1	20.5	16.1	10.7	34.7	31.1	24.7	19.9	17.9
	C_{4-6}	15.6	15.1	10.7	6.3	3.5	2.8	3.2	12.5	9.2	4.8	2.9	2.8
Alkanes	**Methane**	2.0	1.2	1.5	3.3	7.0	14.7	3.1	1.3	1.7	3.6	8.0	10.7
	Propane	16.1	14.0	9.0	4.3	1.6	1.1	5.2	12.1	7.8	3.4	1.2	1.2
Oxygenated	**MeOH**	1.1	0.0	0.1	0.2	0.1	0.2	32.2	0.1	0.1	0.2	0.2	0.2
	DME	1.1	0.0	0.0	0.0	0.0	0.0	35.1	0.4	0.0	0.0	0.0	0.0
EPR / molar		0.95	1.18	1.63	2.38	3.25	4.01	0.94	1.10	1.57	2.53	3.55	3.70
Hydrogen transfer index		0.329	0.310	0.233	0.146	0.072	0.063	0.327	0.259	0.201	0.121	0.057	0.063
			$\Delta_{350-380}$	**$\Delta_{380-450}$**	**$\Delta_{450-480}$**	**$\Delta_{480-500}$**							
Δ_R			1.49	1.22	3.14	2.93							

Table 9. Effect of MTO testing (300 – 500°C) on the catalyst texture properties, coke content and H/C ratio, and coke molecule composition

Temperature / °C			**300**	**350**	**380**	**450**	**480**	**500**
Pore volume $cm^3/g_{SAPO-34}$	V_{Micro}*		0.067	0.135	0.167	0.175	0.144	0.131
	Total		0.270	0.343	0.391	0.408	0.380	0.381
Coke content / wt. %			10.6	6.06	4.17	3.81	5.12	5.55
Coke H/C ratio / atomic			1.22	1.38	1.71	1.89	1.08	0.95
Coke composition	**Adamantanes**	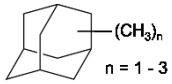	●					
	PMB	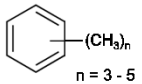	●	●	●	●	●	●
	PCA	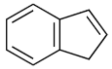	●	●				
		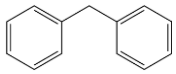	●	●				
		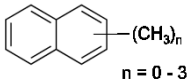	●	●	●	●	●	●
		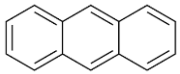	●	●	●	●	●	●
		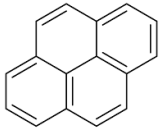				●		

*V_{Micro}: obtained via N_2 isotherm PMB= Polymethylbenzenes PCA= Polycyclic aromatics

4.3.2. Catalytic performances of E-SAPO-34

The effect of temperature in the transformation of methanol to olefins over E-SAPO-34 was investigated in a temperature range between 300 and 500°C. The catalyst performances after 2 and 6 h of reaction were computed and summarized in **Table 8**. The time frame of 2 h was selected as the end of the transient state while 6 h corresponded to the end of the test. The spent catalyst was collected after each reaction and characterized. The results are presented in **Table 9**.

4.3.2.1. Effect of temperature on MTO reaction

At 300°C, the difference between the initial (2 h) and final (6 h) methanol conversion indicated that the E-SAPO-34 catalyst underwent deactivation, as confirmed by the drop in methanol conversion from 61.8 (2 h) to 15.8% (6 h) (**Table 8**). The deactivation was caused by coke accumulation within the E-SAPO-34 micropores, which reached a 10.6%wt. (**Table 9**) after 6 h of time on stream. Such amount of coke was found to be sufficient to occupy 71.7% of the microporous volume, likely nullifying the activity of the active sites close to the external surface. In contrast, methanol access to the remaining active volume (28.3%), which was suspected to be deeper in the SAPO-34 particle, was impeded by coke molecules [121].

The molar concentration of ethylene, propylene and large molecules (C_{4-6}) produced over time are presented in **Figure 32a**. The concentrations of the latter increased rapidly in the early moments to reach a plateau within the first two hours, hereafter followed by a swift drop during the last part of the experiment. The drop in methanol conversion was found to occur along with the onset of dimethyl ether (DME). Methanol and DME concentrations at the reactor outlet are reported in **Figure 32b**. Despite the loss of hydrocarbon production, the catalyst was still active for the partial conversion of methanol to DME. The latter can be attributed to the weak acid sites located on the external surface of SAPO-34, which unaffected by coke deposition, remained functional to catalyze the dehydration of methanol [45].

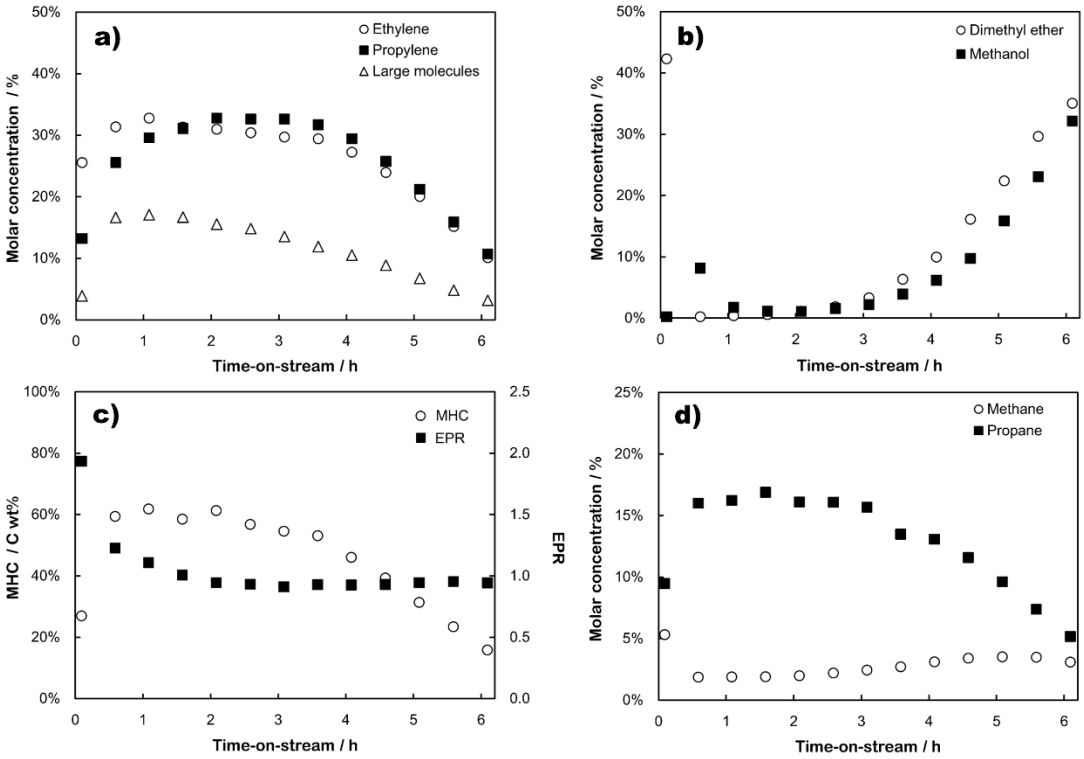

Figure 32. Evolution of the MTO reaction over time at 300°C: (a) molar distribution of light olefins and large molecules (C_{4-6}), (b) molar distribution of oxygenated molecules (methanol and DME), (c) MCH and EPR factors, and (d) molar distribution of light alkanes (methane and propane)

However, the deactivation did not affect the ethylene-to-propylene (EPR) molar ratio, which remained close to 1 (**Figure 32c** and **Table 8**). This is tantamount to the absence of selectivity change during the catalyst deactivation (product shape selectivity) [130], probably due to coke accumulating uniformly along the accessible microporous volume, prompted by the high water content used in the feed (80 wt%).

The evolution of methane and propane molar concentrations over time-on-stream are presented in **Figure 32d**. The tendency found for the production of propane had clear similarities with that of propylene, whereas the methane concentration remained virtually stable. Light alkanes are known to occur in parallel with the accumulation of coke. This is due to the fact that coke molecules require, in addition to the oligomerization, cyclization and condensation reactions, the occurrence as well of hydrogen transfer reactions to be formed. Hydrogen transfer reactions commonly lead to the production of hydrogen-rich species, most prominently propane from propylene [131], while methane is believed to be

generated from surface-methoxy groups. Mechanisms depicting the latter are presented in **Figure 33**.

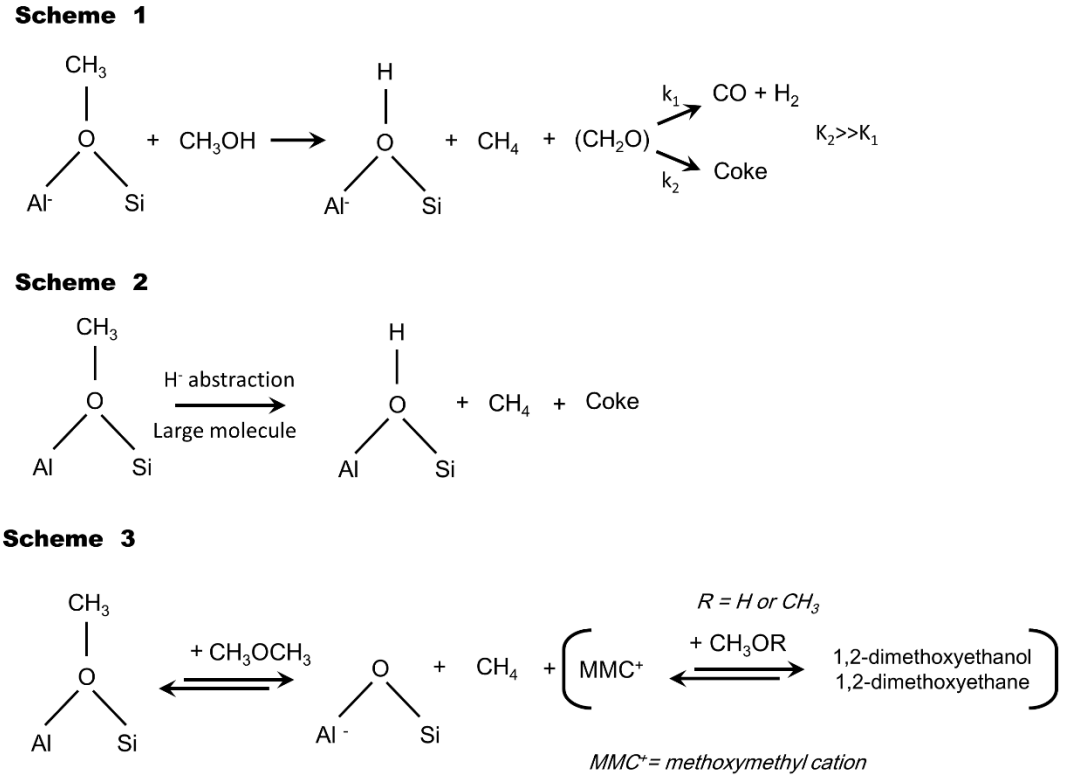

Figure 33. Mechanisms reported in the literature for the formation of methane in the MTO reaction. Scheme 1 was adapted from reference [132], while scheme 2 was extracted from reference [133]. Scheme 3 is a more recent mechanisms developed by Wei and co-workers, in which methane was identified as a by-product of the formation of the early molecules containing the first C-C bond [134]

Overall, the MTO reaction performed at 300°C suggested that methanol conversion to olefins was strongly affected by secondary reactions such as oligomerization and condensation, which are known to be favored at low temperature [76,77]. Such secondary reactions could explain the low production of hydrocarbons and swift deactivation related to the accumulation of coke.

Unlike experiment performed at 300°C, MTO reactions carried out between 350 and 500°C exhibited a quasi-steady state with no evident sign of deactivation between 2 and 6 h of reaction (**Table 8**). By increasing the temperature, it was found that methanol conversion to hydrocarbons evolved sharply to reach a plateau within the first 2 hours corresponding to 74.4, 85.6, 83.5, 83.3 and 84.9% conversion at 350, 380, 450, 480 and 500°C,

respectively. The said plateau was maintained up to the 6 h operation time with standard deviation ranging from 1.5 to 4.6%. Even though no deactivation was observed between 350 and 500°C, a significantly lower ($\Delta_{MCH} \approx$ 10%) methanol conversion was obtained at 350°C as compared to 380, 450, 480 and 500°C. This difference could be ascribed to a fair degree of oligomerization and condensation reactions still occurring at 350°C, but insufficient to lead to catalyst deactivation in the time frame of the experiment. This claim is based on the fact that at 350°C, a lower amount of hydrocarbons is found in the gas phase (see **Table 8**), meanwhile coke in this sample was higher than in the other samples between 350 and 500°C (see **Table 9**). This is further supported by the analysis of the selectivity to carbon in the form of coke as presented in **Table 10**. At 350°C, carbon was being accumulated in the catalyst at a higher rate (with the exception at 300°C).

Table 10. Selectivity to carbon deposition obtained via CHO analysis of the spent catalyst at different temperature

Temperature (°C)	Selectivity to carbon as coke (C wt. %)
350	18.1
380	11.1
450	10.1
480	11.6
500	15.0

Ethylene was found to increase consistently along with temperature between 350 and 500°C, while the production of larger hydrocarbons including propylene and C_{4-6} decreased. Temperature had therefore a positive effect on the EPR, increasing it from 1.18 to 4.01 and 1.10 to 3.70 from 350 to 500°C, at 2 and 6 h respectively. Yet, the effect of the temperature on the EPR was noticed to be stronger above 450°C. Indeed, the computations of the ratios of the consecutive EPR differences and of their related temperature difference (Δ_R) above 450°C ($\Delta_{450-480}$ and $\Delta_{480-500}$) were more than twice of those calculated below 450°C ($\Delta_{350-380}$ and $\Delta_{380-450}$) (**Table 8**). Such finding suggests the occurrence of cracking reactions with increasing temperature, which consequently enhanced ethylene production at the expense of larger molecules. Moreover, it is found that the upsurge of ethylene concentration occurred along with that of methane, which is a species generated from

cracking reactions. Methane concentrations at various temperature (350, 380, 450, 480 and 500°C) are presented in **Figure 34a** which depicts multiple behaviours with raising temperature. At 350 and 380°C, methane concentration was steady at around 2.0%. Then, at 450, 480 and 500°C methane concentration increased to reach maximum values of ca. 3.1, 8.7 and 15.0%, with positive slopes at 450, 480°C and a parabolic plot at 500°C.

In the MTO/SAPO-34 literature, the formation of methane at temperatures above 400°C is commonly ascribed to the mechanism in scheme 2 as reported by Salehirad and co-workers in **Figure 33**. One hypothesis that could explain the high content in methane in our work, besides the aforementioned mechanism, is the occurrence of protolytic cracking reactions involving large molecules [135]. Unlike classic cracking reactions requiring high temperatures (>500°C), protolytic cracking can be triggered at MTO conditions by molecules acting as Lewis acids such as carbocations and/or by Brönsted acid sites (BAS) [131]. This implies that protolytic cracking is therefore impacted by the type and amount of organic molecules (i.e. coke) present in the catalyst. As shown in **Figure 35b**, the suggested mechanism considered that alkene molecules undergo protonation to form an alkoxide intermediate, and next cracking (β-scission) to form a smaller olefin and surface methoxy group (CH_3^+). The suggested mechanism, in fact, complements fairly with the second scheme in **Figure 33**, since methanol and alkenes (with a C=C in the second carbon, i.e. propylene and 2-butene) interacting with BAS become the source of surface methoxy groups. The latter then behave as the H-acceptor molecules leading to the formation of methane, whereas large molecules (R_{LM}) as H-donor. This could explain the increment of coke content and the reduction (in part) of the coke H/C ratio at temperatures above 450°C (**Table 9**).

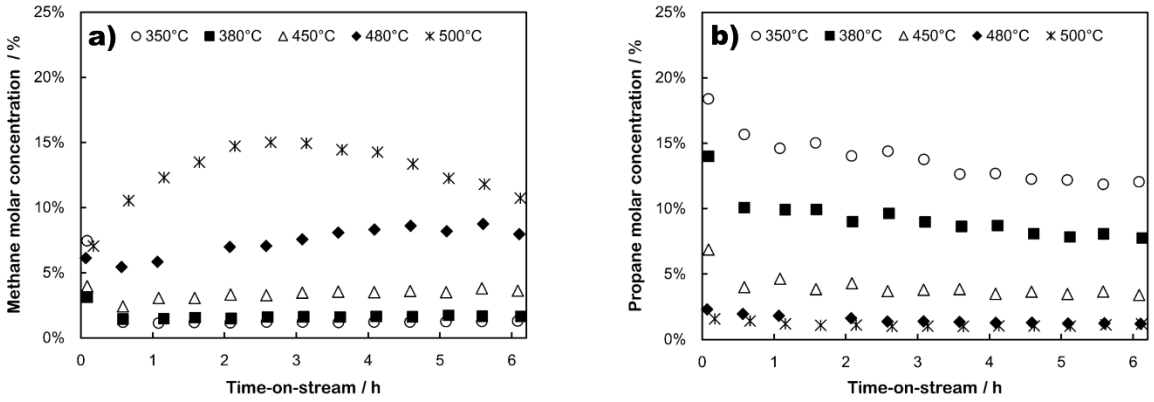

Figure 34. Effect of temperature (350 – 500°C) on the molar concentration of (a) methane and (b) propane over time

This hypothesis is well supported by the drop in production of propylene and large hydrocarbons (C_{4-6}) as temperature reached and/or exceeded 380°C. As presented in **Table 8**, at temperatures ≥380°C, and even though methanol conversion to hydrocarbon and ethylene concentration remained both virtually constant, propylene and large hydrocarbons dropped by 20, 19 and 14% and 48, 39 and 4%, respectively, when temperature was increased from 380 to 450, 480 and 500°C, respectively.

Another hypothesis explaining the high production of methane, and occurring concurrently with the first hypothesis, could be the cracking of substituted aromatics in coke producing methane as result of coke maturation, as explained by Elliott [136] and Milne and co-workers [137]. This hypothesis could explain the drop of the coke H/C ratio found in the spent catalyst above 450°C. Indeed, at 480 and 500°C the H/C ratio decreased to a value ca. 1 for both temperatures suggesting a low amount of substituted aromatics in the coke.

Furthermore, it is important to mention that the reactions suggested above to explain the formation of methane and cracking of hydrocarbons are based on known mechanisms reported in the literature. However, other mechanisms based on radical reactions could be taking place as well, and so they cannot be disregarded. Furthermore, the formation of methane could be favored thermodynamically. The latter is based on the fact that a thermodynamic analysis using the software FACTSAGE 7.0 indicated that feeding methanol, ethylene, propylene, butenes, pentenes or hexenes to a Gibbs equilibrium reactor led to a gas composed of hydrogen, carbon monoxide, carbon dioxide and methane. This result showed that the MTO reaction occurs in a kinetically driven regime.

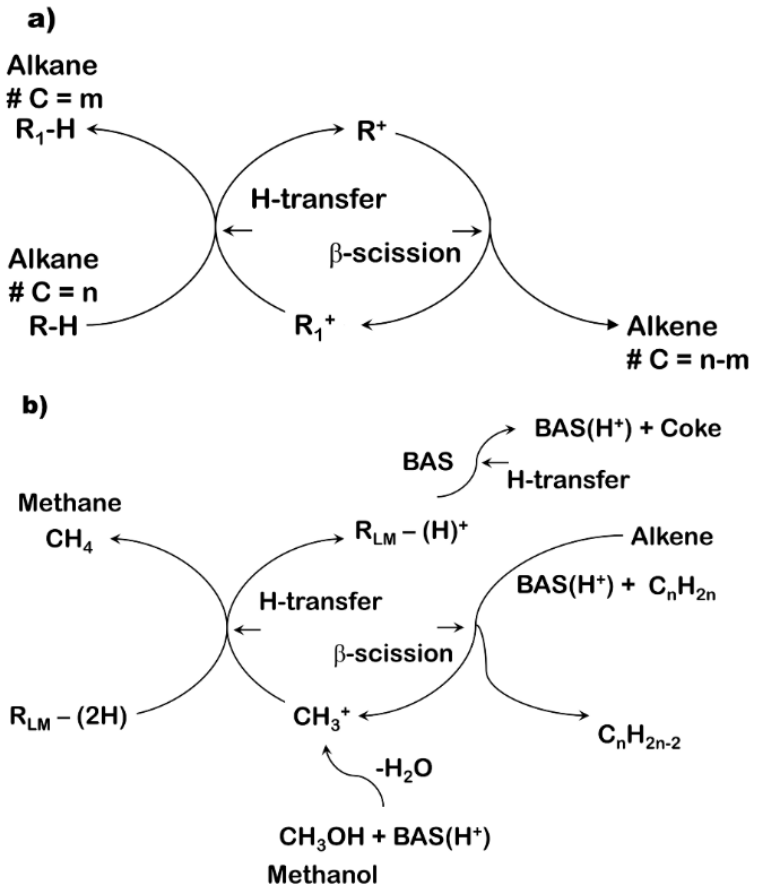

Figure 35. Scheme of (a) the original mechanism proposed by Haag and Dessau in the protolytic cracking of alkanes [135], and (b) the suggested mechanism including the reaction in scheme 2 and protolytic cracking of alkenes explaining the formation of methane at high temperatures

In contrast to methane, propane concentration was found to decrease with increasing the reaction temperature (**Figure 34b**). For instance, propane concentrations decreased steadily from 12.1 to 3.4% in the temperature range between 350 and 450°C above which the concentration remained fairly stable around 1.2% after 6 h reaction. (**Table 8**). The low concentration of propane at 480 and 500°C was unexpected as it was previously shown that propane originated from hydrogen transfer involving propylene, which was still abundant in the medium (above 16%). As propylene was still formed, one could assume that hydrogen transfer reactions were simply not favorable for producing propane at such temperatures. The latter was supported by the drop in the hydrogen transfer index after 6 h (**Table 8**), which decreased from 0.259 at 350°C to a value of 0.057 at 500°C.

The scrutiny of the evolution of light alkanes and the characteristics of coke in the spent catalyst (coke content and coke H/C ratio) showed that the optimal reaction temperature

was 450°C. At this temperature, the olefin production was maximized while light alkanes and coke content were at their lowest values. Furthermore, the coke H/C ratio was the highest indicating the presence of the most adequate coke mixture (polymethylbenzenes) allowing the catalytic conversion of methanol to olefin according to the hydrocarbon pool mechanism.

4.3.2.2. Composition of coke molecules

Coke molecules, formed during methanol transformation in the temperature range studied (300 – 500°C) and trapped inside the micropores of the E-SAPO-34, were extracted with dichloromethane after HF dissolution of the SAPO-34 framework (see the experimental section). Coke molecules were not expected to be formed outside of the catalyst framework given that previous work on the chemical treatment of SAPO-34 (see Chapter 4) had demonstrated it.

The results of identification and quantification of coke molecules are presented together in **Table 9**. Results showed that coke molecules were mainly constituted of polymethylbenzenes and polycyclic aromatics such as indene and benzylbenzene polymethylnaphthalenes, anthracenes, phenanthrene, and pyrenes etc. Interestingly, hydrocarbon diamandoid molecules (methyladamantanes) were also found but only in experiment performed at 300°C. These molecules, which result from the condensation of cyclohexane into an "armchair" configuration, were first reported by Wei and co-workers as the main cause of deactivation at low temperature [75]. The fact that they were only found at 300°C could explain why the deactivation of the catalyst was experienced only at that temperature. In the present work, it was not possible to determine the mass distribution of diamandoid, PMBs and polycyclic aromatics, however, the presence of the former clearly indicates that the temperature was simply not appropriate for the MTO reaction.

PMBs (mono-aromatics) were formed in successive steps where light olefins (ethylene, propylene and butene) first undergo oligomerization followed by cyclization. Products of the latter reaction are then dehydrogenated by molecules acting as H-acceptor (propylene or surface methoxy groups) [119]. A similar mechanism was also proposed by Vedrine and co-workers for the conversion of methanol to aromatics [120]. It is important to emphasize

that for one molecule of mono-aromatic, three molecules of alkanes are formed in parallel, and once the former is created, it becomes the active center governing the hydrocarbon pool mechanism. The presence of PMBs in the spent catalysts explains the activity for olefins formation. Nonetheless, PMBs also act as the precursors of inactive coke molecules by fusing into polycyclic aromatics (naphthalenes, anthracene, phenanthrene and pyrene) [77]. With an increase in the experiment temperature, the reactions leading to coke formation were further exacerbated by molecule retention caused by SAPO-34 micropores, which being narrower than the gyration diameter of the smallest PMB (methylbenzene, 4.64 Å) [63], prevented the aromatic molecules from escaping the SAPO-34 particle.

4.4. Conclusions

An extruded catalyst presenting a "*high*" loading of commercial SAPO-34 (65 wt%) as active part and amorphous silica (35 wt%) as permanent binder was prepared and tested in a bench-scale, fixed-bed reactor for the conversion of methanol to olefins. Comparison of the crystal structure, texture properties and acidity demonstrated that the extrusion process was successful and had no negative effect on the qualities of the active part.

The MTO reaction was tested at temperatures ranging from 300 to 500°C, which led to the following observations:

- At 300°C, E-SAPO-34 showed a poor conversion of methanol to hydrocarbons (61.8% at 2 h) and underwent deactivation after 6 h of reaction (15.8%). Analysis of the coke indicated the presence of diamandoid molecules, polymethylbenzenes and polycyclic aromatics. Diamandoid species were only found at this temperature, which indicated that such temperature was not appropriate for straightforward MTO.
- At higher temperatures (350 ─ 500°C) methanol conversion to hydrocarbons was more prominent and a quasi-steady state was attained for the entire duration of the experiments. Methanol conversion values varied between 72 and 91% and ethylene selectivity was improved with increasing the temperature, which occurred at the expense of larger molecules (C_{3-6}).
- The ethylene-to-propylene ratio was observed to vary greatly, namely, from around a value of 1 to up to 4 in the range between 350 and 500°C. This flexibility in the selectivity could be beneficial for the current dynamic demand facing the market of light olefins.
- Methane concentration was found to increase along with temperature as a result of the combination of protolytic cracking of higher molecules and cracking of substituted aromatics found in the coke.
- Propane concentration was found to decrease with temperature owing to a less favorable hydrogen transfer reaction at higher temperatures.
- 450°C was selected as the optimal temperature for the MTO, as methanol conversion was maximal and the coke content and alkanes were minimal.

Moreover, its H/C ratio indicated a higher amount of substituted polymethylbenzenes, which are acknowledged to be the active coke intermediates for MTO

- The extrusion process was proven convenient as a conditioning process to adapt a modified SAPO-34 catalyst for industrial use.

Chapter 5. MTO reaction: suppression of undesirable products with a SAPO-34 synthesized via an organosilane-directed method

Abstract

A SAPO-34 presenting small dimension features, a low acidity and a complex porosity (hierarchical structure) was synthesized using an organosilane-directed method. The catalyst was then tested and compared to the performance of a purchased SAPO-34 exhibiting a conventional microporous structure for the MTO reaction. During testing, the best performance for the synthesized SAPO-34 was obtained at 450°C, where ethylene and propylene combined selectivity (carbon-based) soared to 79.1%, 4.9% higher than what was obtained with the purchased catalyst. Moreover, the enhancement of the selectivity towards light olefins arose in parallel with a lower selectivity to propane (i.e. 1.6 vs 4.0%) and carbon occurring as coke (i.e. 7.7 vs 10.1%). It was concluded that the higher selectivity to light olefins stemmed from the suppression of olefin secondary reactions, especially those involving propylene.

Keyword: MTO reaction, SAPO-34, hierarchization, intra-particle mesopores, coke deposition.

Réaction MTO: suppression des produits indésirables grâce à une SAPO-34 fabriquée à partir d'une méthode se basant sur les organosilanes

Résumé

Une SAPO-34 présentant de petites particules, une faible acidité et une porosité complexe (structure hiérarchique) a été synthétisée en utilisant une méthode se basant sur les organosilanes. Le catalyseur a ensuite été testé et comparé aux performances d'une SAPO-34 achetée présentant une structure microporeuse conventionnelle pour la réaction MTO. Pendant les essais, la meilleure performance pour la SAPO-34 synthétisée a été obtenue à 450° C, où la sélectivité combinée d'éthylène et de propylène (à base de carbone) a grimpé à 79.1%, 4.9% de plus que ce qui a été obtenu avec le catalyseur acheté. De plus, l'amélioration de la sélectivité vis-à-vis des oléfines légères est apparue parallèlement à une sélectivité plus faible pour le propane (à savoir 1.6 contre 4.0%) et le carbone se manifestant sous forme de coke (à savoir 7.7 contre 10.1%). Il a été conclu que la plus grande sélectivité vis-à-vis des oléfines légères provenait de la suppression des réactions secondaires des oléfines, en particulier celles impliquant le propylène.

Mots clés: MTO reaction, SAPO-34, hierarchization, intra-particle mesopores, coke deposition.

5.1. Introduction

Currently, the production of light olefins originates from energy-intensive, fossil-fueled processes, such as steam cracking of ethane and naphtha (predominantly), fluidized catalytic cracking (FCC) and paraffin dehydrogenation [17,124,138]. Consequently, light olefins production is intimately linked to the availability and cost of fossil fuels utilized in these technologies. As alternative, the Methanol-to-Olefins process (also referred as MTO) was developed by Mobil's scientists in the 70s and presents multiple advantages over steam cracking. Among the latter can be included: a higher carbon-based conversion to light olefins, a better control in the selectivity towards ethylene and propylene, and the potential to diversify the syngas source from which methanol is produced, such as biomass or even municipal solid wastes [139,140]. Thus, employing any of these "*non-petroleum*" sources, in conjunction with the MTO process, could allow the development of "*green*" alternatives to the existing fossil-fueled, historical infrastructure [14,15].

In industry, catalysts employed for the MTO reaction are microporous molecular sieves such as H-ZSM-5 and SAPO-34, whose exceptional performances originates from the combined effect of their internal topology and acidity [3,33]. SAPO-34 has demonstrated a higher selectivity to olefins, in particular ethylene and propylene, which has stimulated the development of commercial processes for the production of polymer-grade olefin streams [35,36]. SAPO-34 is a silicoaluminophosphate presenting a CHA topology with large cages (11.0 × 6.5 Å) and narrow openings (3.8 × 3.8 Å) [44]. This configuration imposes physical constraints on large molecules, to be precise, those presenting four or more carbon atoms, and therefore, favors the diffusion of smaller molecules such as ethylene and propylene. Large molecules retained within the pores lead to coke formation, through oligomerization and fusion reactions, which causes the deactivation of the catalyst [66,73,114–116].

In particular, SAPO-34 is well known to undergo a fast deactivation during the MTO reaction, which has forced commercial systems to employ fluidized-bed reactors to allow the recovery and regeneration of the spent catalyst [33,36]. Deactivation occurs due to the accumulation of inactive molecules (polycyclic aromatics) over acid sites responsible for the reaction, and the ensuing pore blockage transpiring once a critical coke content is

reached [63,65]. Coke deposition does not follow a homogenous distribution in the SAPO-34 microporous volume, given that coke is first formed on the outer layers closer to the external surface [121]. This pattern limits the full utilization of the catalyst active volume, and so, it has been proposed that SAPO-34 lifetime could be "*improved*" by implementing strategies that increase the accessibility to the particle inner layers and limit the occurrence of products secondary reactions [45].

A strategy targeting the suppression of secondary reactions is the use of water in the feedstock. Indeed, water was shown to enhance both light olefin selectivity and catalyst lifetime by acting as a competitor for strong acid sites due to its polar nature [85]. Also, the dilution of methanol, combined with the higher heat capacity of water, allows the latter to behave as a "heat-sink" countering the exothermal nature of the MTO reaction [45]. Furthermore, water has been reported to induce the hydration and conversion of Lewis acid sites to Brönsted types (BAS) [126]. The latter are well known to catalyze the MTO reaction, while the former have been linked to enhancing secondary reactions leading to coke deposition [127].

Other strategies have been implemented during the synthesis of SAPO such as modifying the acidity [141] and/or varying the size and shape of the crystal [70,71,142]. A more recent approach was the introduction of intra-particle mesopores (20 – 500 Å) to obtain a hierarchical-type structure [73,74,143]. This approach relies on the fact that by creating a secondary structure, additional channels within the crystal, would significantly lower the residence time of the products, in addition to rendering accessible the deeper layers of the particle microporous volume [143]. The most successful methods reported include post-chemical treatment of SAPO-34 with HF [117], and the incorporation/removal of a hard template such as carbon-based nanostructures (nanospheres and nanowires) [72] or a soft-templates like in the case of organosilane molecules [102]. The use of soft templates has been recently implemented in SAPO-34, showing positive results in the fabrication of hierarchical-type structures, and also, exhibiting a higher performance for the MTO reaction [73,74].

In this chapter, the catalytic performance of two extruded catalysts exhibiting intrinsically different physico-chemical properties were investigated in the transformation of methanol to olefins. The catalysts studied included a microporous SAPO-34 acquired from Advanced Chemical Supplier (ACS) and a hierarchical SAPO-34 synthesized via an organosilane-directed method. Attention was given to the physico-chemical properties, as they are known to play a key role in the MTO catalytic performance.

5.2. Results and discussion.

5.2.1. Physico-chemical properties.

Table 11. Physico-chemical properties of the catalysts investigated in their pure (P) and extruded (E) forms

Catalyst (loading %)		RC (%)	N_2 adsorption V_{Micro} $cm^3/g_{SAPO-34}$	N_2 adsorption V_{Meso} $cm^3/g_{SAPO-34}$	NH_3-TPD Weak $\mu mol/g_{SAPO-34}$	NH_3-TPD Strong $\mu mol/g_{SAPO-34}$
P	P-MICRO-34	-	0.252	0.000	528	820
	P-MESO-3D	-	0.145	0.261	314	419
	P-MESO-5D	-	0.170	0.216	474	636
	P-MESO-7D	-	0.163	0.192	732	833
E	E-MICRO-34 (65%)	68.3	0.237	0.246	531	839
	E-MESO-3D (55%)	51.2	0.127	0.519	279	437
	E-MESO-5D (55%)	53.4	0.146	0.549	500	566
	E-MESO-7D (55%)	54.2	0.125	0.634	952	475

P: pure catalyst, E: extruded catalyst, RC: relative crystallinity, V_{Micro}: microporous volume, V_{Meso}: mesoporous volume

A total of eight samples were studied, including four pure samples labelled (P-) and their corresponding extruded forms labelled (E-). The samples included a commercial SAPO-34 as well as three SAPO-34 synthesized with crystallization times of 3, 5 and 7 days. Samples were denominated as P-MICRO-34 and E-MICRO-34 for the commercial SAPO-34 in the pure and extruded form, respectively, while P-MESO-#D and E-MESO-#D represented the synthesized catalyst. In the latter, the (#) corresponds to the number of crystallization days. A complete list of the samples nomenclature and physico-chemical properties are presented in **Table 11**.

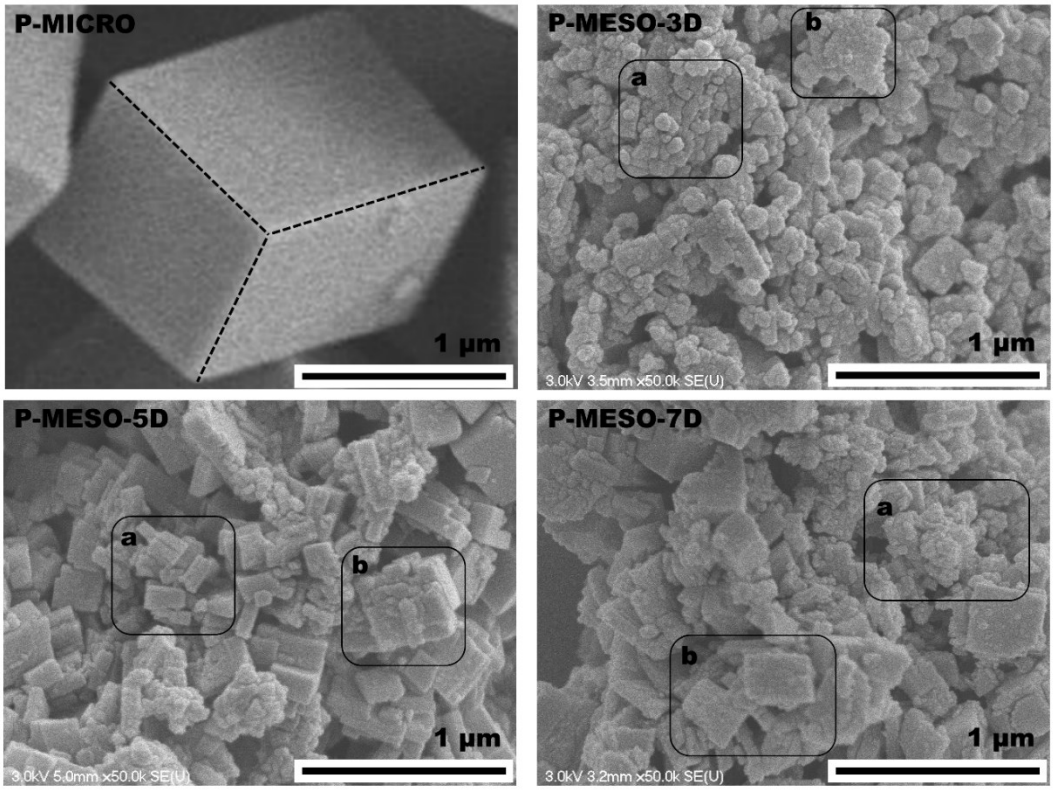

Figure 36. SEM images (50,000 magnification) of P-MICRO-34 (top-left), P-MESO-3D (top-right), P-MESO-5D (bottom-left), and (d) P-MESO-7D (bottom-right). The reference bar represents one micrometer in length. Areas designed by letters ("a" or "b") highlight particular features in the samples. The letter "a" highlight areas where multiple fragments with irregular shapes are observed composing a larger asymmetrical "particle" while the letter "b" indicates areas where fragments have coalesced to form a more seamless particle.

Scanning electron microscope (SEM) images of the purchased SAPO-34 and the synthesized catalysts are presented in **Figure 36**. As shown, the purchased SAPO-34 (P-MICRO-34) presented a well-defined rhombohedral shape resembling that of a prism, a common morphology observed in SAPO-34 particles. Furthermore, the SEM showed that

the surface of the particle was smooth and seamless, indicating no evidence of fractures. In contrast, those synthesized following an organosilane-directed method (P-MESO-3D, 5D and 7D) presented irregular shapes varying from rather spherical forms to "*fractured*" particles displaying in some cases rectangular angles. Sun and co-workers [74] studied the synthesis of SAPO-34 using a similar organosilane-directed method while varying the amount of the mesoporous agent added. The authors found that particles crystallized in the presence of the mesoporous agent were, in fact, the result of the agglomeration of "small cubic-like nanocrystals", in which the silica-containing end of the agent (referred as the "head") was first incorporated into the nanocrystal, while the organic chain (referred as the "tail") provided a "capping effect" that both limited the growth of the "nanocrystal" and the incorporation of Si atoms. In this work, it was observed that these "nanocrystals" are represented by the different fragments highlighted with the letter "a" in **Figure 36**. When analyzing the dimensions of the particles from multiple SEM images with the help of ImageJ software, it was found that these particles (or fragments due to its irregularity) had average sizes of 107, 201 and 282 nm for P-MESO-3D, 5D and 7D, respectively, with standard deviations (STD) between 33 and 45% of the corresponding average value. Remarkably, these dimension values were comparable to those reported by Sun and co-workers of 100 to 500 nm [74]. In contrast, P-MICRO-34 presented a significantly larger dimension average (ca. 2,010 nm) with a lower variability (STD ≈ 25%). Some examples of nano-scale agglomeration can be still observed in the **Figure 36**, but highlighted by the letter "b".

Analysis of the crystal structure of the pure and extruded catalysts was performed using XRD and the measurements are presented in **Figure 37**. XRD patterns showed that the pure and extruded catalysts presented the characteristic crystal planes of SAPO-34 including [101] (strongest signal), [110], [021], [211], [220], [401] and [015] in alignment with their corresponding 2θ angle. The permanent binder was not detected by XRD as the latter was composed of an amorphous silica phase. The calculated relative crystallinity for the extruded catalysts is summarized in **Table 11**. The results indicated that the extruded catalysts retained the initial crystallinity of their corresponding pure catalysts, given that all samples (extruded) exhibited relative crystallinity (RC) values close to their loading

percentages. For instance, a 65% loading led to a crystallinity of 68.3 and loadings of 55% led to relative crystallinity values of 51.2, 53.4 and 54.2% for E-MESO-3D/5D and 7D, respectively. The similarity pointed out a dilution effect caused by the permanent binder, amorphous silica, which has a weak signal in the XRD machine.

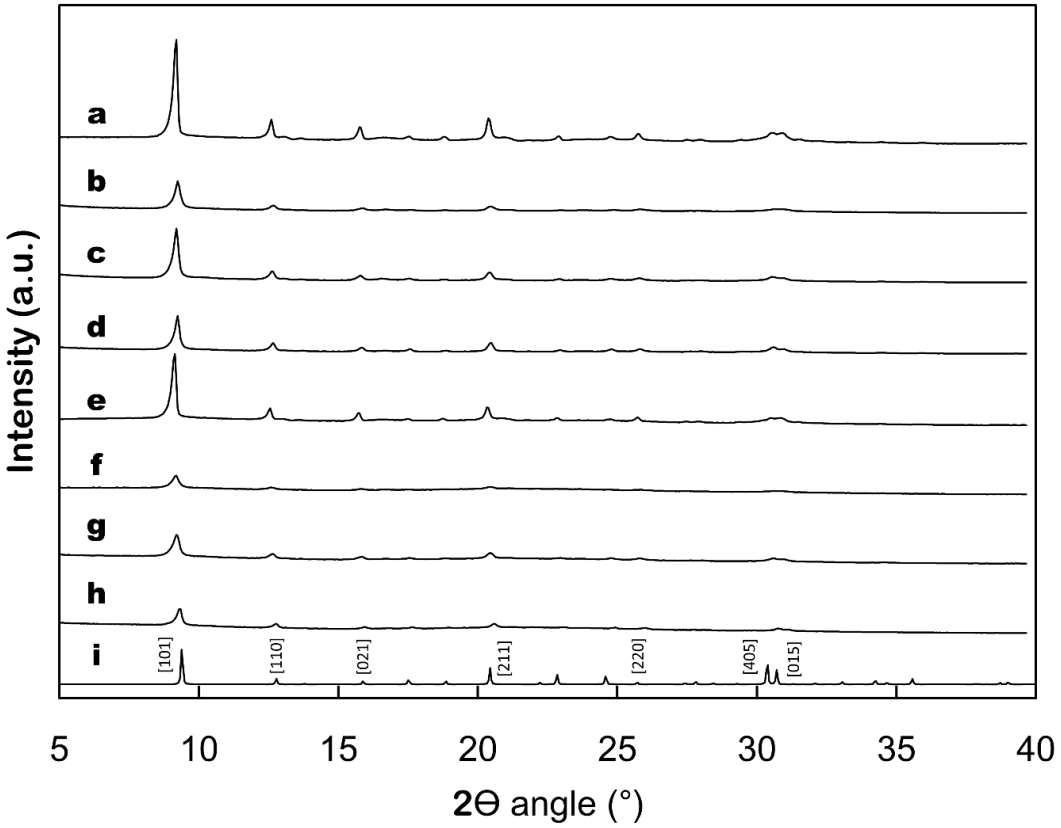

Figure 37. X-ray diffraction patterns of the pure catalysts: P-MICRO-34 (a), P-MESO- 3D (b), P-MESO-5D (c) and P-MESO-7D (d); as the extruded catalysts: E-MICRO-34 (e), E-MESO-3D (f), E-MESO-5D (g) and E-MESO-7D (h), as well as the diffraction pattern of the SAPO-34 from the International Zeolite Association database (i).

The texture properties evaluated via the N_2 adsorption-desorption isotherm are summarized in **Table 11**. P-MICRO-34 was found to be composed solely of a microporous structure (pores with a diameter < 20 Å and type I isotherm), meanwhile the synthesized catalysts in pure form (P-MESO-3D, 5D and 7D) suggested, in addition to the SAPO-34 innate microporous structure, the presence of mesopores with diameter ranging between 20 and 500 Å (IV isotherm) [93]. The latter was considered as an intra-particle type since it was created during the catalyst synthesis stage. The formation of this secondary structure started with the encapsulation of the mesoporous agent (TPAOC) in the SAPO-34 particles

(amorphous), which was formed during the crystallization step. However, during calcination, the trapped organic molecules were burnt out of the structure, leaving behind a secondary network of pores and channels connecting the external surface to the inner layers of the particle. Upon extrusion of the pure catalysts, the resulting samples presented an additional mesoporous volume, which stemmed from the interaction of the permanent binder and the SAPO-34 framework (inter-particle mesopores).

Analysis of the crystallization time showed that the microporous volume attained a maximum value of 0.170 $cm^3/g_{SAPO-34}$ after 5 days, while the minimum value of 0.145 $cm^3/g_{SAPO-34}$ was obtained after 3 days (**Table 11**). Comparison of the microporous volume of the pure and extruded catalysts showed consistently that the extrusion step caused a reduction of this value. For instance, P-MICRO-34 went from 0.252 to 0.237 $cm^3/g_{SAPO-34}$ (-6.0%), while P-MESO-3D, 5D and 7D went from 0.145 to 0.127 $cm^3/g_{SAPO-34}$ (-12.4%), 0.170 to 0.146 $cm^3/g_{SAPO-34}$ (-14.1%) and 0.163 to 0.125 $cm^3/g_{SAPO-34}$ (-23.3%), respectively. The reduction could be ascribed to particle occlusion, a feature reported by Gayubo and co-workers [97] when using large amounts of permanent binder with a conventional SAPO-34 (bentonite/alumina at 75%). In the actual case, a more prominent loss in microporous volume was observed in the synthesized SAPO-34 which could be attributed to a particle size effect, since a larger particle (such as P-MICRO-34) would be more difficult to be fully covered by the permanent binder.

The catalyst acidity, measured via NH_3-TPD, is reported in **Table 11**. Comparison of the total acidity of the synthesized SAPO-34 indicated that increasing the hydrothermal treatment led to a higher acidity, reaching values of 733, 1,110 and 1,565 $\mu mol/g_{SAPO-34}$ after 3, 5 and 7 days of crystallization, respectively. When analyzing the results of the commercial SAPO-34 (P-MICRO-34 and E-MICRO-34), it was noticed that the extrusion step had no impact on the total acidity ($\mu mol/g_{SAPO-34}$) nor the distribution of acid site strength. However, this was not the case for the synthesized catalysts as its acidity decreased consistently upon extrusion, which incidentally occurred in parallel with a redistribution of the acid strength concentration. For example, the pure samples (P-MESO-3D, 5D and 7D) presented weak-to-strong acid site ratios of 0.749, 0.745 and 0.879, respectively. Once extruded, however, the values became 0.638, 0.883 and 2.004,

respectively. The mild loss of acidity and redistribution of the acid strength could be attributed to the presence of a secondary structure created by the mesopores agent, as such could have allowed access and interaction (mild passivation or neutralization) of a small amount of the permanent binder in the liquid form (colloidal silica) with the internal structure of the particle.

5.2.2. Catalytic results in the MTO reaction

The extruded catalysts E-MICRO-34 and E-MESO-3D were tested in the MTO reaction to correlate the effect of the physico-chemical properties, described in the previous section, on the selectivity towards certain products

Of the synthesized catalysts, E-MESO-3D was selected for the catalytic study given that it possessed multiples characteristics that are well known to limit coke deposition [45]. For instance, this catalyst had the smallest dimension features while still retaining the SAPO-34 crystal structure, its acidity was significantly lower than that of the E-MICRO-34, and its structure presented a complex porosity configuration. As for the test conditions, temperatures of 350 and 450°C were selected since they provide different catalytic regimes of coke deposition, and a methanol solution with a H_2O/MeOH molar ratio of 7.12 (20% wt. MeOH) was used.

All experiments, irrespective of the temperature or catalyst used, attained a quasi-steady state within the reaction time (6 h), and so, the conversion, selectivity and other performance parameters were calculated and averaged for the last 4 h of each experiment. At this point, the reaction had already passed the induction period and the gas phase exhibited a stable product concentration.

The selectivity (C wt%) to ethylene (C_2=), propylene (C_3=) and hydrocarbon molecules with four-to-six carbon atoms (C_{4-6}), as well as the conversion of methanol to hydrocarbons are presented in **Figure 38**. Results show that the synthesized catalyst demonstrated a better performance in the MTO reaction at the studied temperatures (350 and 450°C). At 350°C, the extruded microporous catalyst achieved a selectivity to ethylene and propylene of 21.7 (± 1.4) and 24.2% (± 0.7) respectively, while the hierarchical catalyst reached values of

27.3 (± 0.7) and 36.7% (± 1.3). Contrary to light olefins, the selectivity towards C_{4-6} hydrocarbons was higher when using the microporous catalyst, 17.2 ± 0.6 vs 12.8 ± 0.3%.

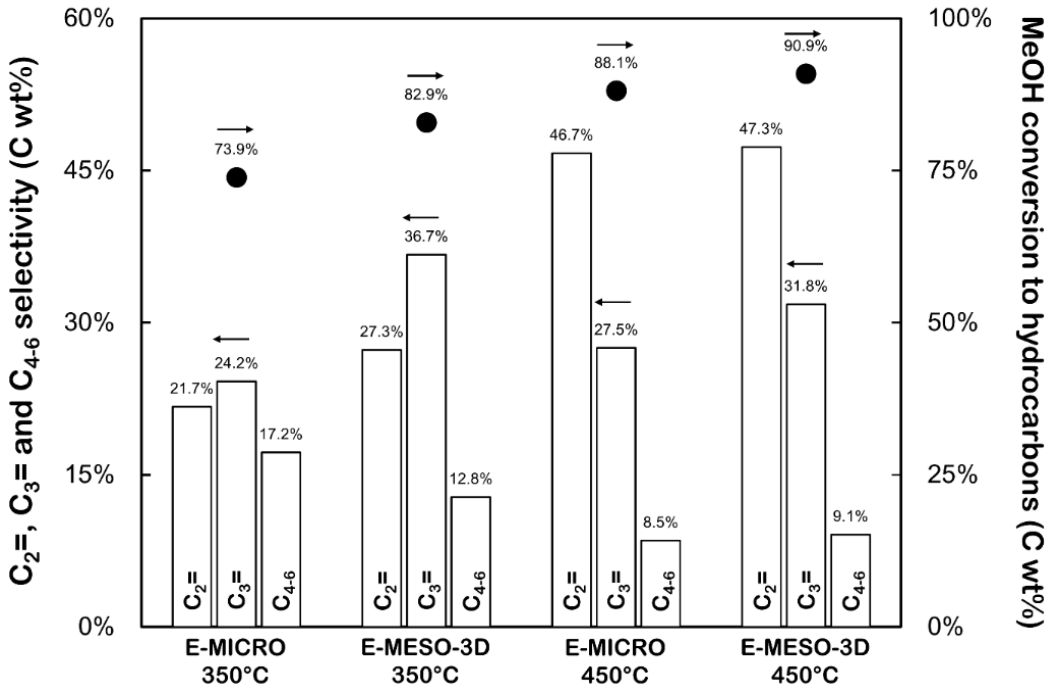

Figure 38.Catalytic performance on the selectivity to ethylene (C_2=), propylene (C_3=) and larger molecules (C_{4-6}) (hollow bars, left-axis), and methanol conversion to hydrocarbons found in the gas phase (black dots, right-axis) for the catalysts tested E-MICRO-34 and E-MESO-3D at 350 and 450°C.

Furthermore, the selectivity (C wt%) to light alkanes, i.e. methane and propane, and coke, are presented in **Figure 39**. The formation of propane and carbon deposited as coke were reduced when using the E-MESO-3D. For instance, the selectivity to propane for the E-MICRO-34 was 7.5% (± 1.0) compared to 3.3% (± 0.7) for the E-MESO-3D. As for the carbon measured in coke, the E-MICRO-34 and E-MESO-3D generated 18.1 and 7.2%, respectively. In the case of methane, the selectivity obtained by both catalysts were comparable, 2.2 (± 0.2) and 1.7% (± 0.5) for the E-MICRO-34 and E-MESO-3D, respectively.

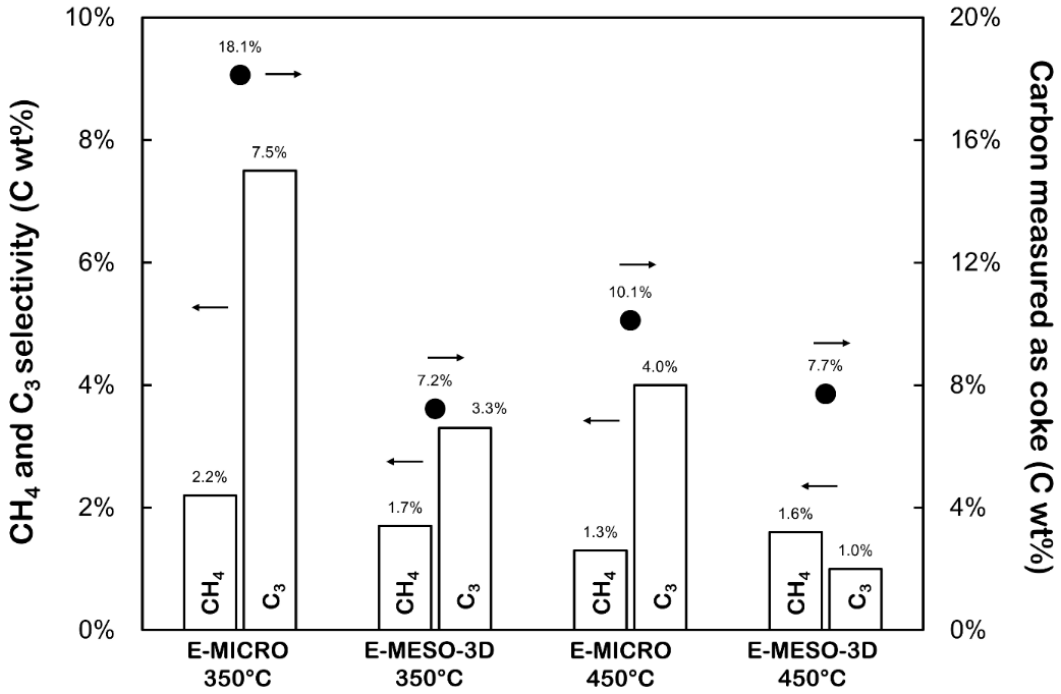

Figure 39. Catalytic performance on the selectivity to methane (CH_4) and propane (C_3) (hollow bars, left-axis), and carbon measured in the spent catalyst coke (black dots, right-axis) for the catalysts tested E-MICRO-34 and E-MESO-3D at 350 and 450°C.

The low deposition of coke translated into a higher conversion of methanol to hydrocarbons, as the E-MESO-3D achieved a conversion of 82.9% (± 1.5), while the E-MICRO-34 reached a value of 73.9 (± 1.3). The results obtained at 350°C clearly indicated the higher performance of the synthesized catalyst (E-MESO-3D) in the MTO reaction, which was attributed to the aforementioned physico-chemical properties (i.e. smaller dimensions, a lower acidity and a more complex porosity). The latter significantly suppressed the secondary reactions leading to coke formation, in particular, H-transfer reactions causing the saturation of olefins to alkanes (i.e. propane from propylene), oligomerization (i.e. C_{4-6} hydrocarbons) and deactivation of active molecules (i.e. carbon measured as coke) [65,76,131]. These reactions are compulsory in the formation of the polymethylbenzenes, the active molecule driving the catalytic cycles in the MTO reaction, according to the "*Hydrocarbon pool*" mechanism [49]. However, the extended retention of product molecules due to long diffusional pathways (i.e. microporous large particles) and the frequent interaction with "strong" acid sites (i.e. high acidity) caused the unwanted consumption of olefins, as observed for the E-MICRO-34.

At 450°C, the difference in performance between the E-MICRO-34 and E-MESO-3D was not as evident as to what was observed at 350°C. For instance, the selectivity towards ethylene, propylene and C_{4-6} hydrocarbons for the E-MICRO-34 and E-MESO-3D were 46.7 (± 0.4), 27.5 (± 0.3), 8.5% (± 0.4) and 47.3 (± 0.3), 31.8 (± 0.1), 9.1% (± 0.3), respectively. Out of the three species, only propylene showed a clear "*relative*" difference with an increase of 15.6% in selectivity, while the other two components (ethylene and C_{4-6} hydrocarbons) showed a gap less than 7.5% (1.3 and 7.1% increase, respectively).

In contrast, the selectivity to propane and carbon deposited as coke showed a clear difference, suggesting that the E-MESO-3D was still more resilient to products secondary reactions. The selectivity to propane for the E-MICRO-34 and E-MESO-3D were 4.0 (± 0.2) and 1.0% (± 0.1), respectively. As for coke content, the E-MICRO-34 and E-MESO-3D led to values of 10.1 and 7.7%, respectively. A close look to the methanol conversion at 450°C showed that no clear statistical difference existed between the catalysts performances, which were 88.1 ± 3.5 and 90.9 ± 3.4% for the microporous and hierarchical catalyst, respectively.

The results obtained at 450°C emphasized the importance of the temperature for reducing secondary reactions through the enhancement of cracking reactions. Indeed, the latter are of great relevance in the MTO reaction, to the extent that the equilibrium between these and oligomerization commonly determines the most adequate condition for olefin production and, on this subject, researchers have identified temperatures between 400 and 450°C as optimal [36,65,144].

Furthermore, the more significant improvement in selectivity to propylene (15.6%) over other olefins (<7.5%) indicated the higher tendency that propylene has for undergoing secondary reactions. Indeed, propylene oligomerization is well known to occur at lower temperatures and higher rates than ethylene over different catalysts [76]. In the MTO reaction, this has been exceptionally demonstrated by Wu and co-workers [85], who studied the reactivity of these species (ethylene, propylene and also butenes) over a conventional SAPO-34. The authors found that the presence of propylene in the feed (methanol or methanol/steam) inhibited the reaction between ethylene and methanol,

ultimately enhancing the selectivity to ethylene. In the actual case, the fact that the selectivity to propylene was the variable most enhanced at both temperatures, demonstrated that the catalyst was capable of limiting the interactions between light olefins, especially propylene, with acid sites which ultimately reduced the formation of propane and coke. In the case of methane, catalyst nor temperature showed any noticeable effect, and so, it was considered to behave as primary reaction product [132,134].

When comparing the accumulation of carbon in the synthesized catalyst (E-MESO-3D) at 350 and 450°C, it was noticed that the lower temperature induced the lesser accumulation of carbon in the catalyst, which was opposite to what was observed with the acquired catalyst (E-MICRO-34). This could be related to a lower conversion of methanol to hydrocarbons with the E-MESO-3D, namely, 82.9 (± 1.5) and 90.9% (± 3.4) for 350 and 450°C, respectively. At 350°C, it was noticed that methanol reforming ($CH_3OH+H_2O \rightleftarrows CO_2+3H_2$) occurred given that a selectivity to CO_2 of 4.6% was obtained, in parallel with the MTO mixture (

Table 12). The spontaneity of the reaction is supported by the calculated reaction Gibbs energy at 350 ($\Delta G_{350°C}$= -5.18 kJ/mol) and 450°C ($\Delta G_{450°C}$= -24. 8 kJ/mol). Nevertheless, the low selectivity (less than 6%) could suggest that such reaction is restricted by its kinetic. A similar finding was reported by Wu and co-workers [78], who studied the MTO reaction over a conventional SAPO-34 in a temperature range between 300 and 500°C. The authors concluded that the combination of low temperature (300 and 350°C) and hypothesized mild basicity of the catalyst could have led to the reforming of methanol since not enough acid sites were activated for the MTO reaction.

Table 12. Summary of the distribution of the carbon atom in the different cuts in the MTO reaction over extruded SAPO-34

Catalysts	**E-MICRO-34**		**E-MESO-3D**	
Temperature (°C)	**350**	**450**	**350**	**450**
Species	**Selectivity (C wt%)**			
Hydrocarbons cut*	73.9	88.1	82.9	90.9
Coke	18.1	10.1	7.2	7.7
CO_2	5.8	-	4.6	-
Total	97.8	98.2	94.07	98.6
Loss**	2.2	1.8	5.3	1.4
Hydrogen concentration (Vol %)***	1.7%	-	1.4%	-

*Hydrocarbons cut is composed of the following species: C_2=, C_3=, C_{4-6}, CH_4 and C_3

**Carbon percentage that was not accounted for, ***CO was not detected in the experiments

5.3. Conclusions

In the present chapter, an organosilane-directed method was used for the synthesis of a SAPO-34 presenting both a microporous and mesoporous structure (hierarchical). In addition, a SAPO-34 presenting a conventional microporous structure was purchased, and both catalyst were tested for the MTO reaction in a bench-scale, fixed-bed reactor following an extrusion procedure. From this work, the following conclusions were drawn:

- The synthesis procedure led consistently to a SAPO-34 composed of both a microporous (innate to the SAPO-34) and an intra-particle mesoporous structure (related to the mesopores agent), displaying small dimension features (≈100 – 280 nm) and low acidity.
- In the case of the purchased SAPO-34, the extrusion step did not have any important impact on the internal properties. However, for the synthesized catalysts, the extrusion step did affect the texture properties and acidity. Occlusion of the catalyst micropores was more prominent (a drop between 12 and 23%), and was attributed to the small dimension of the particles. The acidity showed a consistent mild drop which was quantified between 2.3 – 8.8%, nevertheless, the shift from strong to weak acid sites was evident, and such was ascribed to the interaction of the permanent binder with the acid sites exposed by the secondary structure.
- The selectivity to propylene at 350°C for the E-MESO-3D was the highest because, when compared to the E-MICRO-34 at the same temperature, the former presented features that limited propylene secondary reactions, hence, increasing the propylene output. Meanwhile, to the same catalyst but at 450°C, the higher temperatures favored the cracking of coke precursors (oligomers) to ethylene. Oligomers (coke precursors) are expected to originate from olefin secondary reactions, being propylene the one most affected because it is easier to agglomerate into oligomers than ethylene.
- During MTO testing, it was found that the E-MESO-3D achieved a higher conversion to light olefins (than E-MICRO-34) while reducing the formation of propane and coke. The best result was obtained at 450°C, where light olefin selectivity (C wt%) reached a value of 79.1% (vs 74.2%) while carbon as coke was

7.7% (vs 10.1%). The suppression of propylene secondary reactions was considered to be the important factor reducing the production of unwanted species.

Chapter 6. General conclusions

The present study aimed at developing an effective process for the selective conversion of methanol to light olefins, ethylene and propylene. This was achieved by combining an extrusion process and an organosilane-directed procedure for the fabrication of a hierarchical-type SAPO-34 ready to be tested in a bench-scale, fixed-bed reactor. The results led us to conclude about the impact of multiple parameters such as the catalyst employed (purchase vs synthesized), the extrusion of the catalyst, as well as the reaction temperature of the reaction on the catalyst performance for the MTO reaction.

6.1. Alkaline treatment of a commercial SAPO-34

Our work first focused on the chemical modification of a microporous SAPO-34, in which samples were drenched in different NaOH solutions. The results, however, indicated the limitations that this technique has in SAPO-34, as the analysis of the physico-chemical properties suggested that the treatment led to an indiscriminate elimination of the framework. More importantly, the reduction of the microporous structure (volume) did not induce the formation of a mesoporous one, a feature commonly seen in zeolites like H-ZSM-5 and Mordenite. Moreover, when different samples were tested in the accumulation of coke, treated samples showed a lower capacity (lower amount of acid sites) and a shorter time to reach 90% of the final weight gain. These observations clearly demonstrated that the treatment had no positive effect whatsoever.

However, the analysis confirmed the need of creating a secondary structure since calculations on the ratio acid site to coke molecule indicated a value of 3.5 and 3.7 for untreated and ion-exchanged SAPO-34 (samples that were not treated with NaOH). This demonstrated that coke preferred accumulating in the outer layer of the SAPO-34, leaving behind a large number of acid sites still active. It was concluded that by providing a mesoporous structure to the microporous volume, it could be possible to enhance the lifetime of the catalyst up to three times, that is, if a ratio of 1 were reached during coke deposition.

6.2. Extrusion process of different SAPO-34 catalysts

The extrusion was necessary for testing the catalyst in a bench-scale, fixed bed reactor, which unlike laboratory scale experiments, they require larger amounts of catalyst and this catalyst must be in a "*macroscopic*" forms to avoid clogging. The impact of this step on the overall analysis was based on the changes in the physico-chemical properties, before and after extrusion.

The effect of the extrusion process on the purchased SAPO-34 (P-SAPO-34/P-MICRO-34) was found to be irrelevant. Indeed, the extrusion step had no impact on the internal properties of the active part and though the texture properties (N_2 isotherm) indicated a loss of 6% in the microporous volume. The latter was attributed to some occlusion. Characterization techniques clearly demonstrated that the initial properties of the active part were essentially the same after the extrusion process.

In the case of the synthesized SAPO-34, the extrusion step had a clear impact in both the texture properties and acidity. Occlusion of the catalyst micropores was more prominent (up to 23% drop) and the stronger loss of texture properties was ascribed to the particle size, as the full coverage of the particle with the binder would be easier to occur. One of the main differences between the purchased catalyst and those prepared in the lab was that the latter presented dimensions in the order of a couple hundred nanometers or below. Additionally, the extrusion caused a decrease in acidity and a mild redistribution which was ascribed to binder percolating the internal structure caused by the mesopores and fractures observed via SEM. This access was thought capable of neutralizing acid sites exposed by the added mesoporous structure which explained the mild changes observed in the acidity.

6.3. Effect of temperature on the purchased SAPO-34 (P-SAPO-34/P-MICRO-34)

Temperature was varied from 300 to 500°C to evaluate its effect on the selectivity to hydrocarbons. The purchased SAPO-34 exhibited poor conversion of methanol to hydrocarbons at 300°C. Certainly, the conversion of methanol to hydrocarbons was 61.8%

at 2 h TOS and underwent deactivation after 6 h TOS (15.8%). The loss of hydrocarbon production, though DME was still formed, indicated that secondary reactions such as oligomerization, condensation and hydrogen transfer were favored at this temperature which led to the formation of coke causing the passivation and blocking of acid sites. The subsequent analysis of the spent catalyst showed that the coke was composed of diamandoid molecules, polymethylbenzenes and polycyclic aromatics. More importantly, the presence of diamandoid molecules (methyladamantanes) was revealing of the negative effect of the low temperature, as these molecules, unlike polymethylbenzenes, were incapable to undergo the MTO catalytic cycles to produce olefins.

Increasing the temperature of the MTO reaction between 350 and 500°C led to a higher conversion of methanol to hydrocarbons (between 72 and 91% in punctual values), in addition to observing a quasi-steady state maintained for the entire duration of the experiment (6 h). 450°C was identified as the optimal temperature for the MTO reaction since hydrocarbon production achieved a plateau (83.5 – 86.1% conversion based on carbon), meanwhile coke content and paraffins, which are known to be species to stem from secondary reactions, were minimized (3.81% coke content). Moreover, analysis of the coke indicated that the H/C ratio was highest among the conditions tested (1.89), suggesting the presence of a larger amount of substituted aromatics (i.e. polymethylbenzenes) which are recognized to be the intermediates for the MTO reaction. The dissolution of the spent catalyst with hydrofluoric acid (HF) and the ensuing identification by GC-MS of the trapped molecules further supported the presence of a wide range of aromatic molecules, polymethylbenzenes included.

In the same study, it was found that increasing the temperature had a positive effect in the selectivity to ethylene and methane, while larger molecules including propylene, propane and others (C_4, C_5 and C_6) decreased. Consequently, the ethylene-to-propylene ratio (molar) presented an extraordinary flexibility which ranged from 1.18 at 350°C to 4.01 at 500°C, both measured at 2 h TOS. The higher selectivity to ethylene occurred in parallel with a surge in methane production which was indicative of the cracking reactions, causing the elimination of substituted methyl groups in the aromatic molecules present in the coke. More importantly, this effect was observed to be stronger above 450°C where methane

production increased more drastically. The strong surge above 450°C was linked to a fast drop in the coke H/C ratio, and so, it was concluded that a combination of protolytic cracking and coke maturing were the causes behind the formation of methane at those conditions.

6.4. Performance of the synthesized SAPO-34 (P-MESO-3D)

A hierarchical-type SAPO-34 was synthesized using a three day crystallization time, and after extrusion and MTO testing, the following points are the most significant elements deduced about the connection between their properties and performance.

Overall, the effect of the temperature was similar to that observed in the microporous SAPO-34. For instance, larger molecules were favored at lower temperatures, where oligomerization was more prominent and cracking reactions were having a lower effect on the production of ethylene and methane.

The selectivity towards ethylene and propylene, however, indicated that the extruded form of the synthesized catalyst (E-MESO-3D) showed a higher conversion (79.1%, carbon based) than the microporous-type (E-SAPO-34/E-MICRO-34) (74.2%), which was attributed to the more complex porous structure and lower acidity, which in turn, reduced the secondary reactions, especially those involving propylene, leading to propane and coke accumulation.

6.5. De-alumination of the SAPO-34

Based on the results obtained in the MTO reaction using large volumes of water, one may realize that the SAPO-34 did not exhibit a tendency to lose aluminum due to steam as in the case of zeolites. This is supported by the fact during alkaline treatment, SAPO-34 underwent metal elimination (Al included) and its performance decreased with increasing the concentration of NaOH. However, when different SAPO-34 were tested in the MTO reaction at high water concentration, the extruded SAPO-34 samples showed a "*normal*" performance.

6.1 Traitement alcalin d'une SAPO-34 commercial

Préalablement à la synthèse d'une SAPO-34 hiérarchisée, les travaux ont été dirigés vers la modification chimique d'une SAPO-34 microporeuse, provenant de traitements avec différents solution de NaOH. Les résultats ont, cependant, indiqués les limites que cette technique a pour la SAPO-34, car l'analyse des propriétés physico-chimiques a suggéré que le traitement conduit à une élimination indiscriminée de la charpente. Plus important encore, la réduction de la structure microporeuse (volume) ne conduisait pas la formation d'une structure mésoporeuse, une caractéristique communément observée dans les zéolites comme H-ZSM-5 et Mordenite. De plus, lorsque des échantillons non traités et traités ont été testés par rapport à leur accumulation de coke, les échantillons traités présentaient une capacité inférieure (moins de sites acides) et un temps plus court pour atteindre 90% du gain de poids final (à cause de la déposition de molécules de coke). Ces observations ont clairement démontrés que le traitement n'avait aucun effet positif.

Cependant, l'analyse a confirmé la nécessité de créer une structure secondaire puisque les calculs du coefficient entre site acide et coke indiquent une valeur de 3,5 et 3,7 pour le SAPO-34 non-traitée et ionisée (échantillons non traités avec NaOH), démontrant que les molécules de coke s'accumulent d'abord dans la couche externe du SAPO-34, laissant derrière un grand nombre de sites acides encore actifs. Il a été conclu qu'en fournissant une structure mésoporeuse au volume microporeux, il pourrait être possible d'améliorer la durée de vie du catalyseur d'un facteur 3.

6.2 Procédé d'extrusion de différents catalyseurs SAPO-34

L'extrusion était nécessaire pour tester le catalyseur dans un réacteur à lit-fixe à l'échelle de banc d'essai, ce qui, en contraste aux travaux au niveau laboratoire, nécessite de grandes quantités de catalyseur sous une forme "*macroscopique*" pour éviter le colmatage. L'impact de cette étape dans l'analyse globale était basé sur les changements des propriétés physico-chimiques, avant et après extrusion, observés dans les deux SAPO-34 testés.

L'effet du processus d'extrusion sur la SAPO-34 achetée (P-SAPO-34 / P-MICRO-34) a été jugé nul. En effet, l'étape d'extrusion n'a eu aucun impact sur les propriétés internes de la partie active bien que les propriétés de texture (isotherme de N_2) indiquent une perte de

6% dans le volume microporeux, attribuée à une certaine occlusion. La caractérisation physico-chimique par différent techniques a clairement démontrée que les propriétés initiales de la partie active étaient essentiellement les mêmes après le processus d'extrusion.

Dans le cas de la SAPO-34 synthétisée, l'étape d'extrusion présentait un impact évident à la fois sur les propriétés de texture et sur l'acidité. L'occlusion des micropores du catalyseur était plus importante (jusqu'à 23% de chute). La perte significative des propriétés de texture subies par les catalyseurs synthétisés a été attribuée à la taille des particules. En effet, l'une des principales différences entre le catalyseur acheté et ceux préparés en laboratoire était que ce dernier présentait des dimensions de l'ordre de quelques centaines de nanomètres ou moins, alors que dans le cas du premier, celui-ci étaient constitués de cubes bien formés et avec de côtés de l'ordre de quelques micromètres de longueur. De plus, l'acidité après extrusion a diminué et a subi une légère redistribution qui fut associé à un accès limité du liant permanent dans la structure interne provoqué par les mésopores.

6.3 Effet de la température sur la SAPO-34 achetée (P-SAPO-34/P-MICRO-34)

La température a été variée de 300 à 500°C à fin d'évaluer son effet sur la sélectivité vers hydrocarbures. La SAPO-34 achetée présentait une conversion inferieure du méthanol en hydrocarbures à 300°C. Certes, la conversion du méthanol en hydrocarbures était de 61.8% après 2 h de TOS et a été désactivée après 6 h de TOS (15,8%). La perte de production d'hydrocarbures (bien que le DME soit encore formé) indiquait que des réactions secondaires telles que l'oligomérisation, la condensation et le transfert d'hydrogène étaient favorisées à cette température ce qui a conduit à la formation de coke, entraînant la passivation et le blocage des sites acides. L'analyse subséquente du catalyseur utilisé a démontré que le coke était composé de molécules diamandoïdes, de polyméthylbenzènes et d'aromatiques polycycliques. Plus important encore, la présence de molécules diamandoïdes (méthyladamantanes) révélait l'effet négatif de la basse température, car ces molécules, contrairement aux polyméthylbenzènes, étaient incapables de subir les cycles catalytiques de la réaction MTO pour produire des oléfines.

L'augmentation de la température de la réaction MTO entre 350 et 500°C a conduit à une conversion plus élevée du méthanol en hydrocarbures (entre 72 et 91% en valeurs ponctuelles), en plus d'observer un état quasi stationnaire maintenu pendant toute la durée de l'expérience (6 h). 450°C a été identifiée comme la température optimale pour la réaction MTO puisque la production d'hydrocarbures a atteint un plateau (83.5 – 86.1% de conversion basée sur le carbone), tandis que la teneur en coke et les paraffines, connues pour être formées à partir de réactions secondaires, ont été minimisées (teneur en coke de 3.81%). De plus, l'analyse du coke a indiqué que le rapport H/C était le plus élevé parmi les conditions testées (1.89), suggérant la présence d'une plus grande quantité d'aromatiques substitués (polyméthylbenzènes) qui sont reconnus comme intermédiaires pour la réaction MTO. La dissolution du catalyseur utilisé avec de l'acide fluorhydrique (HF) et l'identification par GC-MS des molécules piégées ont confirmé la présence d'une large gamme de molécules aromatiques, y compris les polyméthylbenzènes.

Dans la même étude, il a été trouvé que l'augmentation de la température avait un effet positif sur la sélectivité en éthylène et en méthane, tandis que les molécules plus grandes incluant le propylène, le propane et d'autres (C_4, C_5 et C_6) diminuaient. En conséquence, le rapport de l'éthylène au propylène (molaire) présentait une flexibilité extraordinaire qui variait de 1.18 à 350°C à 4.01 à 500°C, les deux mesurés à 2 heures de TOS. La plus grande sélectivité vis-à-vis de l'éthylène s'est produite parallèlement à une augmentation du méthane, indiquant des réactions de craquage entraînant l'élimination de groupes méthyle substitués dans les molécules aromatiques présentes dans le coke. Plus important encore, cet effet a été observé plus fort au-dessus de 450°C où la production de méthane a augmenté plus radicalement. La forte poussée au-dessus de 450°C a été liée à une chute rapide du rapport H/C dans le coke, et il a été conclu qu'une combinaison de craquage protolytique et de maturation du coke étaient les causes de la formation de méthane dans ces conditions.

6.4 Performance de la SAPO-34 synthétisée (P-MESO-3D)

Une SAPO-34 hiérarchisée a été synthétisée en utilisant un temps de cristallisation de trois jours, et ainsi, après l'extrusion et le test MTO, les points suivants ont pu être obtenus par rapport aux propriétés et performances.

Dans l'ensemble, l'effet de la température était similaire à celui observé pour la SAPO-34 microporeuse. Par exemple, des molécules plus grosses étaient favorisées à des températures plus basses où l'oligomérisation était plus importante et les réactions de craquage affectaient moins la production d'éthylène et de méthane.

Cependant, la sélectivité envers l'éthylène et le propylène indique que la forme extrudée du catalyseur synthétisé (E-MESO-3D) montre une conversion plus élevée (79.1%, à base de carbone) que le type microporeux (E-SAPO-34/E-MICRO-34) (74.2%), qui a été attribuée à la structure poreuse plus complexe et à une acidité plus faible, ce qui a réduit les réactions secondaires, en particulier celles impliquant le propylène, conduisant à l'accumulation de propane et de coke.

6.4 De-alumination de la SAPO-34

Sur la base des résultats obtenus dans la réaction de MTO en utilisant de grands volumes d'eau, on peut se rendre compte que le SAPO-34 n'avait pas tendance à perdre de l'aluminium à cause de la vapeur comme dans le cas des zéolithes. Ceci est soutenu par le fait pendant le traitement alcalin, SAPO-34 a subi une élimination des métaux (Al inclus) et sa performance a diminué avec l'augmentation de la concentration de NaOH. Cependant, lorsque différents SAPO-34 ont été testés dans la réaction de MTO à une concentration élevée en eau, les échantillons de SAPO-34 extrudés ont montré une performance « normale ».

Chapter 7. Recommendations and outlook

Incorporation of different metals such as nickel and cerium in the SAPO-34 Framework has been reported in the literature as a method to improve selectivity to light olefins in the MTO reaction. In particular, nickel is well-known to favor the production of ethylene, meanwhile the cerium has shown to improve selectivity for both light olefins (ethylene and propylene). The following recommendations aim the incorporation of these metals onto the SAPO-34 Framework.

7.1. Incorporation of Nickel into the SAPO-34 framework

The incorporation of Nickel can be considered a conservative approach as a wide number of publications have been done on the matter (see **Chapter 1**). One element that has not been studied yet is the synergic effect between hierarchization and Ni incorporation. It is noteworthy to mention that both optimization techniques were developed in different periods. Nickel incorporation to SAPO-34 occurred during the 90s, while hierarchization has only been done in the last decade. Both techniques look to decrease the formation of coke. Nickel is hypothesized to achieve this by lowering the acid strength of the catalyst, whereas hierarchization by lowering the residence time of the products. The fact that both have an impact in different "parts" of the reaction could imply that these could be mixed to re-create a SAPO-34 catalyst more resilient to coke deposition, while enhancing the formation of ethylene.

7.2. Combining a Ce-SAPO-34 and a CO_2 atmosphere during MTO

One element still not studied in the MTO/SAPO-34 system is the effect of using a carbon dioxide atmosphere during the reaction. For this, it is imperative that the SAPO-34 be loaded with a metal, preferentially an alkaline type so carbon dioxide, an acid molecule, can be adsorbed and rendered reactive on the surface through the reverse Boudouard reaction. As mentioned in the literature review (**Chapter 1**), Ca-ZSM-5 has been studied

under a carbon dioxide atmosphere and this led to the formation of carbon monoxide which was attributed to coke consumption.

Another option as co-catalyst is the Cerium oxide. This component has been loaded on the SAPO-34 with positive effects in the selectivity to ethylene and propylene. However, this oxide is also known to work as an "*oxygen pump*", which could be useful in the combustion of coke. By combining the carbon dioxide atmosphere and the cerium oxide, it could be possible to find a synergic effect that rivals that of water. This system, however, differs from other systems in that higher temperatures could be needed to enhance the effect of Ce/CO_2. This is because carbon dioxide activity may require a boost from the temperature which unfortunately could enhance the formation of coke. Under this scenario, the study would focus on finding the right conditions in which the accumulation of coke and the reverse Boudouard Reaction could neutralize each other.

This could lead to a novel route in the production of light olefins where conversion and selectivity could be sacrificed (to an extent) while still employing a fixed-bed reactor system, which as shown in the present work, it is not the adequate reactor type for the MTO reaction when using a SAPO-34 as catalyst.

7.3. Fluidized-bed reactor system

For this project, the selection of the fixed-bed reactor was based on the fact that such system is more accessible for the exploration and optimization of parameters, and to this point, catalyst and temperature have been investigated. However, it is understood that there are still other elements to optimize such as the loading of the SAPO-34 framework, the amount of such loading, as well as, perhaps, the WHSV and water content.

The research of fluidized-bed reactor should aim at a long-term work, which is after the improvement of aforementioned parameters. This line of research is suggested considering that all commercial SAPO-34 systems (polymer-grade olefins) rely on fluidized-bed reactors. In spite of this suggestion, the use of fixed-bed reactor for scaling up is completely feasible as other systems such as the MTP (methanol to propylene) process from LURGI employs fixed-bed reactors and H-ZSM-5 as catalyst.

A rule of thumb for selecting between a fixed- or fluidized-bed reactors is the time of deactivation of the catalyst. For instance, it is believed that a catalyst that deactivates in a matter of minutes should be set for a fluidized-bed reactor, while hours, days and weeks is more appropriate for fixed-beds. For our catalyst, deactivation occurs between of 2 and 3 hrs for a WSHV (MeOH) of 1. The latter is a WHSV a little less that employed by UOP/Hydro, which ranges between 1.5 and 3.

The current results place the system still in gray area since a 2 to 3 hrs for deactivation may still be short for scaling-up, and so, more research should be encouraged.

Chapter 8. References

[1] Mokrani, T. et Scurrell, M. (2000). Gas Conversion to Liquid Fuels and Chemicals: The Methanol Route-Catalysis and Processes Development. Catalysis Review, 51, 1, p. 1–145.

[2] Zhu, G., Xie, C. et Li. Z., (2010). Catalytic processes for light olefin production. In: Robinson, Hsu. Springer Handbook of Petroleum Processing, p. 149–168.

[3] Stöcker, M. (1999). Methanol-to-hydrocarbons: catalytic materials and their behavior, Microporous Mesoporous Materials, 29, 1–2, p. 3–48.

[4] Gidarakos, E., Havas, G. et Ntzamilis, P., (2006). Municipal solid waste composition determination supporting the integrated solid waste management system in the island of Crete. Waste Management, 26, 6, p. 668–679.

[5] Malkow, T., (2004). Novel and innovative pyrolysis and gasification technologies for energy efficient and environmentally sound MSW disposal. Waste Management, 24, 1, p. 53–79.

[6] Olah, G.A., Goeppert, A. et Prakash, G.K.S., (2009). Beyond Oil and Gas: The Methanol Economy. Wiley-VCH Verlag GmbH & Co. KGaA, Second Edition, 334 p.

[7] McMillan, M. (2010). Waste Management Industry Survey: Business and Government Sectors (16F0023X). Statistics Canada, 40 p.

[8] Woodhouse, C. (2011). Waste to Energy: A Technical Review of Municipal Solid Waste Thermal Treatment Practices (Final Report). Stantec Consulting Ltd. and British Columbia Ministry of Environment 335 p.

[9] Dalai A.K., Batta, N., Eswaramoorthi, I. et Schoenau, G.J. (2009). Gasification of refuse derived fuel in a fixed bed reactor for syngas production. Waste Management, 29, 1, p. 252–258.

[10] van Bennekom, J.G., Venderbosch, R.H., Winkelman, J.G.M., Wilbers, E., Assink, D., Lemmens, K.P.J. et Heeres, H.J. (2013). Methanol synthesis beyond chemical equilibrium. Chemical Engineering Science, 87, 1, p. 204–208.

[11] Larson, E.D., Worrel, E. et Chen, J. (1996). Clean fuels from Municipal Solid Waste for Transportation in New York city and other Major metropolitan Areas (PU/CEES Report No. 293). Center for Energy and Environmental Studies/Princeton University, Princeton, NJ, 55 p.

[12] Alberta Oil, A methanol renaissance in Canada refuels the biofuels debate, Alberta Oil Mag. (n.d.). https://www.albertaoilmagazine.com/2014/09/refueling-biofuels-debate/ (accessed October 2, 2017).

[13] Enerkem Alberta Biofuels (2017). http://enerkem.com/facilities/enerkem-alberta-biofuels/ (accessed October 2, 2017).

[14] Chornet, E., Valsecchi, B., Avila, Y., Nguyen, B. et Lavoie, J.M. (2008). Production of ethanol from methanol, US 8080693.

[15] Gil-Coba, J., Marie-Rose, S.C. et Lavoie, J.M. (2016). Effect of water content and catalysts acidity in the products distribution ruring propylene synthesis with a mixture of DME and methanol. Catalysis Letters, 146, 12, p. 2534–2542.

[16] ACS Materials (2017), https://www.acsmaterial.com/sapo-1010.html (accessed September 26, 2017).

[17] Bellussi, G. et Pollesel P., (2005). Industrial applications of zeolite catalysis: production and uses of light olefins. Studies in Surface Science and Catalysis, 158, 2, p. 1201–1212.

[18] Chang, C.D. (1983). Hydrocarbons from Methanol. Catalysis Review, 25 , 1, p. 1–118.

[19] Barger, P.T., Vora, B.V., Pujadó, P.R. et Chen, Q. (2003). Converting natural gas to ethylene and propylene using the UOP/HYDRO MTO process. Studies in Surface Sciences and Catalysis, 145, 1, p. 109–114.

[20] Eramo, M. (2013). Ethylene market outlook. in: Ethylene Forum. Los Angeles, US, 43 p.

[21] IHS Markit (2017), https://www.ihs.com/index.html (accessed October 2, 2017).

[22] IHS Markit (2017). Ethylene - Chemical Economics Handbook. https://www.ihs.com/products/ethylene-chemical-economics-handbook.html (accessed July 25, 2017).

[23] IHS Markit (2017). Propylene World Analysis. https://www.ihs.com/products/world-petro-chemical-analysis-propylene.html (accessed July 25, 2017).

[24] De Jose, B. (2002). Olefins conversion technology applications (WPC-32270). 17th World Petroleum Congress, p. 503–511.

[25] ICIS Chemical Business. (2003). Lurgi scales up Propylur process for demonstration. https://www.icis.com/resources/news/2003/01/24/188728/lurgi-scales-up-propylur-process-for-demonstration/ (accessed August 22, 2017).

[26] Sadrameli, S.M. (2016). Thermal/catalytic cracking of liquid hydrocarbons for the production of olefins: A state-of-the-art review II: Catalytic cracking review. Fuel, 173, 1, p. 285–297.

[27] Chenier, P.J. (2002). Survey of Industrial Chemistry. Springer US (on-line), US, Third Edition, 515 p.

[28] Ren, T., Patel, M. et Blok, K. (2006). Olefins from conventional and heavy feedstocks: Energy use in steam cracking and alternative processes. Energy, 31, 4, p. 425–451.

[29] Ren, T., Patel, M.K. et Blok, K. (2008). Steam cracking and methane to olefins:

Energy use, CO_2 emissions and production costs. Energy, 33, 5, p. 817–833.

[30] Long, J., Zhu, Y., Tian, H., Chen, Z., Guo, Y., Da, Z., Zhang, J. et He, M. (2004). Molecular sieve-containing catalyst for cracking hydrocarbons and method for preparing the same. US 0266608A1.

[31] IHS Markit (2017), Propylene - Chemical Economics Handbook. https://www.ihs.com/products/propylene-chemical-economics-handbook.html (accessed July 25, 2017).

[32] Kirk-Othmer (1993). Encyclopedia of Chemical Technology, WILEY, Fouth Edition, New York, US, 22950 p.

[33] Keil, F.J. (1999). Methanol-to-hydrocarbons: process technology. Microporous Mesoporous Materials, 29, 1–2, p. 49–66.

[34] Chang, C.D. et Silvestri, A.J. (1977). The conversion of methanol and other O-compounds to hydrocarbons over zeolite catalysts. Journal of Catalysis, 47, 2, p. 249–259.

[35] Chen, J.Q., Bozzano, A., Glover, B., Fuglerud, T. et Kvisle, S. (2005). Recent advancements in ethylene and propylene production using the UOP/Hydro MTO process. Catalysis Today, 106, 1–4, p. 103–107.

[36] Tian, P., Wei, Y., Ye, M. et Liu, Z. (2015). Methanol to olefins (MTO): From fundamentals to commercialization, ACS Catalysis, 5, 3, p. 1922–1938.

[37] Bare, S.R. (2007). Methanol to Olefins (MTO): Development of a commercial catalytic process. oral presentation, 98 p.

[38] Kim, H.S., Lee, S.G., Kim, Y.H., Lee, D.H., Lee, J.B. et Park, C.S. (2013) Improvement of lifetime using transition metal-incorporated SAPO-34 catalysts in conversion of dimethyl ether to light olefins. Journal of Nanomaterials, Article ID 679758, p. 1–9.

[39] International Zeolite Agency (2017). http://www.iza-online.org/ (accessed October 2, 2017).

[40] Tanabe, K. (1999). Industrial application of solid acid–base catalysts. Applied Catalysis A: General, 181, 2, p. 399–434.

[41] Froment, G.F., Dehertog, W.J. et Marchi, A.J. (1992). Zeolite catalysis in the conversion of methanol into olefins. in: Catalysis (Royal Chemical Society), 9, p. 1–64.

[42] Al-Dughaither, A.S. et De Lasa, H. (2014). Neat dimethyl ether conversion to olefins (DTO) over HZSM-5: Effect of SiO_2/Al_2O_3 on porosity, surface chemistry, and reactivity. Fuel, 138, 1, p. 52–64.

[43] Lok, B.M., Messina, C.A., Patton, R.L., Gajek, R.T., Cannan, T.R. et Flanigen, E.M. (1984). Silicoaluminophosphate molecular sieves: another new class of microporous crystalline inorganic solids. Journal of the American Chemical Society, 106, 20, p.

6092–6093.

[44] Wilson, S. et Barger, P. (1999). The characteristics of SAPO-34 which influence the conversion of methanol to light olefins. Microporous Mesoporous Materials, 29, 1–2, p. 117–126.

[45] Chen, D., Moljord, K. et Holmen, A. (2012). A methanol to olefins review: Diffusion, coke formation and deactivation on SAPO type catalysts. Microporous Mesoporous Materials, 164, 1, p. 239–250.

[46] Dessau, R.M. et LaPierre, R.B. (1982). On the mechanism of methanol conversion to hydrocarbons over HZSM-5. Journal of Catalysis, 78, 1, p. 136–141.

[47] Mole, T., Whiteside, J.A. et Seddon, D. (1983). Aromatic co-catalysis of methanol conversion over zeolite catalysts. Journal of Catalysis, 82, 2, p. 261–266.

[48] Dahl, I.M. et Kolboe, S. (1996). On the reaction mechanism for hydrocarbon formation from methanol over SAPO-34. Journal of Catalysis, 161, 1, p. 304–309.

[49] Dahl, I.M. (1994). On the reaction mechanism for hydrocarbon formation from methanol over SAPO-34 I. Isotopic labeling studies of the co-Reaction of ethene and methanol. Journal of Catalysis, 149,2 p. 458–464.

[50] Arstad, B. et Kolboe, S. (2001). The reactivity of molecules trapped within the SAPO-34 cavities in the Methanol-to-Hydrocarbons reaction. Journal of the American Chemical Socieity, 123, Journal of the American Chemical Society, 123, 33, p. 8137–8138.

[51] Arstad, B. et Kolboe, S. (2001). Methanol-to-hydrocarbons reaction over SAPO-34. Molecules confined in the catalyst cavities at short time on stream. Catalysis Letters, 71, 3–4, p. 209–212.

[52] Song, W., Haw, J.F., Nicholas, J.B. et Heneghan, C.S. (2000). Methylbenzenes are the organic reaction centers for methanol-to-olefin catalysis on HSAPO-34. Journal of the American Chemical Society, 122, 43, p. 10726–10727.

[53] Bjørgen, M. (2003). Coke precursor formation and zeolite deactivation: mechanistic insights from hexamethylbenzene conversion. Journal of Catalysis, 215, 1, p. 30–44.

[54] Goguen, P.W., Xu, T., Barich, D.H., Skloss, T.W., Song, W., Wang, Z., Nicholas, J.B. et Haw, J.F. (1998). Pulse-quench catalytic reactor studies reveal a carbon-pool mechanism in Methanol-to-Gasoline chemistry on zeolite HZSM-5. Journal of the American Chemical Society, 120, 11, p. 2650–2651.

[55] Olsbye, U., Bjørgen, M., Svelle, S., Lillerud, K.P. et Kolboe, S. (2005). Mechanistic insight into the methanol-to-hydrocarbons reaction. Catalysis Today, 106, 1–4, p. 108–111.

[56] Sullivan, R.F., Egan, C.J., Langlois, G.E. et Sieg R.P. (1961). A new reaction that occurs in the hydrocracking of certain aromatic hydrocarbons. Journal of the American Chemical Society, 83, 5, p. 1156–1160.

[57] Mole, T., Bett, G. et Seddon, D. (1983). Conversion of methanol to hydrocarbons over ZSM-5 zeolite : An examination of the role of aromatic hydrocarbons using ^{13}carbon- and deuterium-labeled feeds. Journal of Catalysis, 84, 2, p. 435–445.

[58] Xu, S., Zheng, Z., Wei, Y., Chen, J., Li, J., Chu, Y., Zhang, M., Wang, Q., Zhou, Y., Wang, J., Deng, F. et Liu, Z. (2013). Direct observation of cyclic carbenium ions and their role in the catalytic cycle of the Methanol-to-Olefin reaction over Chabazite zeolites. Angewandte Chemie International Edition, 52, 44, p. 11564–11568.

[59] Bos, A.N.R., Tromp, P.J.J. et Akse, H.N. (1995). Conversion of methanol to lower olefins. Kinetic modeling, reactor simulation, and selection. Industrial and Engnieering Chemistry Research, 34, 11, p. 3808–3816.

[60] Chen, D., Grønvold, A., Moljord, K. et Holmen, A. (2007). Methanol conversion to light olefins over SAPO-34: Reaction network and deactivation kinetics. Industrial and Engnieering Chemistry Research, 46, 12, p. 4116–4123.

[61] Chen, D., Moljord, K. et Holmen, A. (2000). The effect of the particle size on methanol conversion to light olefins. in: 12th International Congress of Catalysis. p. 2651–2656.

[62] Chen, D., Rebo, H.P., Moljord, K. et Holmen, A. (1997). Influence of coke deposition on selectivity in zeolite catalysis. Industrial and Engineering Chemistry Research, 36, 9, p. 3473–3479.

[63] Luo, M., Zang, H., Hu, B., Wang, B. et Mao, G. (2016). Evolution of confined species and their effects on catalyst deactivation and olefin selectivity in SAPO-34 catalyzed MTO process. RSC Advances, 6, 1, p. 17651–17658.

[64] Song, W., Fu, H. et Haw, J.F. (2001). Selective synthesis of methylnaphthalenes in HSAPO-34 cages and their function as reaction centers in methanol-to-olefin catalysis. Journal of Physical Chemistry B, 105, 51, p. 12839–12843.

[65] Rostami, R.B., Ghavipour, M., Di, Z., Wang, Y. et Behbahani, R.M. (2015). Study of coke deposition phenomena on the SAPO_34 catalyst and its effects on light olefin selectivity during the methanol to olefin reaction. RSC Advances, 5, 100, p. 81965–81980.

[66] Chen, D., Rebo, H.P., Grønvold, A., Moljord, K. et Holmen, A. (2000). Methanol conversion to light olefins over SAPO-34: kinetic modeling of coke formation. Microporous Mesoporous Materials, 35–36, p. 121–135.

[67] Liu, Z., Sun, C., Wang, G., Wang, Q. et Cai, G. (2000). New progress in R&D of lower olefin synthesis. Fuel Processing Technology, 62, 2–3, p. 161–172.

[68] Chen, D., Moljord, K., Fuglerud, T. et Holmen, A. (1999). The effect of crystal size of SAPO-34 on the selectivity and deactivation of the MTO reaction. Microporous Mesoporous Materials, 29, 1–2, p. 191–203.

[69] Wang, P., Yang, D., Hu, J., Xu, J. et Lu (2013). Synthesis of SAPO-34 with small and tunable crystallite size by two-step hydrothermal crystallization and its catalytic

performance for MTO reaction. Catalysis Today, 212, p. 62.e1-62.e8.

[70] Sun, Q., Ma, Y., Wang, N., Li, X., Xi, D., Xu, Deng, F., Yoon, K.B., Oleynikov, P., Terasaki, O. et Yu, J. (2014). High performance nanosheet-like silicoaluminophosphate molecular sieves: synthesis, 3D EDT structural analysis and MTO catalytic studies. Journal of Material Chemistry A, 2, 42, p. 17828–17839.

[71] Wang, C., Yang, M., Tian, P., Xu, S., Yang, Y., Wang, D., Yuan, Y. et Liu, Z. (2015). Dual template-directed synthesis of SAPO-34 nanosheet assemblies with improved stability in the methanol to olefins reaction. Journal of Material Chemistry A, 3, 10, p. 5608–5616.

[72] Schmidt, F., Paasch, S., Brunner, E. et Kaskel, S. (2012). Carbon templated SAPO-34 with improved adsorption kinetics and catalytic performance in the MTO-reaction. Microporous Mesoporous Materials, 164, p. 214–221.

[73] Yang, S.T., Kim, J.Y., Chae, H.J., Kim, M., Jeong, S.Y. et Ahn, W.S. (2012). Microwave synthesis of mesoporous SAPO-34 with a hierarchical pore structure. Materials Reseach Bulletin, 47, 11, p. 3888–3892.

[74] Sun, Q., Wang, N., Xi, D., Yang, M. et Yu, J. (2014). Organosilane surfactant-directed synthesis of hierarchical porous SAPO-34 catalysts with excellent MTO performance. Chemistry Communications (Camb), 50, 49, p. 6502–6505.

[75] Wei, Y., Li, J., Yuan, C., Xu, S., Zhou, Y., Chen, J., Wang, Q., Zhang, Q. et Liu Z. (2012). Generation of diamondoid hydrocarbons as confined compounds in SAPO-34 catalyst in the conversion of methanol. Chemistry Communications (Camb), 48, 25, p. 3082–3084.

[76] Sanati, M., Hörnell, C. et Järäs. (1999). The oligomerization of alkenes by heterogeneous catalysts. in: Catalysis (Royal Chemical Society), 14, Chapitre 7, p. 236–287.

[77] Guisnet, M. et Magnoux, P. (2001). Organic chemistry of coke formation. Applied Catalysis A: General, 212, 1–2, p. 83–96.

[78] Wu, X., Abraha, M.G. et Anthony, R.G. (2004). Methanol conversion on SAPO-34: Reaction condition for fixed-bed reactor. Applied Catalysis A: General A, 260, 1, p. 63–69.

[79] Obrzut, D.L., Adekkanattu, P.M., Thundimadathil, J., Liu, J., Dubois, D.R. et Guin, J.A. (2003). Reducing methane formation in methanol to olefins reaction on metal impregnated SAPO-34 molecular sieve. Reaction Kinetics and Catalysis Letters, 80, 1, p. 113–121.

[80] Dubois, D.R., Obrzut, D.L., Liu, J., Thundimadathil, J., Adekkanattu, P.M, Guin, J.A., Punnoose, A. et Seehra, M.S. (2003). Conversion of methanol to olefins over cobalt-, manganese- and nickel-incorporated SAPO-34 molecular sieves. Fuel Processing Technology, 83, 1–3, p. 203–218.

[81] Djieugoue, M.A., Prakash, A.M. et Kevan, L. (2000). Catalytic study of Methanol-to-Olefins conversion in four small-pore silicoaluminophosphate molecular sieves:

Influence of the structural type, nickel incorporation, nickel location, and nickel concentration. Journal of Physical Chemistry B, 104, 27, p. 6452–6461.

[82] Tan, J., Liu, Z., Bao, X., Liu, X., Han, X., He, C. et Zhai, R. (2002). Crystallization and Si incorporation mechanisms of SAPO-34. Microporous Mesoporous Materials, 53, 1–3, p. 97–108.

[83] Xu, L., Du, A., Wei, Y., Wang, Y., Yu, Z., He, Y., Zhang, X. et Liu, Z. (2008). Synthesis of SAPO-34 with only Si(4Al) species: Effect of Si contents on Si incorporation mechanism and Si coordination environment of SAPO-34. Microporous Mesoporous Materials, 115, 3, p. 332–337.

[84] Liu, G., Tian, P., Xia, Q. et Liu, Z. (2012). An effective route to improve the catalytic performance of SAPO-34 in the methanol-to-olefin reaction. Journal of Natural Gas Chemistry, 21, 4, p. 431–434.

[85] Wu, X. et Anthony, R.G.G. (2001). Effect of feed composition on methanol conversion to light olefins over SAPO-34. Applied Catalysis A: General, 218, 1–2, p. 241–250.

[86] Sardesai, A. et Lee, S. (2005). Alternative Source of Propylene. Energy Sources, 27, p. 489–500.

[87] Man, J.J., Zhang, Q.Q., Xie, H.H., Pan, J.J., Tan, Y. et Han, Y. (2011). Effects of reaction atmosphere on dimethyl ether conversion to propylene process over Ca/ZSM-5. Journal of Fuel Chemistry and Technology, 39, 1, p. 42–46.

[88] Xu, L., Liu, Z., Du, A., Wei, Y. et Sun, Z. (2004). Synthesis, characterization, and MTO performance of MeAPSO-34 molecular sieves. Studies in Surface Science and Catalysis, 147, p. 445–450.

[89] Salmasi, M., Fatemi, S. et Najafabadi, A.T. (2011). Improvement of light olefins selectivity and catalyst lifetime in MTO reaction; using Ni and Mg-modified SAPO-34 synthesized by combination of two templates. Journal of Industrial and Engineering Chemistry, 17, 4, p. 755–761.

[90] Inui, T., Phatanasri, S. et Matsuda, H. (1990). Highly Selective Synthesis of Ethene from Methanol on a Novel Nickel-Silicoaluminophosphate Catalyst. Journal of the Chemistry Society, 20, 3, p. 205–206.

[91] Thomas, J.M., Xu, Y., Catlow, C.R.A. et Couves, J.W. (1991). Synthesis and characterization of a catalytically active nickel-silicoaluminophosphate catalyst for the conversion of methanol to ethene. Chemistry of Materials, 3, 4, p. 667–672.

[92] Inui, T. (1994). Process for synthesis of lower olefins from methanol. EP0418142B1.

[93] Leofanti, G., Padovan, M., Tozzola, G. et Venturelli, B. (1998). Surface area and pore texture of catalysts. Catalysis Today, 41, 1–3, p. 207–219.

[94] Magnoux, P., Roger, P., Canaff, C., Fouche, V., Gnep, N.S. et Guisnet, M. (1987). New technique for the characterization of carbonaceous compounds responsible for

zeolite deactivation. in the 4th International Symposium in Catalysis, Elsevier, p. 317–330.

[95] Freiding, J., Patcas, F.C. et Kraushaar-Czarnetzki, B. (2007). Extrusion of zeolites: Properties of catalysts with a novel aluminium phosphate sintermatrix. Applied Catalysis A: General, 328, 2, p. 210–218.

[96] Michels, N.L., Mitchell, S. et Pérez-Ramírez, J. (2014). Effects of binders on the performance of shaped hierarchical MFI zeolites in methanol-to-hydrocarbons. ACS Catalysis, 4, 8, p. 2409–2417.

[97] Gayubo, A.G., Aguayo, A.T., Sánchez del Campo, A.E., Tarrío, A.M. et Bilbao, J. (2000). Kinetic modeling of methanol transformation into olefins on a SAPO-34 catalyst. Industrial Engineering Chemistry Research, 39, 2, p. 292–300.

[98] Bedard (2010). Zeolites in Industrial Separation and Catalysis, Wiley-VCH Verlag GmbH & Co. KGaA, First Edition, Weinheim, Germany, 618 p.

[99] Flanigen, E.M. et Grose, R.W. (1974). Phosphorus Substitution in Zeolite Frameworks. in Molecular Sieve Zeolites-I. Chapter 5, p. 76–101.

[100] Wilson, S.T., Lok, B.M. et Flanigen, E.M. (1990). Crystallite metallophosphate compositions. US 4310440.

[101] Verboekend, D., Milina, M. et Pérez-Ramírez, J. (2014). Hierarchical silicoaluminophosphates by postsynthetic modification: Influence of topology, composition, and silicon distribution. Chemistry Materials, 26, 15, p. 4552–4562.

[102] Choi, M., Cho, H.S., Srivastava, R., Venkatesan, C., Choi, D.H. et Ryoo, R. (2006). Amphiphilic organosilane-directed synthesis of crystalline zeolite with tunable mesoporosity. Nature Materials, 5, p. 718–723.

[103] Groen, J.C., Peffer, L.A.A., Moulijn, J.A. et Pérez-Ramírez, J. (2005). Mechanism of hierarchical porosity development in MFI zeolites by desilication: the role of aluminium as a pore-directing agent. Chemistry - A European Journal, 11, 17, p. 4983–4994.

[104] Bjørgen, M., Joensen, F., Holm, M.S., Olsbye, U., Lillerud, K.P. et Svelle, S. (2008). Methanol to gasoline over zeolite H-ZSM-5: Improved catalyst performance by treatment with NaOH. Applied Catalysis A: General, 345, 1, p. 43–50.

[105] Ogura, M., Shinomiya, S., Tateno, J., Nara, Y., Nomura, M., Kikuchi, E. et Matsukata, M. (2001). Alkali-treatment technique — new method for modification of structural and acid-catalytic properties of ZSM-5 zeolites. Applied Catalysis A: General, 219, 1–2, p. 33–43.

[106] Van Laak, A.N.C., Zhang, L., Parvulescu, A.N., Bruijnincx, P.C.A., Weckhuysen, B.M., de Jong, K.P. et de Jongh P.E. (2011) Alkaline treatment of template containing zeolites: Introducing mesoporosity while preserving acidity. Catalysis Today, 168, 1, p. 48–56.

[107] Vennestrøm, P.N.R., Grill, M., Kustova, M., Egeblad, K., Lundegaard, L.F.,

Joensen, F., Christensen, C.H. et Beato, P. (2011). Hierarchical ZSM-5 prepared by guanidinium base treatment: Understanding microstructural characteristics and impact on MTG and NH_3-SCR catalytic reactions. Catalysis Today, 168, 1, p. 71–79.

[108] van Laak, A.N.C, Sagala, S.L., Zečević, J., Friedrich, H., de Jongh, P.E. et de Jong, K.P. (2010). Mesoporous mordenites obtained by sequential acid and alkaline treatments – Catalysts for cumene production with enhanced accessibility. Journal of Catalysis, 276, 1, p. 170–180.

[109] Li, X., Prins, R. et van Bokhoven, J.A. (2009). Synthesis and characterization of mesoporous mordenite. Journal of Catalysis, 262, 2, p. 257–265.

[110] Verboekend, D. et Pérez-Ramírez, J. (2011) Design of hierarchical zeolite catalysts by desilication. Catalysis Science and Technology, 1, 6, p. 879–890.

[111] Li, S., Falconer, J.L. et Noble, R.D., SAPO-34 membranes for CO_2/CH_4 separation. Journal of Membrane Science, 241, 1, p. 121–135.

[112] Jänchen, J., Ackermann, D., Weiler, E, Stach, H. et Brösicke, W. (2005). Calorimetric investigation on zeolites, $AlPO_4$'s and $CaCl_2$ impregnated attapulgite for thermochemical storage of heat. Thermochimica Acta, 343, 1–2, p. 37–41.

[113] Hong, M., Li, S., Falconer, J.L. et Noble, R.D. (2008). Hydrogen purification using a SAPO-34 membrane. Journal of Membrane Science, 307, 2, p. 277–283.

[114] Park, J.W., Lee, J.Y., Kim, K.S., Hong, S.B. et Seo, G. (2008). Effects of cage shape and size of 8-membered ring molecular sieves on their deactivation in methanol-to-olefin (MTO) reactions Applied Catalysis A: General, 339, 1, p. 36–44.

[115] Park, J.W. et Seo, G. (2009). IR study on methanol-to-olefin reaction over zeolites with different pore structures and acidities. Applied Catalysis A: General, 356, 2, p. 180–188.

[116] Marchese, L., Frache, A., Gianotti, E., Martra, G., Causà et M., Coluccia, S. (1999). AlPO-34 and SAPO-34 synthesized by using morpholine as templating agent. FTIR and FT-Raman studies of the host–guest and guest–guest interactions within the zeolitic framework. Microporous Mesoporous Materials, 30, 1, p. 145–153.

[117] Chen, X., Vicente, A.A., Qin, Z., Ruaux, V., Gilson, J.P. et Valtchev, V.P. (2016). Preparation of hierarchical SAPO-34 crystals by post-synthesis fluoride etching. Chemistry Communications, 52, 17, p. 3512–3515.

[118] Prakash, A.M. et Unnikrishnan, S. (1994). Synthesis of SAPO-34: High Silicon Incorporation in the presence of morpholine as template. Journal of the Chemical Society - Faraday Transactions, 90, 15, p. 2291-2296.

[119] Magnoux, P., Rabeharitsara, A. et Cerqueira, H.S. (2006). Influence of reaction temperature and crystallite size on HBEA zeolite deactivation by coke. Applied Catalysis A: General, 304, 1, p. 142–151.

[120] Vedrine, J.C., Dejaifve, P., Garbowski, E.D. et Derouane, E.G. (1980). Aromatics

Formation from Methanol and Light Olefins Conversions on H-ZSM-5 Zeolite,: Mechanism and Intermediate Species. Studies in Surface Science and Catalysis, 5, 1, p. 29-37.

[121] Mores, D., Stavitski, E., Kox, M.H.F.F., Kornatowski, J., Olsbye, U. et Weckhuysen, B.M. (2008). Space- And time-resolved in-situ spectroscopy on the coke formation in molecular sieves: Methanol-to-olefin conversion over H-ZSM-5 and H-SAPO-34. Chemistry - A European Journal, 14, 36, p. 11320–11327.

[122] Amghizar, I., Vandewalle, L.A., Van Geem, K.M. et Marin, G.B. (2017). New Trends in Olefin Production. Engineering, 3, 2, p. 171–178.

[123] Plotkin, J.S. (2005). The changing dynamics of olefin supply/demand. Catalysis Today, 106, 1, p. 10–14.

[124] Chen, X. et Yan, Y. (2008). Study on the technology of thermal cracking of paraffin to alpha olefins. Journal of Analytical and Applied Pyrolysis, 81, 1, p. 106–112.

[125] Weissermel, K. et Arpe, H.J. (1997). Industrial Organic Chemistry. WILEY-VCH Verlag GmbH & Co. KGaA, Fourth Edition, New York, US, 467 p.

[126] Wolthuizen, J.P., van den Berg, J.P. et van Hooff, J.H.C. (1980). Low temperature reactions of olefins on partially hydrated zeolite H-ZSM-5. Studies in Surface Science and Catalysis, 5, 1, p. 85–92.

[127] Müller, S., Liu, Y., Kirchberger, F.M., Tonigold, M., Sanchez-Sanchez, M. et Lercher, J.A. (2016). Hydrogen Transfer Pathways during Zeolite Catalyzed Methanol Conversion to Hydrocarbons. Journal of the American Chemical Society, 138, 49, p. 15994–16003.

[128] Haw, J.F., Song, W., Marcus, D.M. et Nicholas, J.B. (2003). The Mechanism of Methanol to Hydrocarbon Catalysis. Accounts of Chemical Reseachr, 36, 5, p. 317–326.

[129] Cui, Y., Zhang, Q., He, J., Wang, Y. et Wei, F. (2013). Pore-structure-mediated hierarchical SAPO-34: Facile synthesis, tunable nanostructure, and catalysis applications for the conversion of dimethyl ether into olefins. Particuology, 11, 4, p. 468–474.

[130] Hereijgers, B.P.C., Bleken, F., Nilsen, M.H., Svelle, S., Lillerud, K.P., Bjørgen, M., Weckhuysen, B.M. et Olsbye, U. (2009). Product shape selectivity dominates the Methanol-to-Olefins (MTO) reaction over H-SAPO-34 catalysts. Journal of Catalysis, 264, 1, p. 77–87.

[131] Ilias, S. et Bhan, A. (2012). Mechanism of the Catalytic Conversion of Methanol to Hydrocarbons. ACS Catalysis, 3, 1, p. 18–31.

[132] Hutchings, G.J. et Hunter, R. (1990). Hydrocarbon formation from methanol and dimethyl ether: a review of the experimental observations concerning the mechanism of formation of the primary products. Catalysis Today, 6, 3, p. 279–306.

[133] Salehirad, F. et Anderson, M.W. (1996). Solid-State 13 C MAS NMR study of

Methanol-to-Hydrocarbon chemistry over H-SAPO-34. Journal of Catalysis, 314, 2, p. 301–314.

[134] Wei, Z., Chen, Y.Y., Li, J., Wang, P., Jing, B., He, Y., Dong, M., Jiao, H., Qin, Z., Wang, J. et Fan, W. (2016). Methane formation mechanism in the initial methanol-to-olefins process catalyzed by SAPO-34. Catalysis Science and Technology, 6, 14, 5526–5533.

[135] Kotrel, S., Knözinger, H. et Gates, B. (2000). The Haag-Dessau mechanism of protolytic cracking of alkanes. Microporous Mesoporous Materials, 35–36, p. 11–20.

[136] Elliott, D.C. (1988). Relation of Reaction Time and Temperature to Chemical Composition of Pyrolysis Oils. in: Pyrolysis Oils from Biomass. Chapter 6, p. 55–65.

[137] Milne, A.T., Evans, R.J. et Abatzaglou, N. (1998). Biomass Gasifier " Tars ": Their Nature , Formation , and Conversion (NREL/TP-570-25357). Golden, US, 204 p.

[138] Mathieu, Y., Corma, A., Echard, M. et Bories, M. (2014). Single and combined Fluidized Catalytic Cracking (FCC) catalyst deactivation by iron and calcium metal-organic contaminants. Applied Catalysis A: General, 469, p. 451–465.

[139] Kumar, A., Jones, D.D. et Hanna, M.A. (2009). Thermochemical biomass gasification: A review of the current status of the technology. Energies, 2, 3, p. 556–581.

[140] Sansaniwal, S.K., Pal, K., Rosen, M.A. et Tyagi, S.K. (2017). Recent advances in the development of biomass gasification technology: A comprehensive review, Renewable and Sustainable Energy Reviews, 72, p. 363–384.

[141] Liu, G., Tian, P., Zhang, Y., Li, J., Xu, L., Meng, S. et Liu, Z. (2008). Synthesis of SAPO-34 templated by diethylamine: Crystallization process and Si distribution in the crystals. Microporous Mesoporous Materials, 114, 1–3, p. 416–423.

[142] Álvaro-Muñoz, T., Sastre, E. et Marquez-Alvarez, C. (2014). Microwave-assisted synthesis of plate-like SAPO-34 nanocrystals with increased catalyst lifetime in the methanol-to-olefins reaction. Catalysis Science and Technology, 4, 12, p. 4330–4339.

[143] Gueudré, L., Milina, M., Mitchell, S. et Pérez-Ramírez, J. (2014). Superior mass transfer properties of technical zeolite bodies with hierarchical porosity. Advanced Functional Materials, 24, 2, p. 209–219.

[144] Wei, Y., Yuan, C., Li, J., Xu, S., Zhou, Y., Chen, J., Wang, Q., Xu, L., Qi, Y., Zhang, Q. et Liu, Z. (2012). Coke formation and carbon atom economy of Methanol-to-Olefins reaction, Chemistry and Sustainability Energy and Materials, 5, 5, p. 906–912.